Universität Hamburg

DER FORSCHUNG | DER LEHRE | DER BILDUNG

Functional Polymethylenes: Synthesis and Post-Polymerization Modification

Dissertation
with the aim of achieving the doctoral degree at the Faculty of
Mathematics, Informatics and Natural Sciences

submitted to the
Department of Chemistry
University of Hamburg

Tim Walter Krappitz

2017 in Hamburg

The following evaluators recommend the admission of the dissertation:

1. Evaluator: Prof. Dr. Patrick Théato

2. Evaluator: Prof. Dr. Gerrit A. Luinstra

Date of the oral defense: 07.04.2017

1. Chairman of the examination board: Prof. Dr. Patrick Théato

2. Examiner: Prof. Dr. Martin Trebbin

3. Examiner: Dr. Werner Pauer

Approved for publication: 07.04.2017

Table of Contents

List of Publications

1. **T. Krappitz**, P. Theato, *J. Polym. Sci. Pol. Chem.*, Comparative Study on Post-Polymerization Modification of C1 Poly(benzyl 2-ylidene-acetate) and Its C2 Analog Poly(benzyl acrylate), **2016**, 54, 686–691.

This study is part of the discussion in chapter 3.1.

2. **T. Krappitz**, D. Brauer, P. Theato, *Polym. Chem.*, Synthesis of Poly(allyl 2-Ylidene-Acetate) and Subsequent Post-Polymerization Modification via Thiol–ene Reaction, **2016**, 7, 4525–4530.

This study is part of the discussion in chapter 3.2.

3. **T. Krappitz**, P. Feibusch, C. Aroonsirichock, V. P. Hoven, P. Theato, *Macromolecules*, Synthesis of Poly(glycidyl 2-ylidene-acetate) and Functionalization by Nucleophilic Ring-Opening Reactions, **2017**, 50, 1415-1421.

This study is part of the discussion in chapter 3.3.

List of Abbreviations

Abbreviation	Full name
AdDA	adamantyl 2-diazoacetate
AIBN	azobisisobutyronitrile
ATR	attenuated total reflectance
ATRP	atom transfer radical polymerization
BnDA	benzyl 2-diazoacetate
ChDA	cholesteryl 2-diazoacetate
COD	1,5-cyclooctadiene
DBU	1,8-diazabicyclo[5.4.0]undec-7-ene
DMeCOD	1,5-dimethyl-1,5-cyclooctadiene
DMPA	2,2-dimethoxy-2-phenylacetophenone
dNbpy	4,4´-dinonyl-2,2´-dipyridyl
DSC	differential scanning calorimetry
EDA	ethyl 2-diazoacetate
EEGE	ethoxy ethyl glycidyl ether
FRP	free radical polymerization
FT-IR	fourier transform infrared
c-HDA	cyclohexyl 2-diazoacetate
n-HDA	n-hexyl 2-diazoacetate
MMA	methyl methacrylate
MWCO	molecular weight cut-off
M_n	number average molecular weight
MW	molecular weight
M_w	weight average molecular weight
NHC	N-heterocyclic carbenes
NMR	nuclear magnetic resonance
o.n.	overnight
PAA_C1	poly(allyl 2-ylidene-acetate)
PBIEA_C1	poly(2-(2-bromoisobutyryloxy)ethyl 2-ylidene-acetate)
PBnA_C1	poly(benzyl 2-ylidene-acetate)
PBnA_C2	poly(benzyl acrylate)
PEA_C1	poly(ethyl 2-ylidene-acetate)
PGA_C1	poly(glycidyl 2-ylidene-acetate)
PGMA_C2	poly(glycidyl methacrylate)
PProA_C1	poly(propargyl 2-ylidene-acetate)
PMMA	poly(methyl methacrylate)

Abbreviation	Full name
PPhMA	poly(phenyl methacrylate)
RDRP	reversible-deactivation radical polymerization
SEC	size exclusion chromatography
SLS	static light scattering
TGA	thermogravimetric analysis
THF	tetrahydrofurane
TM	transition metal
Tz	1,2,4-triazole

Abstract

Despite the fact that polyolefins are highly important materials in today's society, it is still an issue to synthesize these polymers with a high density of functional side groups. In this context, novel rhodium mediated C1 polymerization leads to functional polymethylene scaffolds bearing a (polar) functional group at every main chain carbon atom. However, the scope of monomers investigated for C1 polymerizations and in turn the accessibility of materials is still limited. Therefore, post-polymerization modification with its broad toolbox of suitable and highly efficient reactions is a promising approach to provide access to diversely functionalized polymethylenes, leading to new materials. Nonetheless, the applicability of the already established toolbox of post-polymerization modifications for sterically demanding precursor polymers derived from C1 polymerization is unknown.

This thesis demonstrates various approaches for the post-modification of functional polymethylenes. Various functional polymethylenes bearing benzyl, allyl, propargyl and glycidyl esters as side groups were prepared and characterized. Subsequently, successful post-polymerization modifications by ester cleavage, thiol-ene, azide-alkyne and ring-opening reactions are presented. Conformities and differences with the structural analog acrylate or methacrylate structures of the functional polymethylenes are revealed and discussed. Furthermore, a functional polymethylene-macroinitiator for a subsequent atom transfer radical polymerization (ATRP) was prepared and is discussed.

All of the presented and examined studies emphasize C1 polymerization in combination with the toolbox of post-polymerization modification as a highly promising approach towards the synthesis of a large variety of densely functionalized polymeric materials.

Zusammenfassung

Polyolefine haben sich im Laufe der Zeit zu einer der wichtigsten Polymerklassen entwickelt, jedoch stellt es noch immer ein großes Problem dar, Polyolefine mit einer hohen Dichte an funktionellen Seitengruppen zu synthetisieren. Die Rhodium vermittelte C1 Polymerisation ermöglicht die Synthese von funktionellen Polymethylenen mit einer (polaren) funktionellen Gruppe an jedem Kohlenstoffatom der Hauptkette. Aktuell ist diese neue Polymerisationsvariante noch nicht ausreichend hinsichtlich ihrer vollständigen Monomertragweite erforscht. Eine Möglichkeit, die Produktpalette dieser Polymerklasse zu erweitern, ist die Verwendung von polymeranalogen Reaktionen (engl.: *post-polymerization modification*). Die verfügbare Vielfalt an möglichen, hoch effizienten Modifikationen könnte eine vielversprechende Alternative zur Darstellung verschiedenster funktioneller Polymethylene sein.

Die vorliegende Dissertation demonstriert die Möglichkeit, unterschiedliche polymeranaloge Reaktionen an funktionellen Polymethylenen durchzuführen. Hierfür wurden unterschiedliche funktionelle Polymethylene mit Benzyl, Allyl, Propargyl und Glycidylestern synthetisiert. Anschließend wurden polymeranaloge Reaktionen an diesen Prekursorpolymeren durchgeführt, dazu zählen Substitutionsreaktionen an Estern, Thiol-en Reaktionen, Azid-Alkin-Cycloadditionen und ringöffnende Additionsreaktionen. Die generelle Übertragbarkeit von polymeranalogen Reaktionsbedingungen, die ursprünglich für Polymere mit geringerer Seitengruppendichte entwickelt wurden, auf funktionelle Polymethylene wird erfolgreich demonstriert. Zudem werden Übereinstimmungen und Unterschiede zwischen den strukturell analogen C1 und C2 Polymeren aufgezeigt und diskutiert. Weiterhin wurde ein Makroinitiator mit dem Grundgerüst eines Polymethylens synthetisiert und ist Teil der Diskussion der vorliegenden Arbeit. Alle präsentierten Forschungsergebnisse empfehlen die Verwendung von C1 Polymerisationen in Kombination mit den vielen Möglichkeiten der polymeranalogen Modifikationen hinsichtlich eines erfolgversprechenden Ansatzes zur Synthese einer Vielfalt von hochfunktionalisierten Polymermaterialien.

1. Theory and Introduction

Polymer materials are ubiquitously used in our daily life, e.g. for packaging, electronics and construction. Ever since Staudinger,[1] who was later awarded the Nobel Prize in Chemistry (1953), devised the term "macromolecules", the rapid development of polymers, that kept momentum throughout the last century, started. In many cases, polymers are irreplaceable by conventional materials, such as wood or metal. Especially their unexcelled utilization in high tech applications, such as sensors,[2] optoelectronics[3] (e.g. OLEDs) and biohybrids,[4] is a key driving force for polymer research, one of the most vibrant fields of contemporary science. The reason why polymers are indispensable for many applications is that they cover a broad range of designable properties. Owing to the robust polymerization conditions and broad monomer scope, free radical polymerization is by far the most prevalent polymerization technique utilized by the chemical industry. However, high tech applications, being one of the key driving forces for present polymer research, require a distinct control of the final polymer properties. A major contribution to the final properties originates from the chosen monomer species and its functionalities as well as the density of functional groups along a polymer chain, largely affecting the physical parameters and chemical reactivity of a polymer. Toughness, surface properties, rheological properties, adhesion and miscibility with other polymers are some of the polymer characteristics that are affected by functionalities.[5] Additional influences originate from the polymerization technique, e.g. free radical polymerization (FRP) or reversible-deactivation radical polymerization (RDRP). The polymerization techniques are important factors determining the molecular weight distribution and dispersity as well as the tacticity of a polymer.

In conclusion, the final polymer characteristics are determined and connected by many individual parameters. Numberless research efforts target the development of novel polymers and polymerization techniques as well as the improvement of already existing techniques.

1.1. Polyolefins - The Predominant Industrial Polymers

Up to date, industrial polymers are mostly based on the polymerization of vinyl compounds. Their present C=C double bonds allow for facile polymerization by conventional techniques, either via radical polymerization concepts, ionic polymerization (cationic or anionic) or transition-metal mediated polymerization. Out of the multiplicity of polyolefins prepared from a vinyl monomer feedstock, polyethylene is by far the most prevailing commercial polymer. The chain-growth polymerization of polyethylene or its

functional derivatives proceeds via the addition of two carbon atoms per growing step (C2 polymerization). Without doubt, FRP of vinyl compounds is the most widely used conventional polymerization technique for the industrial production of high-molecular weight polymers.[6] It can be utilized for the polymerization of a wide range of monomers due to its tolerance towards a large variety of functional groups and reaction conditions. Furthermore, FRPs are relatively easy to perform. The initial step, called "initiation" during which radicals capable to propagate are formed, often involves the thermally or photochemically induced homolytic bond cleavage of a radical initiator and addition of this radical initiator to one monomer unit. Subsequently, the chain grows up to a certain polymerization degree until all monomer is consumend or the chain is terminated. FRP is, in an ideal case, solely terminated via radical combination or disproportionation events between two growing chains.
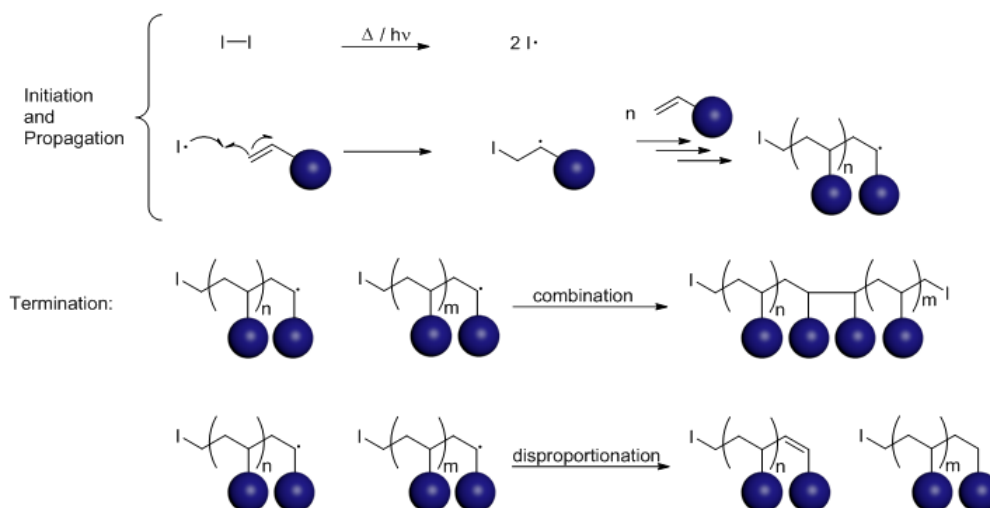

Scheme 1.1.: C2 polymerization utilizing vinyl compounds. This polymerization concept leads to the formation of polyolefins, also called functional polyethylenes.

Notably, conventional polymerization techniques are often suffering from limitations originating from multiple (polar) functionalities on monomer C=C double bonds.[7,8] For instance, it is possible to convert methyl methacrylate (MMA) via radical homopolymerization to poly(methyl methacrylate) (Plexiglas®, PMMA) or methacrylic acid to poly(methacrylic acid) (Eudragit®); however, the homopolymerizaton of maleic anhydride via classical approaches is not facile or remains even impossible (Scheme 1.2).* Furthermore, transition-metal catalyzed polymerizations of polar functional vinyl compounds are often subject to catalyst poisoning.[8,10] In order to cope with limitations by conventional polymerization techniques, regarding highly (polar) functionalized monomers, novel promising research approaches are aiming at different monomer

---

*There is one exception, *Müllen* and co-workers reported the feasibility of this route to synthesize poly(methylene amine). They were utilizing 1,3-diacetyl-4-imidazolin-2-one as a monomer, and for the first time, successfully synthesized a polymer bearing an amino group at each carbon atom of the polymer backbone.[9]

sources or alternative concepts such as post-polymerization modification.
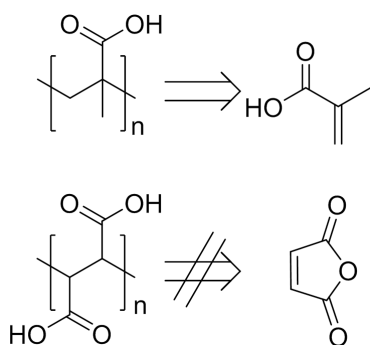
Scheme 1.2.: Illustration of the limitations for C2 polymerizations in terms of multiple functional groups attached to the double bond. Radical polymerization of methacrylic acid is possible; however, hompolymerization of maleic anhydride remains impossible.

## 1.2. Functional Polymethylenes via C1 Polymerization

Polymethylenes are structural equivalents of polyethylenes. In the case of C1 polymerization, they are built by one carbon atom per growing step of the backbone. The first C1 polymerization reported is the thermal decomposition (explosion) of diazomethane in 1898 resulting in polymethylene, the structural analog to polyethylene, and it is, thereby, also the very first report of polyethylene formation.[11] However, it took a century until synthetically practical and safe concepts for C1 polymerization of carbene precursors were developed. Novel C1 polymerization (also termed "polyhomologation",[12] "poly(substituted) methylene synthesis"[13] or "carbene (insertion) polymerization"[14]) is an alternative approach towards highly functionalized polymethylenes (refer to reviews[8,10,15]). In these approaches, Lewis acids as well as transition-metals (TM) are utilized, the latter ones are capable of mediating a carbene insertion into TM-C bonds, thereby forming polymethylenes. Most commonly, sulfoxonium ylides and diazo compounds are utilized as carbene precursors and monomer source (Scheme 1.3).
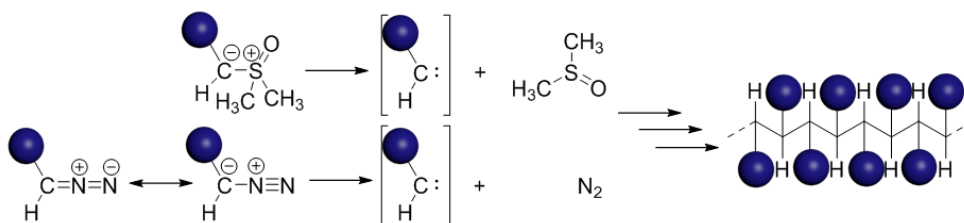
Scheme 1.3.: C1 polymerization utilizing carbene precursors such as sulfoxonium ylides or diazo compounds. This polymerization concept leads to the formation of functional polymethylenes.

1.2.1. C1 Polymerization - Boron Mediated

Shea and co-workers developed one kind of C1 polymerization. They utilized boron moieties (Lewis acids) as mediators for living C1 polymerization of sulfoxonium ylides since 1997 (Scheme 1.4).[12] Their approach results in good yields up to 85-95%, narrow molecular weight distributions (Đ = 1.01-1.20) and high molecular weights up to 500 kDa.[8,16] Furthermore, to this day, a lot of different topologies, such as three-arm star polymers, cyclic structures and giant tubelike structures were synthesized via boron mediated C1 polymerization.[16,17] Initially, this approach was inspired by the homologation of organoborane structures to oligomers reported by *Tufariello* and *Lee* already in 1966.[18,19]
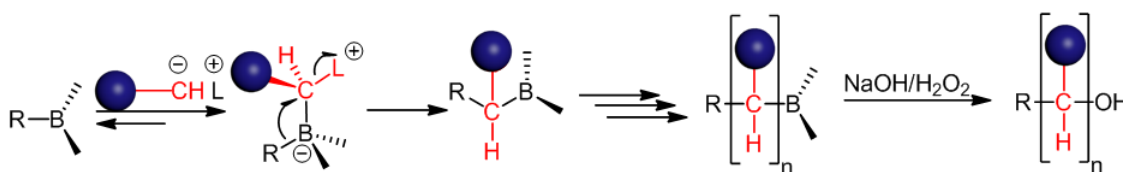
Scheme 1.4.: The mechansim of boron mediated C1 polymerization. Adapted from reference[16] .

The mechanism involves the addition of ylide to the boron moiety with subsequent 1,2-migration insertion as well as cleavage of the ligand (L) as by-product of the reaction. In case of sulfoxonium ylides, the ligand L equals dimethylsulfoxide (DMSO). In this way, the Lewis acid is regenerated and further chain growth can occur. The growth proceeds until the excess of ylide is consumed. Afterwards, the formed polyorganoborane can be cleaved with suitable nucleophiles at the boron center. In this way, up to three identical linear, atactic polymer chains can be formed. The topology can be altered via the chosen boron mediator as well as via alteration of the cleaving nucleophile. One major drawback of this polymeirzation is the difficult synthesis of suitable polar functional monomers.[20]

1.2.2. C1 Polymerization - Transition-Metal Mediated

In the earliest reports around 1900, especially, gold[21] and copper[22,23] catalysts were investigated for C1 polymerization of diazo alkanes as carbene precursors. Further reports described the use of many other heterogeneous and homogeneous metal catalysts for C1 polymerization of diazo alkanes as summarized in a recent review by *de Bruin* and co-workers.[10] However, the synthesis of functional polymethylenes via the utilization of polar functional diazo compounds is much more challenging due to their increased stability. The very first examples of a successful transition-metal (TM) catalyzed C1 polymerization utilizing α-diazocarbonyl compounds were almost

simultaneously reported by the groups of *Liu*[14] (copper promoted C1 polymerization of allyl 2-diazoacetate) and *Ihara*[24] (palladium promoted C1 polymerization of alkyl 2-diazoacetates). Amongs the multitude of possible C1 polymerization concepts, two concepts for the conversion of α-diazocarbonyl compounds stand out. Presently, the best performing transition-metal catalysts for the C1 polymerization of α-diazocarbonyl compounds are based on palladium[13,25–29] and rhodium.[30–32]

1.2.2.1. Palladium Mediated C1 Polymerization

Palladium-catalyzed C1 polymerization was almost exclusively developed by *Ihara* and co-workers. Mainly Pd^{II}- catalytic species are utilized, resulting in atactic functional polymethylenes.[24,25] Furthermore, a large variety of polymethylenes bearing ester or acyl functionalities as side groups are accessible via this approach. For example, functional polymethylenes bearing OH groups and oxyethylene chains at each main chain carbon atom were reported.[13,29] In certain cases, as for example for the synthesis of poly(acylmethylene)s, the undesired incorporation of azo functionalities in the backbone was reported.[25] Some studies highlight the possibility to polymerize even monomers with bulky substituents, such as cholesteryl 2-diazoacetate (ChDA) (Scheme 1.5).[28,33]
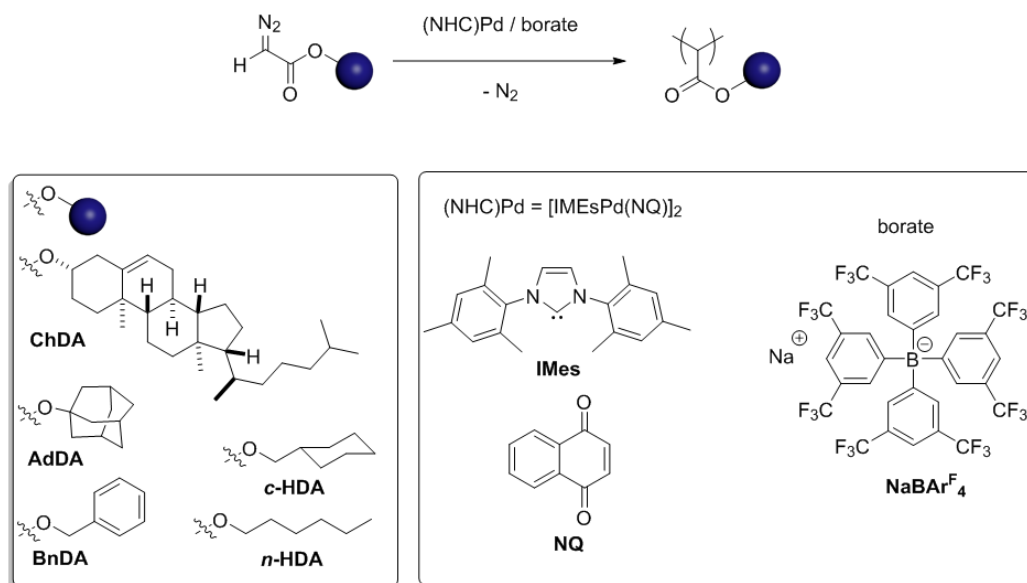
Scheme 1.5.: The illustration shows the palladium catalyzed C1 polymerization with (NHC)Pd/borate as catalytic system and various diazoacetates as monomers.

Other reported diazoacetate-monomers include adamantyl 2-diazoacetate (AdDA), cyclohexyl 2-diazoacetate (*c*-HDA), n-hexyl 2-diazoacetate (*n*-HDA) and benzyl 2-diazoacetate (BnDA). The authors utilized a palladium catalyst for the C1 polymerizations with *N*-heterocyclic carbenes (NHC) as ligand in conjunction with borate

as co-catalyst (i.e. (NHC)Pd/borate); borate = tetraarylborate (NaBAr$_4$)). The proposed active catalytic species is generated by the oxidation of (NHC)Pd^{0}to the cationic [(NHC)Pd^{II}H]$^+$species via reaction with the borate NaBAr$^F_4$.[27] With the depicted catalytic system in Scheme 1.5, a polymer poly(cholesteryl 2-ylidene-acetate) with a number average molecular weight of M$_n$ = 18900 g mol^{-1} and a dispersity of Đ = 1.34 was obtained. Recently, *Ihara* and co-workers also reported the first example of transition-metal (i.e. palladium) mediated C1 polymerization of diazoacetates resulting in a narrow molecular weight distribution.[34]Up to date, this is the first report on controlled C1 polymerization of diazocarbonyl compounds to yield narrow molecular weight distributions.

1.2.2.2. Rhodium Mediated C1 Polymerization

Homogeneous rhodium-mediated C1 polymerization (Scheme 1.6) has been invented by a joint effort of *Reek* and co-workers and *de Bruin* and co-workers and was reported for the first time in 2006.[30]
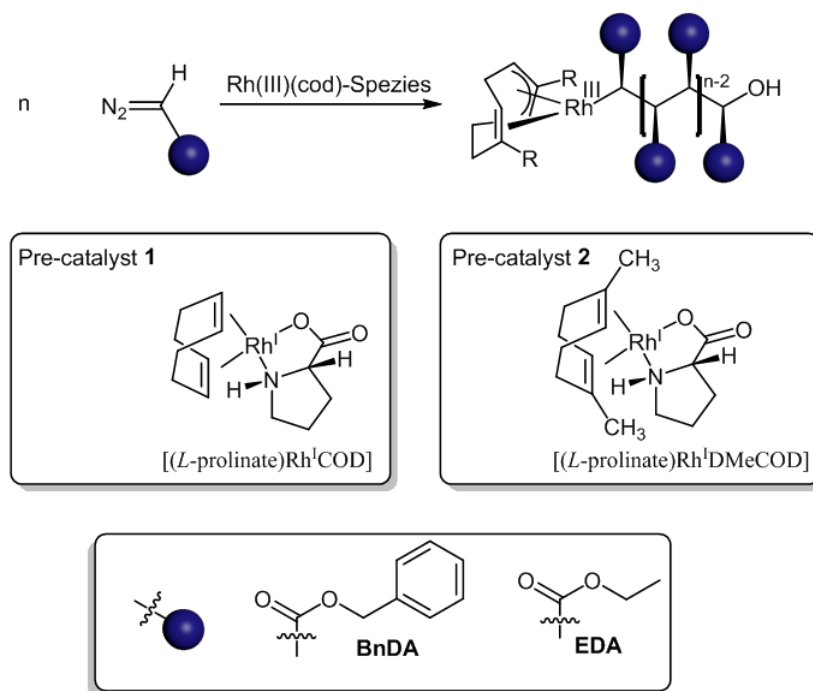

Scheme 1.6.: C1 polymerization of diazo compounds via rhodium catalysis, resulting in syndiotactic functional polymethylenes. Two commonly employed pre-catalysts are illustrated, namely [(*L*-prolinate)Rh^I(1,5-cyclooctadiene)] ([(*L*-prolinate)Rh^I(COD)] and [(*L*-prolinate)Rh^I(1,5-dimethyl-1,5-cyclooctadiene)] ([(*L*-prolinate)Rh^I(DMeCOD)]. Most studies on rhodium mediated C1 polymerization utilize benzyl 2-diazoacetate (BnDA) and ethyl 2-diazoacetate (EDA) as monomers.

The utilization of rhodium catalysts [(*N,O*-ligand)Rh^I(diene)], compared to other TM-

catalysts, resulted by far in the highest molecular weights (M_w up to 540 kDa) and polymers were obtained in good yields (up to 95 %).[35] However, the polymerization results in large dispersities in contrast to the boron mediated living polymerization. Furthermore, the polymer yield and molecular weight is strongly dependent on the employed catalytic system and the monomer species. In addition to the formation of high molecular weight polymethylenes, low molecular weight oligomers and di- and trimers are formed. The obtained functional polymethylenes are highly interesting due to their stereoregularity (syndiotactic polymethylenes) in combination with densely packed functional side groups.[36] This stereoregularity can be oversved by the very sharp signals in solution NMR spectra. As a consequence of the stereoregularity, several of the functionalized and highly crystalline polymethylenes show liquid crystallinity.[37] The liquid crystallinity originates from the polymers self-assembly into higher-order aggregates, i.e. poly(ethyl 2-ylidene-acetate) assembles into a triple-helical supramolecular structure, leading to rod-like behavior. The majority of reported studies utilized rhodium(I) precatalysts consisting of *L*-prolinate as *N,O*-ligand and commercially available 1,5-cyclooctadiene (COD) or 1,5-dimethyl-1,5-cyclooctadiene (DMeCOD) as diene ligands (Scheme 1.6). The *N,O*-ligand does not show a significant influence on the polymerization, thus it is assumed that it is cleaved of in the initial steps and solely influences slightly the kinetics of initiation.[30] Furthermore, the initial Rh[I](diene) catalyst is oxidized to a Rh[III](diene) species in a multistep activation process. Afterwards, C1 polymerization via rhodium catalysis follows a migratory carbene insertion mechanism.[35,38–43] The fundamental migration insertion mechanism is depicted in Scheme 1.7, with the rate limiting step (elimination of nitrogen) being highlighted in green.
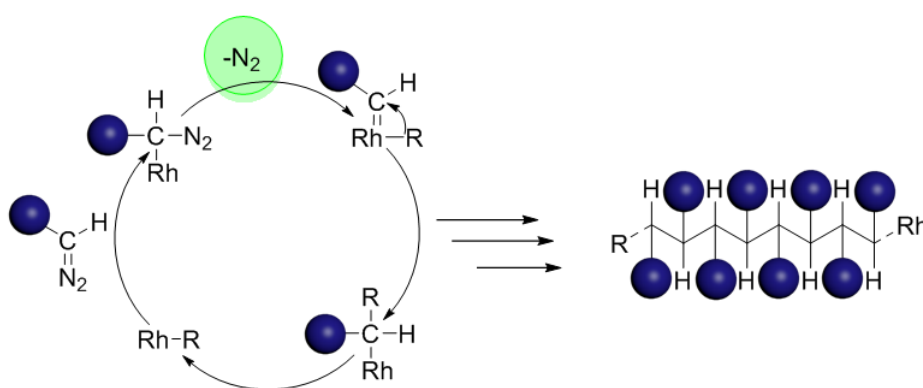

Scheme 1.7.: The basic insertion migration mechansim of rhodium mediated C1 polymerization. Adapted from reference.[43]

1.2.2.3. Kinetic Studies of Transition-Metal Mediated C1 Polymerizations

Previous research targeted kinetic studies of C1 polymerizations utilizing ethyl 2-diazoacetate as monomer. Widely varied polymerization rates were reported by utilization of N_2-gas formation measurement.[40] Full monomer conversion was observed in the range of minutes and up to 10 hours, depending on the catalyst selection. Greater details were revealed by the utilization of *real-time in situ* FT-IR spectroscopic measurements.[44] Because a first-order kinetics for the polymerization of ethyl 2-diazoacetate with [(*L*-prolinate)Rh^I(1,5-cyclooctadiene)] and [(*L*-prolinate)Rh^I(2,5-norbornadiene)] was found, the authors suggested the formation of Rh-carbenoid species as the rate-determining step of this polymerization. Also, palladium catalysts, such as *bis*(acetonitrile)-dichloropalladium, palladium acetate and and palladium chloride were utilized and identified as zero-order reactions. The rate determining step for palladium catalyzed C1 polymerization of ethyl 2-diazoacetate was identified as the formation of a monomer-palladium transition state complex by coordination.

1.2.3. Diazocarbonyl Compounds - Safe Carbene Precursors

Theodor Curtius was the first to discover diazocarbonyl compounds in 1883, marking the point of origin for the rapid development of this vast field of organic chemistry by reporting the synthesis of ethyl diazoacetate.[45] Well-known diazo reactions include their utilization as carbene precursors, e.g. in the *Wolff* Rearrangement, to yield carboxylic acid derivatives.[46,47] Diazocarbonyl compounds are more stable - and thus safer - compared to aliphatic diazo compounds, hence, they are frequently used as a carbene source in organic chemistry.[48] The reason for their increased stability can be explained by the formation of a delocalized π-electron system with the carbonyl group as illustrated by the mesomeric stabilization in Scheme 1.8.
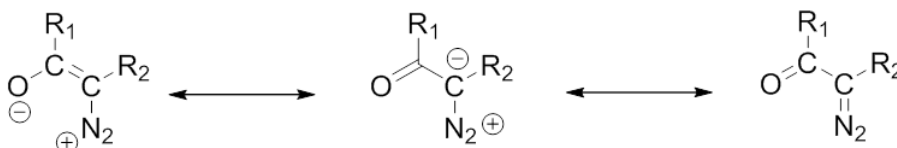

Scheme 1.8.: The increased stability of diazocarbonyl compounds compared to aliphatic diazo compounds explained by mesomeric structures.

Numerous synthetic methodologies were developed to synthesize diazocarbonyl compounds and two recently described facile synthetic procedures towards the synthesis of diazo acetates are depicted in Scheme 1.9.[49,50] Synthesis of α-diazocarbonyl compounds generally starts from the respective alcohol. This alcohol can then be converted with bromoacetyl bromide, as shown in Scheme 1.9A and subsequently be transformed by

N,N-ditosylhydrazine as precursor to the diazo group. The overall process benefits from its mild reaction conditions and good yields.
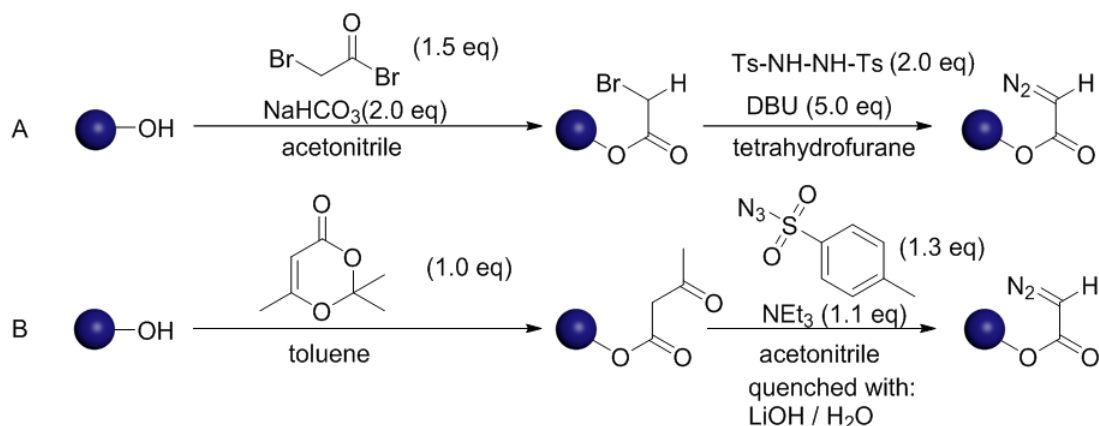
Scheme 1.9.: Two synthetic approaches (A & B) are shown leading to α-diazocarbonyl compounds.[49,50]

The second illustrated synthesis (Scheme 1.9B), proceeds via initial reaction of the alcohol with 2,2,6-trimethyl-4H-1,3-dioxin-4-one (precursor for the reactive acetyl ketene) to afford the β-keto ester. Subsequently, a diazo transfer reaction utilizing tosyl azide results in the targeted α-diazocarbonyl compound. The synthesis requires rather harsh reaction conditions compared to the previously described method **A** but requires less synthetic work.
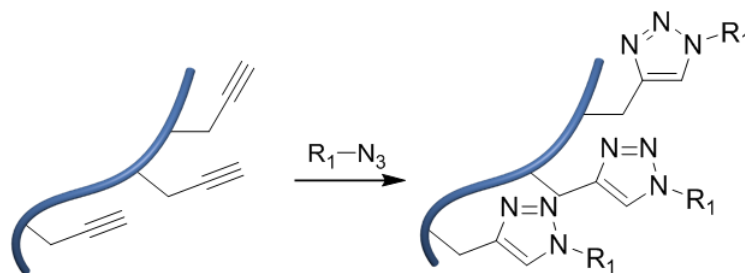
1.3. Post-Polymerization Modification - One Way to Introduce Functionality

In many cases, it remains impossible or at least highly challenging to synthesize and/or polymerize (polar) functional monomers, as, for example, stated above for homopolymerization of maleic anhydride. Hence, the polymer community searched for alternative pathways to overcome these limitations, and, thereby, make the desired polymer structures accessible. The concept of C1 polymerization has been summarized above and is one approach to achieve novel desired structures by utilization of a new monomer class and a new polymerization technique. Other approaches focus on the modification of previously synthesized monomers. Among the multitude of possible strategies, post-polymerization modification (*Staudinger*[1] initially devised the term "*polymer analogous reaction*") evolved as an important concept for altering the functionalities of an existing precursor polymer. Thus, post-polymerization modification has the tremendous benefit to change the functionalities, and thus, the properties, of a polymer without changing the degree of polymerization. In particular, it is possible to

synthesize a reactive precursor polymer from a single reactive monomer. Subsequently, this polymeric precursor can be altered with ease and can lead to a vast diversification in the chemical structure of the polymer. Among the numerous reported approaches for post-polymerization modification, there are a few techniques resulting in quantitative and selective conversions at moderate conditions.[51,52]

1.3.1. Huisgen 1,3-Dipolar Cycloaddition

This reaction of azides with alkynes is named after the pioneering chemist *Rolf Huisgen*, who initially noticed the of scope of these reactions.[53] Later, with the designated concept of click-chemistry*[51]*, it had a renaissance and is frequently utilized as the copper(I) catalyzed variant also referred to as copper(I)-catalyzed Azide-Alkyne Cycloaddition (CuAAC). One of the great advantages of azide-alkyne coupling reactions is their orthogonality to many functional groups, including amines, alcohols, and esters. Furthermore, CuAAC can even be performed in aqueous media (Scheme 1.10).[54]

Scheme 1.10.: Post-polymerization modification of polymers bearing glycidyl side groups with various nucleophiles.

Azide-alkyne reactions for post-polymerization modification can be conducted via a precursor polymer bearing either an azide functionality or a terminal alkyne.[55] For example poly(propargyl methacrylate)[56] or poly(3-azidopropyl methacrylate)[57] can be utilized as starting materials.
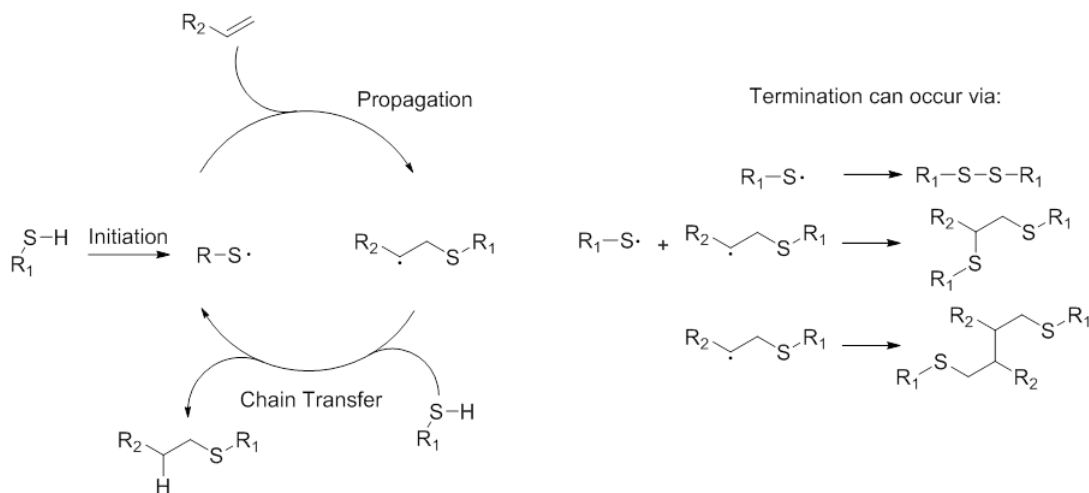
1.3.2. Thiol-Ene Reactions

The concept of thiol-ene chemistry was initially started by the observation of *Posner* in 1905, reporting the reaction of mercaptanes (thiols) with unsaturated C=C bonds via addition.[58] Subsequently, thiol-ene modifications were mainly utilized in organic chemistry, and it took almost a century (early 2000s) until their true potential for post-polymerization modification was recognized.[59]

In general, the ligation via thiol-ene reactions can commence via either a radical pathway[60] or a nucleophilic addition to the double bond. In case of activated double

bonds, it is also called "thiol-Michael" addition.[61] The proposed mechanism[59] for the versatile radical thiol-ene reaction is depicted in Scheme 1.11.

Scheme 1.11.: Reaction mechanism of a radical thiol-ene reaction.

The radical mechanism involves homolytic bond cleavage of the S-H bond by either thermal or photochemical activation e.g. utilizing radical initiators such as azobisisobutyronitrile (AIBN) or dimethoxy-2-phenylacetophenone (DMPA). Subsequently, the reactive thiyl radical adds to an unsaturated bond (propagation) and the usually observed anti-Markovnikov product is obtained after hydrogen transfer from free thiols (chain transfer). However, other termination events can occur as well and refer to the combination of two radical species. Furthermore, intramolecular cyclization was reported for thiol-ene post-modified polymers, such as 1,2-polybutadienes (Scheme 1.12).[62]
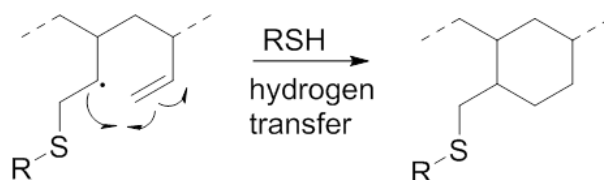

Scheme 1.12.: This illustration shows intramolecular ring-closure, as partially observed for thiol-ene post-polymerization modification of 1,2-polybutadienes.

This undesired ring-closure was prevented by increasing of the distance between the intermediately formed radical and the adjacent double bond.[63]
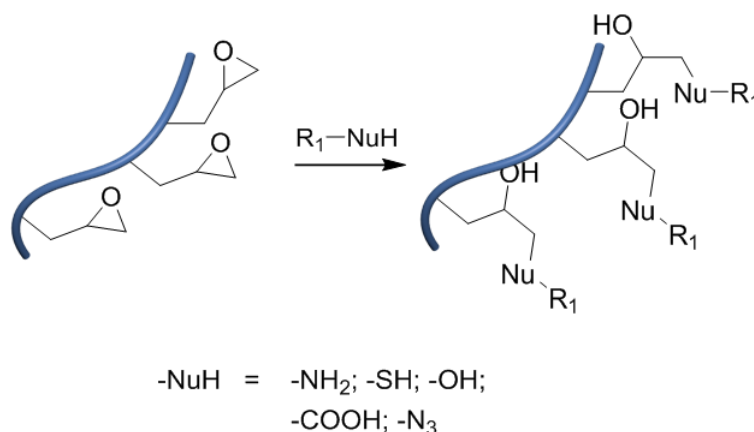
1.3.3. Epoxide Ring-Opening Reactions

The impact of epoxides (oxiranes) on polymer chemistry originates from an inherent high reactivity due to the strained three-membered ring.[51,64] Hence, epoxides can be easily polymerized via different approaches, such as cationic[65] or anionic[66,67] ring-opening polymerization. For example, ethoxy ethyl glycidyl ether (EEGE) the protected version

of glycidol can be polymerized via anionic ring opening polymerization as shown in Scheme 1.13.
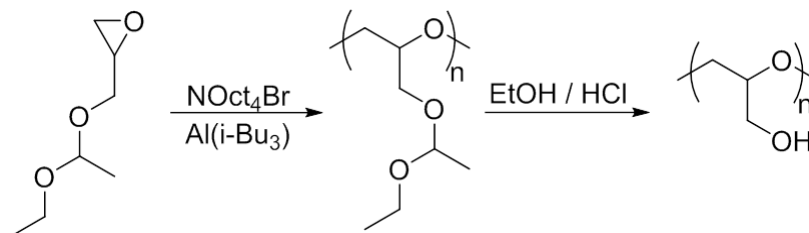
Scheme 1.13.: Anionic ring-opening polymerization of ethoxy ethyl glycidyl ether (EEGE) using a catalytic system consisting of triisobutylaluminum (Al(i-Bu$_3$)) and tetraoctylammonium bromide (NOct$_4$Br).

In order to utilize the oxirane group for post-polymerization modification, suitable polymers with side group containing oxirane moieties need to be prepared (Scheme 1.14). Poly(glycidyl methacrylate) can be easily prepared by FRP and is a commonly selected precursor polymer with side group oxirane moieties.[68]

Scheme 1.14.: Post-polymerization modification of polymers bearing glycidyl side groups with various nucleophiles.

Ring-opening reactions of the reactive side groups can easily occur with many different nucleophiles, such as amines, thiols, alcohols, acids or azides. If weak nucleophiles are utilized, the ring-opening to occur requires the addition of an auxiliary base. The nucleophilic attack usually takes place at the less substituted carbon of the epoxide moiety.

1.3.4. Amidations and Transesterifications

Amidations and transesterifications have been known for a very long time in organic synthesis. However, these reactions usually require rather harsh conditions if the ester is non-reactive, i.e. it does not consist of an electron withdrawing moiety weakening

the ester bond. In 1972, the synthesis of activated ester polymers as precursors for post-polymerization modifications was independently reported by the groups of *Ferruti*[69] and *Ringsdorf*.[70] Some of the mainly used active esters are based on *N*-hydroxysuccinimide,[71] pentafluorophenol,[72] 4-nitrophenol[73] or acetone oxime[74] (Scheme 1.15).
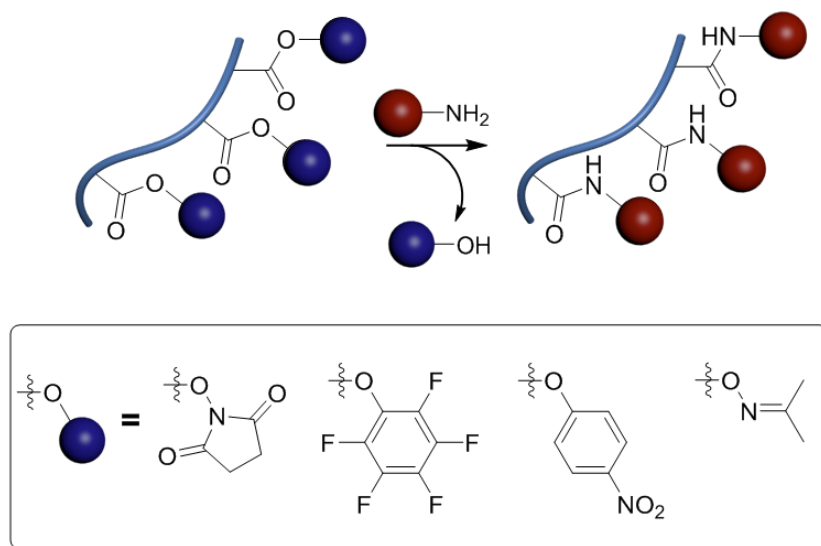
Scheme 1.15.: Amidation of polymers bearing active ester moieties.

These ester moieties can be easily cleaved, requiring only moderate reaction conditions for quantitative conversion and can be regarded as click-chemistry as they fulfill many of the prerequisites, yet not all.

Non-activated ester can be modified utilizing elevated temperatures and/or by the addition of suitable catalysts or bases. One example, initially reported by *Yang* and *Birman*[75] for organic synthesis, was recently transferred by *Theato* and co-workers to the functionalization of stable polymethacrylates (Scheme 1.16).[76]
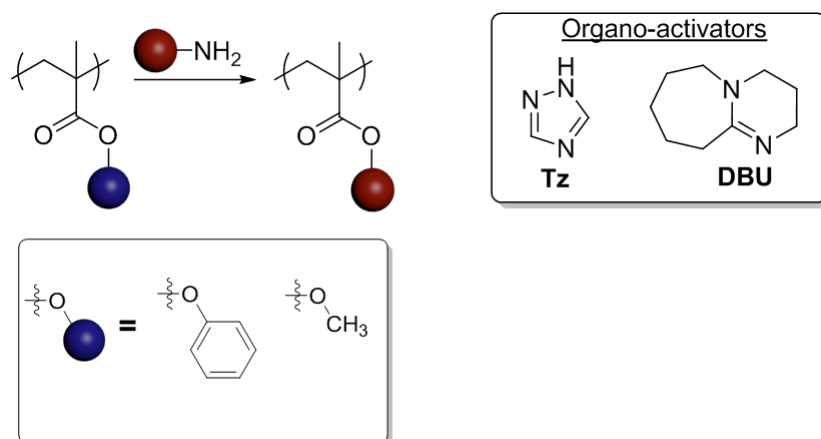
Scheme 1.16.: Organo catalytic amidation of polymers bearing stable ester moieties.

1. Theory and Introduction

It demonstrates the acyl-transfer catalysis of polyacrylates. The reaction involves the utilization of organo-activating agents 1,8-diazabicyclo [5.4.0]undec-7-ene (DBU) and 1,2,4-triazole (Tz) in a 1:3 ratio as well as elevated temperatures (120 °C) for high conversion, i.e. >99% for poly(phenyl methacrylate) (PPhMA) and >70% for poly(methyl methacrylate) (PMMA).

2. Concept and Motivation

Conventional polymerizations (C2 polymerizations) of vinyl compounds are often limited if more than one polar functional group is attached to the monomers C=C double bond. In contrast, the latest attempts in C1 polymerization of carbene precursors via Lewis acid or transition-metal catalysis offer a good access to functional polymethylenes. However, the monomer scope is still rather limited or remains uncertain as polar functional groups exhibit tremendous influence on the polymerization (e.g. on yield, molecular weight and dispersity). The concept of post-polymerization modification can be regarded as the method of choice to cope with these limitations and tremendously broaden the accessibility of polymethylene functionalities. The critical parameter that limits the ligation chemistry of functional polymethylenes compared to polyolefins, is their inherent high functional side group density.

This project aims at elucidating the influence of polymer side group density on post-polymerization modification. Especially intriguing is a direct comparison of the post-modified functional polymethylenes with the respective structural analogous polyolefins, utilizing the same reaction conditions for post-polymerization modification. It is commonly acknowledged and known for decades that side groups tremendously influence final polymer properties.[5] In addition, some studies reported that the side group density of polymers impacts the final polymer properties,[77] and influences on post-polymerization modification were noted as well, with regard to the side group density.[63] However, a detailed study on the influence of densely packed side groups, as apparent for functional polymethylenes, on post-polymerization modification has never been reported.

In a first step, appropriate polymethylenes bearing reactive functionalities that are accessible to post-polymerization modification have to be prepared. Suitable groups are going to be screened by selecting from the known prosperous toolbox of ligation techniques. Rhodium mediated C1 polymerization with previously reported rhodium pre-catalysts is the preferably chosen transition-metal catalyzed technique, as it allows for the highest molecular weights and a stereoregular control. Additionally, the preparation of α-diazocarbonyl compounds as monomer species is less challenging than the formation of polar functional ylide structures required for boron mediated C1 polymerization. Once the preparation of suitable functional polymethylenes is achieved, post-polymerization modification experiments and comparison with the structural analog functional polyethylenes will lead to information on the impact of side group density on post-polymerization modifications.

An in-depth study of the feasibility to transfer the existing toolbox of post-polymerization modification to functional polymethylenes is presented.

3. Results and Discussion

The following five chapters 3.1-3.5 will cover the results of my doctoral research.
The initial approach was the eludication of the general possibility to post-modify functional polymethylenes. Therfore, a known functional polymethylene was synthesized via C1 polymerization and testified for the feasibility to conduct post-polymerization modification. The next steps targeted the synthesis and utilization of suitable functional polymethylenes, enabling facile and selective post-polymerization modification.

Graphical Overview

Chapter 3.1 discusses the results of a comparative study between poly(benzyl 2-ylidene-acetate) and poly(benzyl acrylate) to elucidate the general feasibility of post-polymerization modification on functional polymethylenes (Figure 3.1).
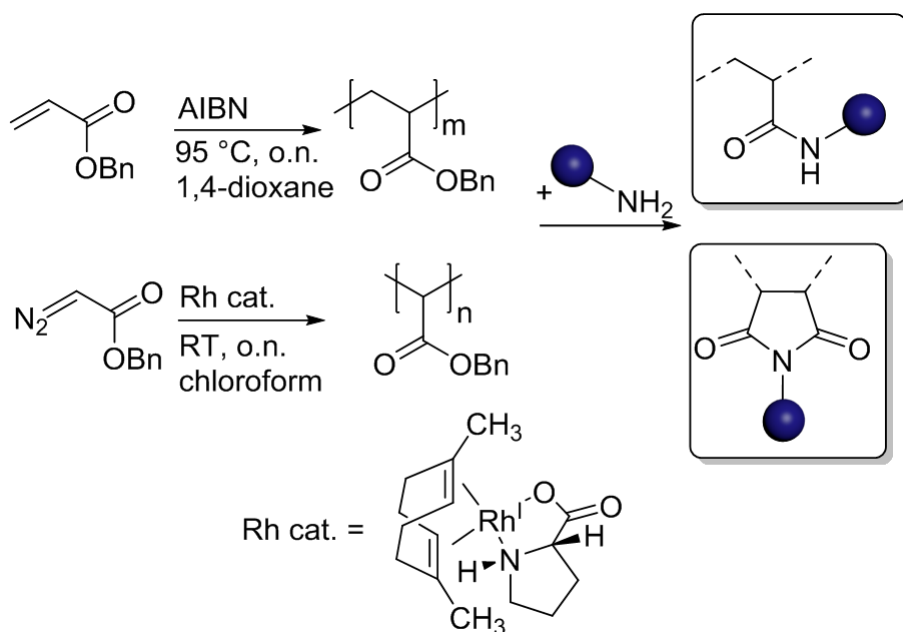
Fig. 3.1.: Graphical illustration covering the work discussed in chapter 3.1.

Chapter 3.2 discusses a first approach towards a suitable functional polymethylene for a facile post-polymerization modification. In this regard, poly(allyl 2-ylidene-acetate) was investigated (Figure 3.2).

real-time in situ FT-IR   **contact angle measurements**
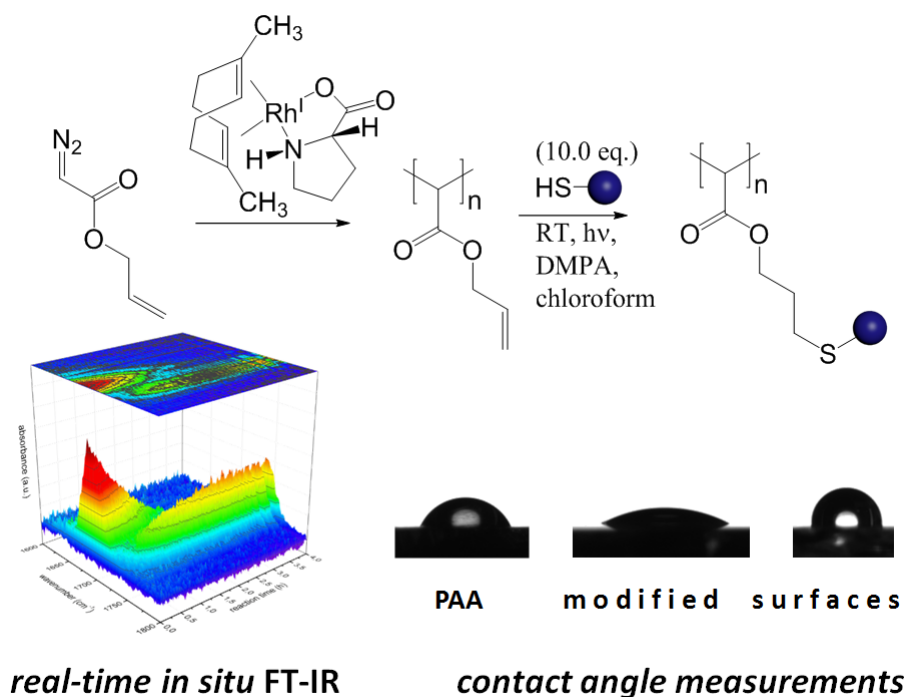
Fig. 3.2.: Graphical illustration covering the work discussed in chapter 3.2.

Chapter 3.3 highlights poly(glycidyl 2-ylidene-acetate) as the currently most versatile functional polymethylene for a facile and controlled post-polymerization modification (Figure 3.3).
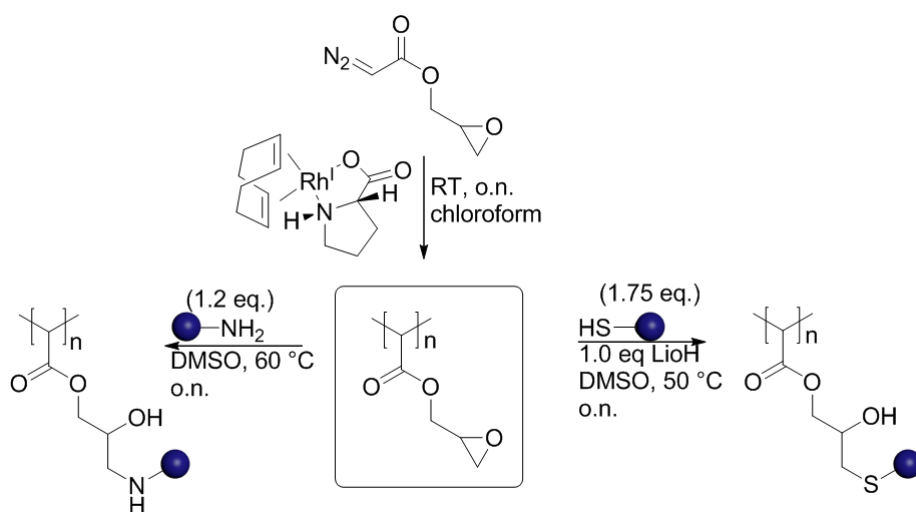
Fig. 3.3.: Graphical illustration covering the work discussed in chapter 3.3.

Chapter 3.4 is an approach towards multiple polymerizations of propargyl 2-diazoacetate (Figure 3.4).
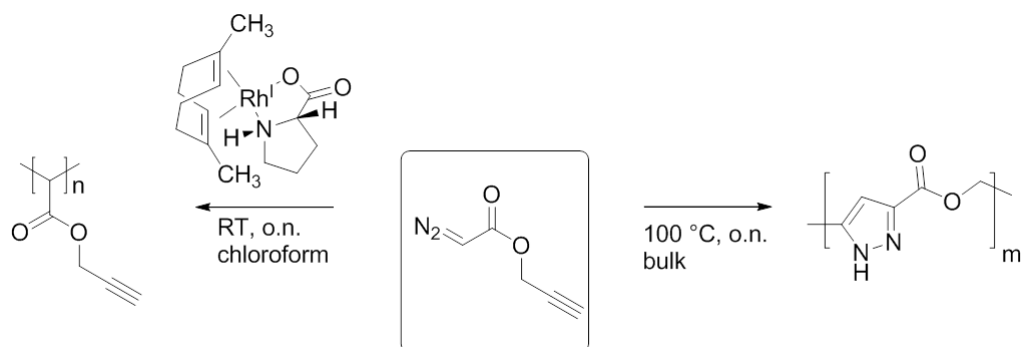
Fig. 3.4.: Graphical illustration covering the work discussed in chapter 3.4.

Chapter 3.5 enlightens the possibility to synthesize an ATRP macroinitiator with a functional polymethylene scaffold, that is suitable to initiate a copolymerization in the side groups (Figure 3.5). Thereby, bottle-brush copolymers with an extremely high grafting density were targeted.
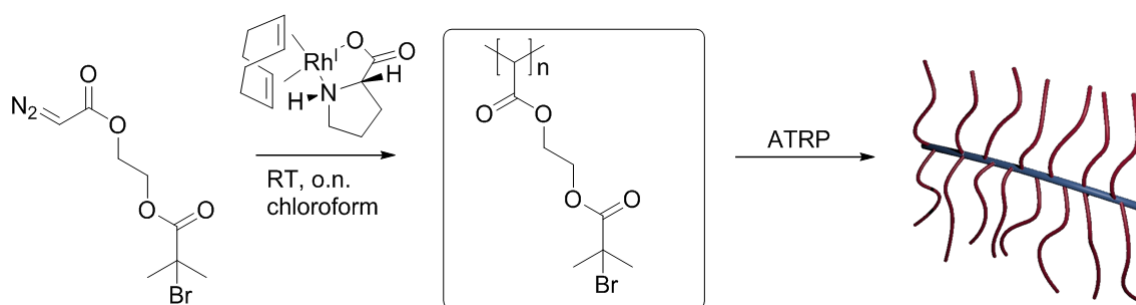
Fig. 3.5.: Graphical illustration covering the work discussed in chapter 3.5.

3.1. General Feasibility to Post-Modify Functional Polymethylenes

This chapter is partially adapted from Ref.[78] - *J. Polym. Sci. Pol. Chem.*, **2016**, 54, 686–691 - with permission from Wiley Periodicals, Inc.

The online content can be accessed by using the following URL:

`http://doi.wiley.com/10.1002/pola.27891`

3.1.1. Introduction

Poly(ethyl 2-ylidene-acetate) **PEA_C1** and poly(benzyl 2-ylidene-acetate) **PBnA_C1** are often used as a benchmark polymers to elucidate the performance of transition-metal mediated C1 polymerizations. Their synthesis is well studied, and especially rhodium mediated C1 polymerization leads to a high molecular weight. Furthermore, rhodium catalysis results in stereoregular (syndiotactic) functional polymethylenes exhibiting a highly symmetric microstructure. The high molecular weight and high crystallinity enable simple purification and facilitate the interpretation of NMR spectra due to sharp signals as a direct result of the stereoregularity. In addition, the synthesis is straightforward and requires only little synthetic effort, i.e. there is no requirement of inert conditions.[40] The synthetic handling proved to be simple compared to the atactic and highly viscous functional polymethylenes obtained by palladium mediated C1 polymerization. Thus, the rhodium mediated technique was selected to synthesize the known **PBnA_C1** for an initial study on the general possibility of post-polymerization modification of functional polymethylenes. The main aim was to find a suitable modification route to achieve a significant conversion of the initial precursor polymer. As stated in the preliminary chapter 1.3.4, stable polyacrylates were successfully modified with amines via organo catalysis utilizing a system composed of the organo activators 1,8-diazabicyclo[5.4.0]undec-7-ene (DBU) and 1,2,4-triazole (Tz).[76] Herein, I tried to transfer this concept to **PBnA_C1** and targeted the amidation with primary and secondary amines.

3.1.2. Synthesis and Characterization of Benzyl 2-diazoacetate

Benzyl 2-diazoacetate was prepared via method **B** in Scheme 1.9 and characterized by nuclear magnetic resonance (^{1}H NMR, ^{13}C NMR) and Fourier transform infrared (FT-IR) spectroscopy.

The^{1}H NMR spectrum is illustrated in Figure 3.6. The spectrum exhibits a broad small singlet signal at 4.81 ppm originating from the N_2CH group. Furthermore, the aromatic

protons give rise to a signal at 7.37 ppm and the methylene group results in a signal at 5.22 ppm.
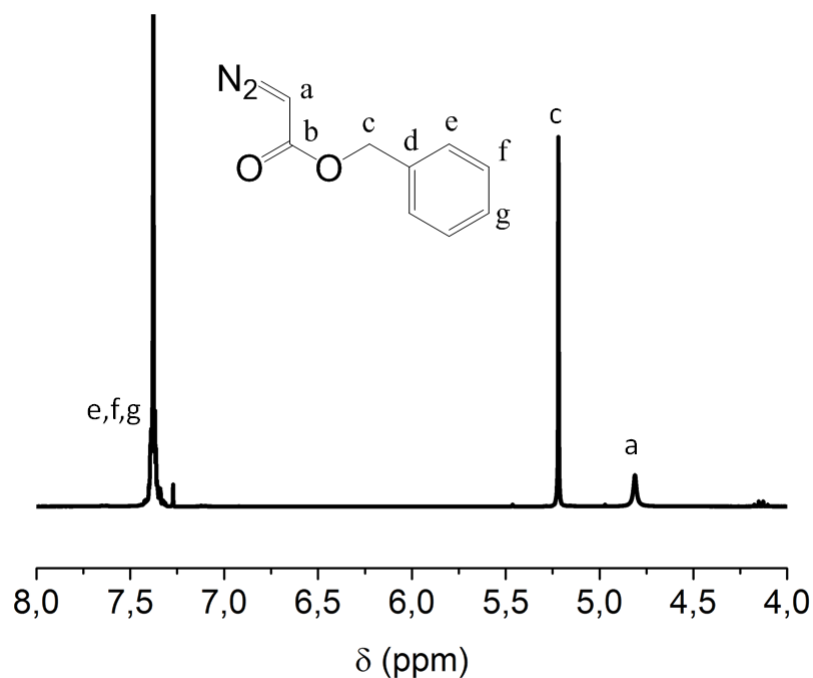

Fig. 3.6.: ^{1}H NMR spectrum of benzyl 2-diazoacetate in CDCl$_3$ (300 MHz spectrum).

The monomer was also identified in the ^{13}C NMR spectrum (Figure 3.7). Especially the backbone signal at 46.4 ppm is commonly observed in the proximity of 46 ppm for functional polymethylenes bearing ester side groups.
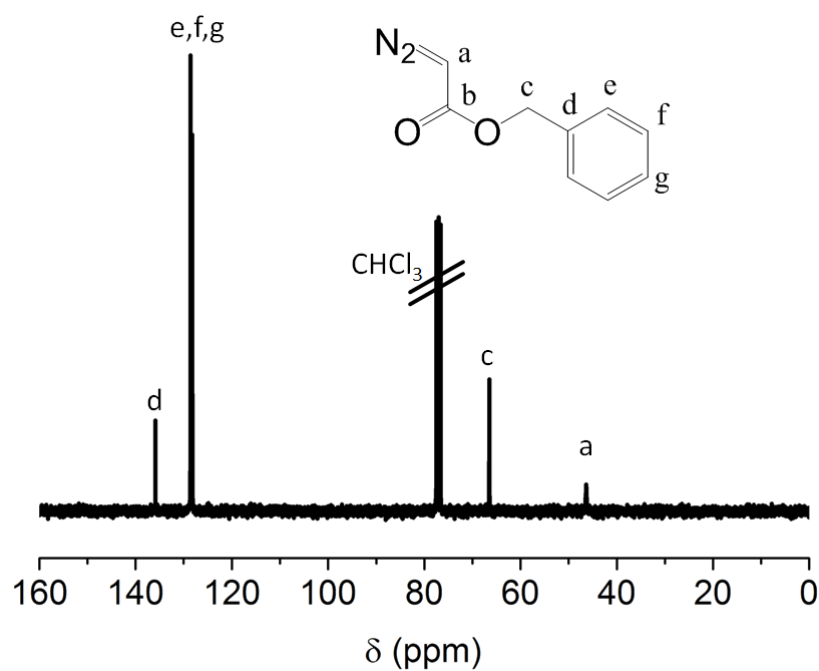

Fig. 3.7.: ^{13}C NMR spectrum of benzyl 2-diazoacetate in CDCl$_3$ (75 MHz spectrum).

Most characteristic for diazo compounds is their strong N_2 vibration band in the FT-IR spectrum (Figure 3.8). For benzyl 2-diazoacetate, the diazo group results in a strong signal at $2106\,cm^{-1}$, as well as a small signal from the C-H vibration of the N_2CH group at $3112\,cm^{-1}$.
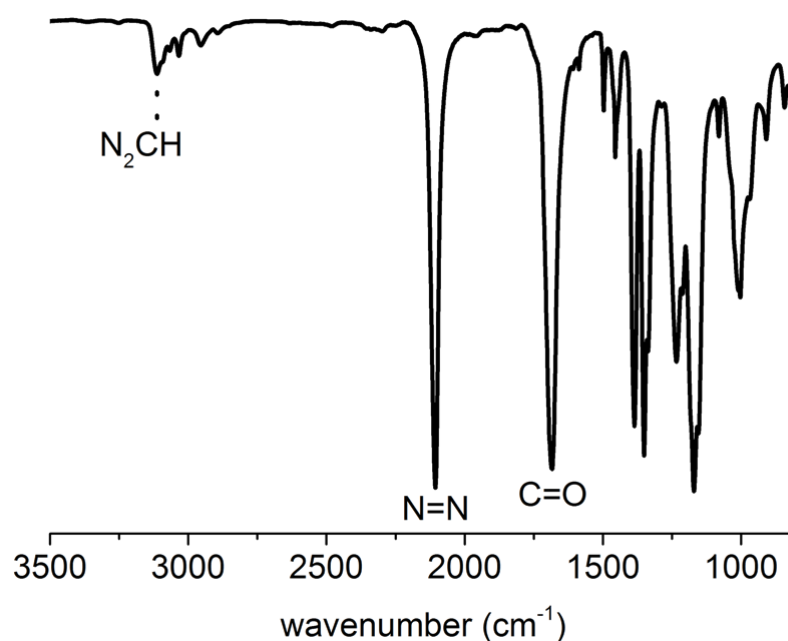
Fig. 3.8.: FT-IR spectrum of benzyl 2-diazoacetate.

3.1.3. Synthesis and Characterization of Poly(benzyl 2-ylidene-acetate) and Poly(benzyl acrylate)

In order to elucidate the general feasibility of functional polymethylene ligation chemistry, an appropriate C1 precursor polymer and a comparable, at best structural analog functional polyethylene was required. Poly(benzyl 2-ylidene-acetate) **PBnA_C1** as well as poly(benzyl acrylate) **PBnA_C2** bear benzyl ester side groups and are well investigated C1 and C2 polymers. Hence, these polymers represent ideal compounds to commence this preliminary study (Scheme 3.1). Benzyl acrylate was used for the preparation of **PBnA_C2** by FRP using AIBN as thermal initiator at 95 °C in 1,4-dioxane overnight. **PBnA_C1** was obtained by rhodium mediated C1 polymerization at room temperature, utilizing $2\,mol\%$ [(*L*-Prolinate)Rh^{I}(1,5-Dimethyl-1,5-cyclooctadiene)] as catalyst and benzyl 2-diazoacetate as monomer. The polymerization was performed overnight. The polymerization conditions were adapted from *Jellema* et. al., utilizing chloroform as solvent and performing the reaction overnight.[79]
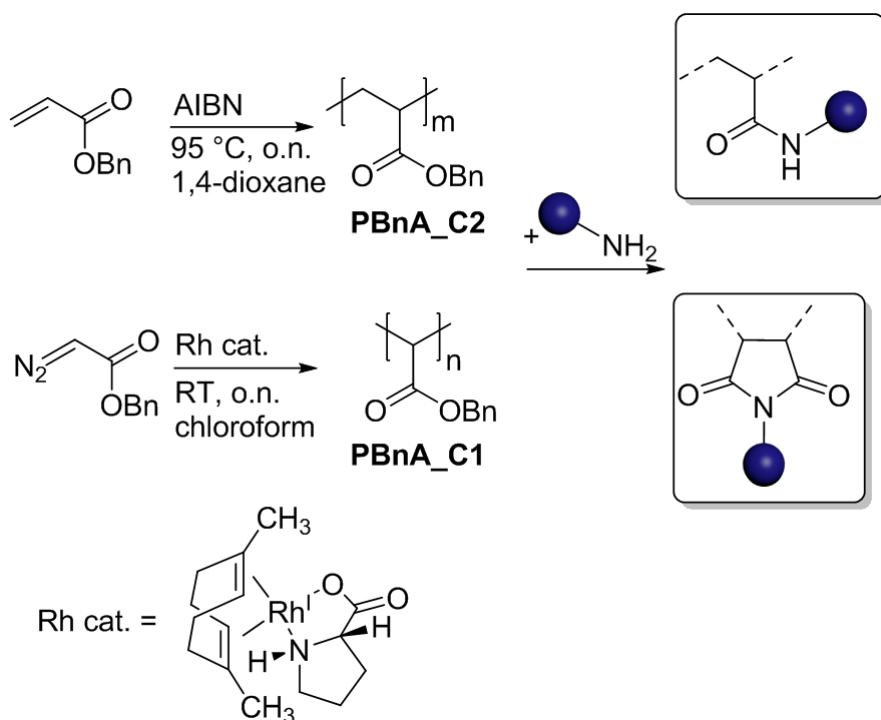
Scheme 3.1.: This illustration shows C2 polymerization of benzyl acrylate and C1 polymerization of benzyl 2-diazoacetate, followed by post-polymerization modification with primary amines. As a result, amides or imides are obtained as predominant product species.

Both polymers, **PBnA_C1** and **PBnA_C2** were fully characterized by nuclear magnetic resonance (^{1}H NMR, ^{13}C NMR) and Fourier transform infrared (FT-IR) spectroscopy as well as by size exclusion chromatography (SEC). Especially interesting for the course of the further discussion are the FT-IR spectra of both polymers (Fig. 3.9).
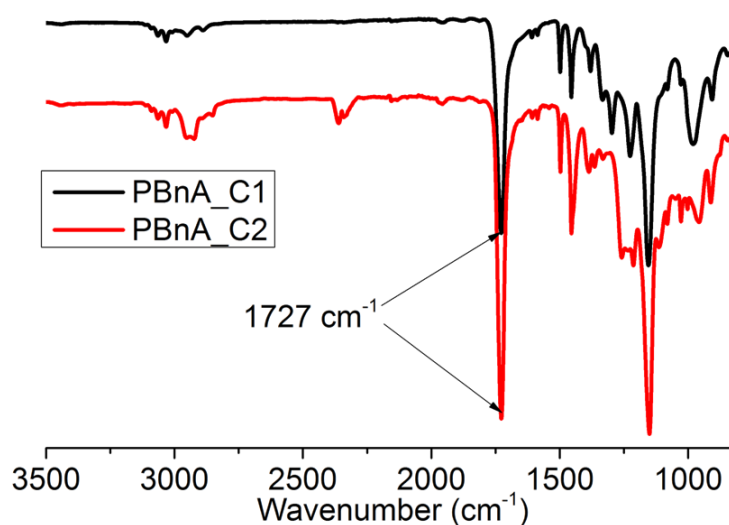
Fig. 3.9.: FT-IR spectra of poly(benzyl 2-ylidene-acetate) **PBnA_C1** (black line) and poly(benzyl acrylate) **PBnA_C2** (red line).

Both spectra exhibit a peak of the $C=O_{stretch}$- vibration at 1727 cm^{-1}, thus indicating no influence of the side group density on the $C=O_{stretch}$ - vibration.

Molecular weights as recorded by SEC are listed in Table 3.1. The results demonstrate good yields, high molecular weights and a relatively broad molecular weight distribution. As a result, these polymers, solely differing in their functional side group density, can be regarded as suitable starting materials for further studies aiming at a comparative post-polymerization modification study.

Table 3.1.: Selected polymer characteristic data of poly(benzyl acrylate) **PBnA_C2** and poly(benzyl 2-ylidene-acetate) **PBnA_C1**.

Polymer	M_n (g mol^{-1})	M_w (g mol^{-1})	Đ (M_w/M_n)	Yield (%)
PBnA_C2	25,000	96,000	3.9	69
PBnA_C1	68,000	316,200	4.6	58

3.1.4. Post-Polymerization Modification of Poly(benzyl acrylate) (C2 Polymer)

At first, an amidation of **PBnA_C2** was targeted in anisole with 3.0 eq. *n*-hexylamine at 120 °C for 17 hours and in the presence of the organo activators 1,8-diazabicyclo[5.4.0]-undec-7-ene (DBU) and 1,2,4-triazole (Tz). This resulted in a conversion of 87.5% according to the ^{1}H NMR spectrum (Fig. 3.10 C). The conversion was calculated by the integral ratio between the methylene group of the precursor polymer **PBnA_C2** and the methyl group of the *n*-hexylamine functionalized product. Evidence for a successful amidation is given by the appearance of alkyl chain signals in the grey marked region at 0.73 - 1.55 ppm. For comparison purposes, the initial spectrum of **PBnA_C2** (Fig. 3.10 A) and the spectrum of poly(*n*-hexyl acrylamide) (Fig. 3.10 B) are illustrated additionally. Noteworthy, no conversion in anisole was observed after the same time in the absence of DBU and Tz. Thus, the results clearly highlight the benefits of the organo catalytic concept for the successful amidation of stable polyacrylates as precursor polymers (refer to chapter 1.3.4). Noteworthy, a conversion of at least up to 74% was obtained if the reaction was performed at 120 °C for 17 hours in bulk (25 eq. *n*-hexylamine) without additional catalyst.
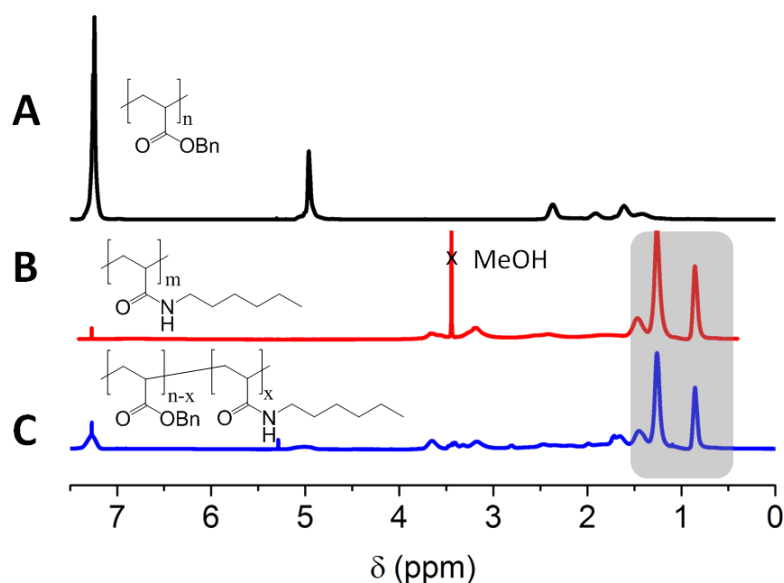
Fig. 3.10.: (**A**)^{1}H NMR spectra of **PBnA_C2**; (**B**) poly(n-hexyl acrylamide) and (**C**) **PBnA_C2** after functionalization with n-hexylamine. All spectra were recorded in CDCl$_3$.

The corresponding FT-IR spectrum of **PBnA_C2** after functionalization with n-hexylamine exhibits the expected and characteristic amide vibration bands (Fig. 3.11). The two depicted lines, black-dashed (reaction performed at $100\,°C$) and blue-dotted (reaction performed at $120\,°C$), show an increased conversion at higher temperatures after the same reaction time.
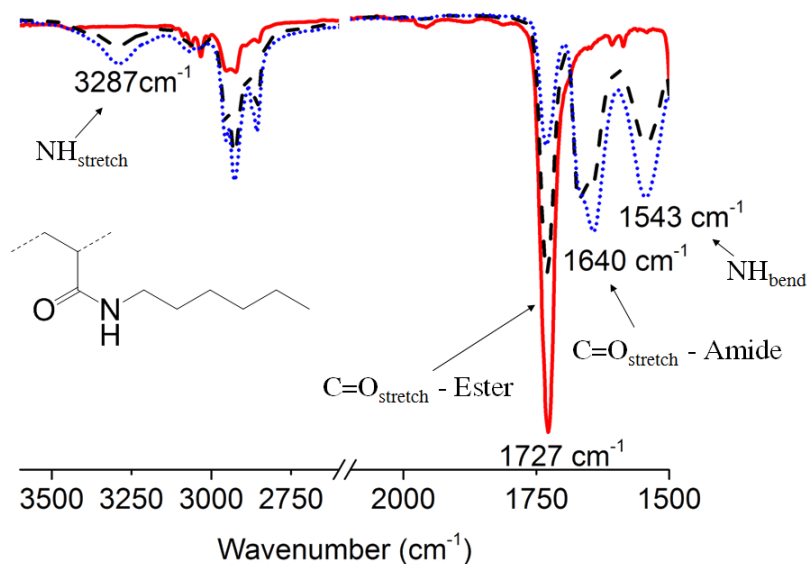
Fig. 3.11.: FT-IR spectra of poly(benzyl acrylate) (red solid line) and poly(benzyl acrylate) after amidation in bulk with n-hexylamine (25 eq.) at $100\,°C$ (black dashed line) and $120\,°C$ (blue dotted line). All reactions were performed for 17 hours.

Signals resulting from the $NH_{stretch}$ - vibration at $3287\,cm^{-1}$ and the NH_{bend} - vibration at $1543\,cm^{-1}$ as well as the resultant signal of the amide $C{=}O_{stretch}$ - vibration at $1640\,cm^{-1}$ are commonly observed for amides. In addition, the signal of the initial ester $C{=}O_{stretch}$- vibration at $1727\,cm^{-1}$ significantly decreased after the amidation process.

3.1.5. Post-Polymerization Modification of Poly(benzyl 2-ylidene-acetate) (C1 Polymer)

Next, I aimed to compare the post-polymerization modification products of **PBnA_C2** with the functional polymethylene **PBnA_C1**. The selected amines utilized for the modification of **PBnA_C1** are listed in Table 3.1.

Table 3.2.: Amines investigated for post-polymerization modification of poly(benzyl 2-ylidene-acetate) **PBnA_C1**.

Amine	Conversion in bulk reaction[a] (%)
1-Hexylamine	82[b]
2-Ethylhexylamine	35
Piperidine	75[b]
Dihexylamine	0
Benzylamine	nd[bc]

[a] Conversions calculated by ^{1}H NMR do not account for the proposed imide formation.
[b] Conversion greater than 50% according to the FT-IR spectrum (*vide infra*).
[c] Conversion not determined due to signal overlapping.

The following discussion will focus on the ligation reactions of **PBnA_C1** with 1-hexylamine, piperidine and benzylamine. These amines show the most pronounced and interesting results regarding their size, conversion as well as functionality. Further analytical data such as supporting NMR spectra for successful functionalizations, TGA, DSC and SLS data are part of appendix A.1. Noteworthy, no comparison between the precursor polymer **PBnA_C1** and the functionalized products by means of SEC is presented as the functionalized polymers were not detectable with the utilized refractive index detector in chloroform, the solvent which was utilized as eluent for SEC analysis of **PBnA_C1**. On the other hand, **PBnA_C1** was not soluble in other tested solvents for SEC. However, all polymers were dialyzed prior to their characterization, utilizing a membrane tube with a molecular weight cut-off $MWCO = 6000\,Da$, indicative for a retained high molecular weight. Furthermore, the molecular weight of **PBnA_C1** functionalized with *n*-hexylamine, utilizing bulk conditions at $120\,°C$ with no additional organo activators and solvent, was determined by SEC with tetrahydrofurane as eluent. The results ($M_n = 15000\,gmol^{-1}$; $M_w = 34900\,gmol^{-1}$) support a non-degraded polymeric

structure after modification. Even though these data provide clear evidence of a macromolecule, they are rather unsatisfactory for a comparative discussion with pristine **PBnA_C1** due to different eluents. Thus, molecular weights of **PBnA_C1** prior to and after functionalization with n-hexylamine were determined via static light scattering (SLS). The SLS results are solely depicted in the supporting information (Appendix A.1; Fig. A.10 and Fig. A.11) as they were obtained from a different batch of polymer; however, they show the expected molecular weight decrease upon functionalization of **PBnA_C1** with the investigated n-hexylamine and a predominant imide formation.

Initially, the same reaction conditions as utilized for **PBnA_C2** for the organo activator DBU/Tz system and n-hexylamine were studied, resulting in a conversion of roughly 60%, thus, being less effective as for the corresponding C2 system (*vide supra*). Presumably, this can be attributed to a sterical hindrance in the mechanism of the DBU/Tz system. In addition, it was intriguing to see that the system without the organo activators gave rise to at least 30% conversion compared to no conversion for the structural analog C2 polymer **PBnA_C2**. These results, in the absence of organo activators, suggest a certain tension of the C1 polymer backbone, resulting in an increased reactivity compared to the C2 system. Subsequently, experiments to increase the conversion of **PBnA_C1** were conducted. Utilizing bulk conditions with 25 eq. n-hexylamine resulted in the highest conversion (82%) of the C1 polymer. The conversion was calculated for the originally anticipated amidation from the ^{1}H NMR spectrum shown in Figure 3.12A. The ^{1}H NMR spectrum exhibits the same signals in the alkyl region (0.58 - 1.77 ppm) as previously observed for the functionalized **PBnA_C2**. However, the FT-IR spectrum illustrated in Figure 3.12C reveals an unexpected and significant difference between the two polymers **PBnA_C1** and **PBnA_C2**.
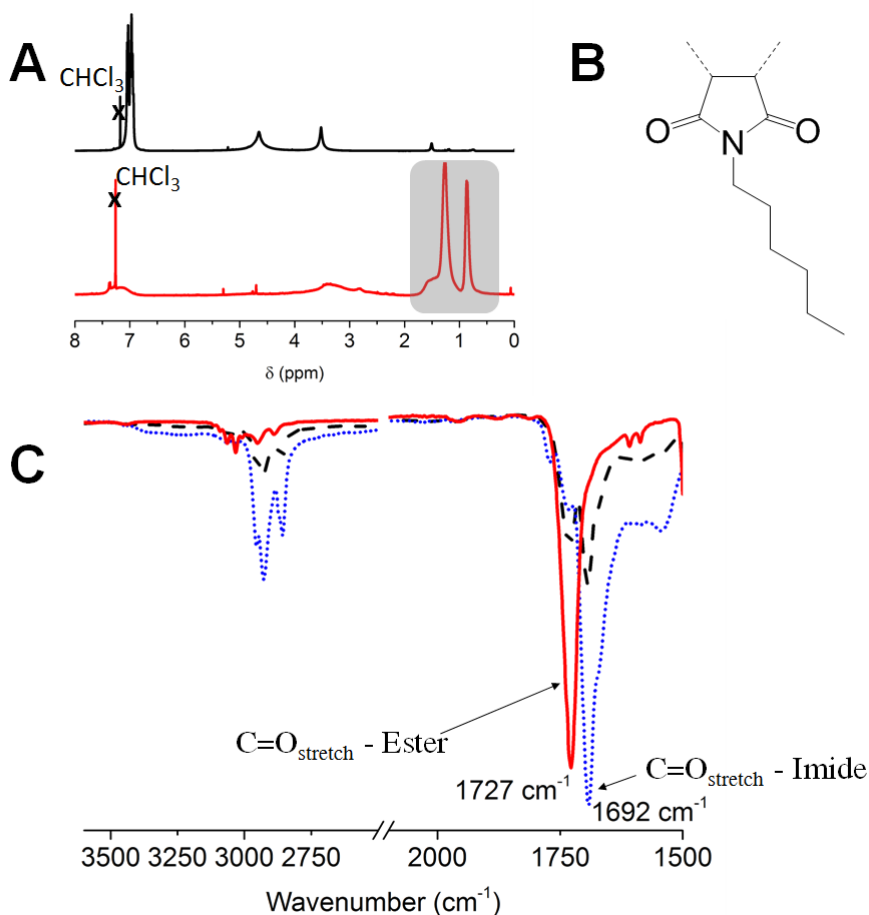
Fig. 3.12.: (**A**) ^{1}H NMR spectra of poly(benzyl 2-ylidene-acetate) before (top) and after (bottom) reaction with 25 eq. n-hexylamine. The spectra were recorded in CDCl$_3$; (**B**) Proposed imide structure; (**C**) FT-IR spectra of poly(benzyl 2-ylidene-acetate) (red solid line) and poly(benzyl 2-ylidene-acetate) after amidation in bulk with n-hexylamine (25 eq.) at 100 °C (black dashed line) and 120 °C (blue dotted line). All reactions were performed for 17 hours.

The NH$_{stretch}$ - vibration for the expected amidation was not observed and the NH$_{bend}$ - vibration is missing as well. Additionally, a shorter wavenumber-shift for the C=O$_{stretch}$ - vibration of the functionalized **PBnA_C1** compared to the functionalized **PBnA_C2** was noticed. The initially recorded signal from the ester bond at 1727 cm^{-1} decreased and a new signal occurred at 1692 cm^{-1}. The previously shown FT-IR spectra of **PBnA_C1** and **PBnA_C2** in Figure 3.9 clearly exhibit the same wavenumber for the C=O$_{stretch}$ vibration mode of the ester at 1727 cm^{-1}. Hence, the same wavenumber was anticipated for a potentially formed amide. Taking these data into account, the predominant formation of cyclic imides in case of **PBnA_C1** is proposed. This 5-membered ring is probably formed due to a subsequent reaction of the initially formed amide with a neighboring ester group. With the recorded spectral data, it is impossible to distinguish between a predominantly formed imide species and the minor amide formation. Hence, no exact conversion could be calculated. Nonetheless, the FT-IR spectrum indicates

a transformation of more than 50% of the converted ester moieties into the proposed imide structures. Earlier studies by *de Bruin* and co-workers reported the formation of similar 5-membered ring anhydrides upon ester cleavage.[79] However, they observed the formation of crosslinked insoluble materials upon ester cleavage at high temperatures. In contrast, the proposed imide formation seems to occur mainly within the chains, i.e. intramolecular, and without intermolecular cross-coupling reactions, supporting the formation of 5-membered cyclic imides.

Next, piperidine was investigated for the modification of **PBnA_C1**. These investigations were aimed at confirming the predominant formation of imide structures. Piperidine is not capable to form an imide structure as it is a secondary amine in contrast to *n*-hexylamine. Hence, the products of **PBnA_C1** and **PBnA_C2** after functionalization with piperidine are expected to show the $C=O_{stretch}$ - vibration at the same wavenumber. This anticipation was, indeed, correct, as illustrated by the FT-IR spectra in Figure 3.13. Both polymers exhibit a $C=O_{stretch}$ - vibration at $1626\,cm^{-1}$. Consequently, these data can be regarded as proof for a predominant imide formation of **PBnA_C1** after post-polymerization modification with *n*-hexylamine.
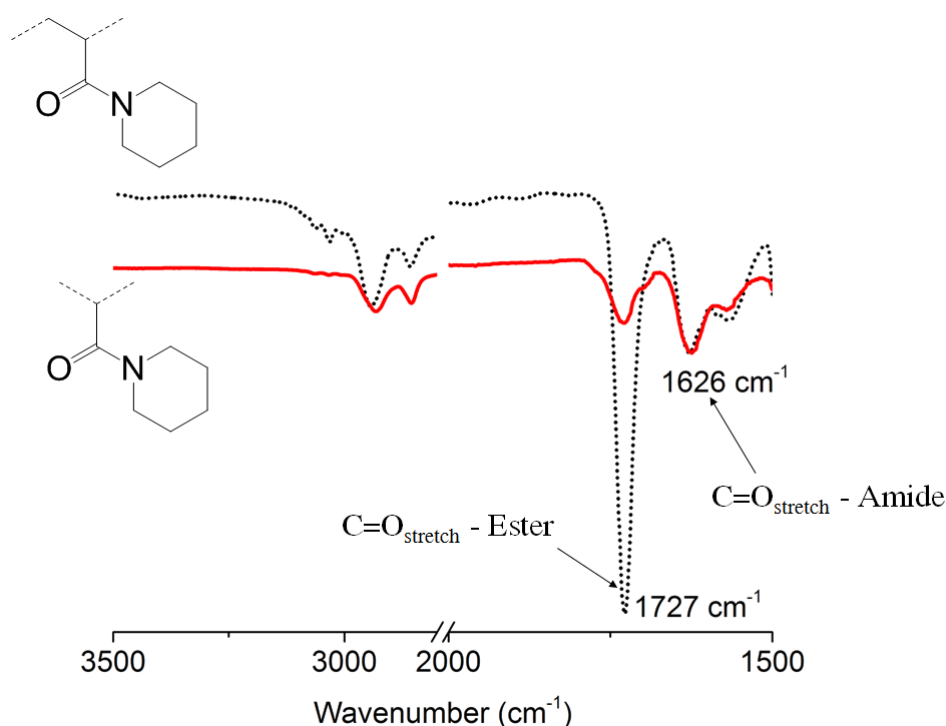
Fig. 3.13.: FT-IR spectra of poly(benzyl 2-ylidene-acetate) (red solid line) and poly(benzyl acrylate) (black dotted line) after ligation reaction with 25 eq. piperidine. The reaction was performed in bulk at $120\,°C$ overnight.

The conversion with piperidine can be estimated by the ratios of the remaining $C=O_{stretch}$ ester vibration and the $C=O_{stretch}$ - vibration bands of the product. Again, a significantly higher conversion (>50%) after the same reaction time was observed for the C1 system,

possibly due to tension resulting from a high functional side group density.

With regard to the issue of steric hindrance, benzylamine was considered to be a third highly interesting substitutent. Benzylamine is anticipated to exhibit a similar steric demand as benzyl alcohol. Hence, the general feasibility to post-modify highly dense functionalized polymethylenes will be highlighted by a conversion of **PBnA_C1** with benzylamine. Indeed, as shown by the ^{1}H NMR and FT-IR spectrum in Figure 3.14, a conversion higher than 50% is achieved. This conversion is estimated by the C=O$_{stretch}$ intensities in the FT-IR spectrum.
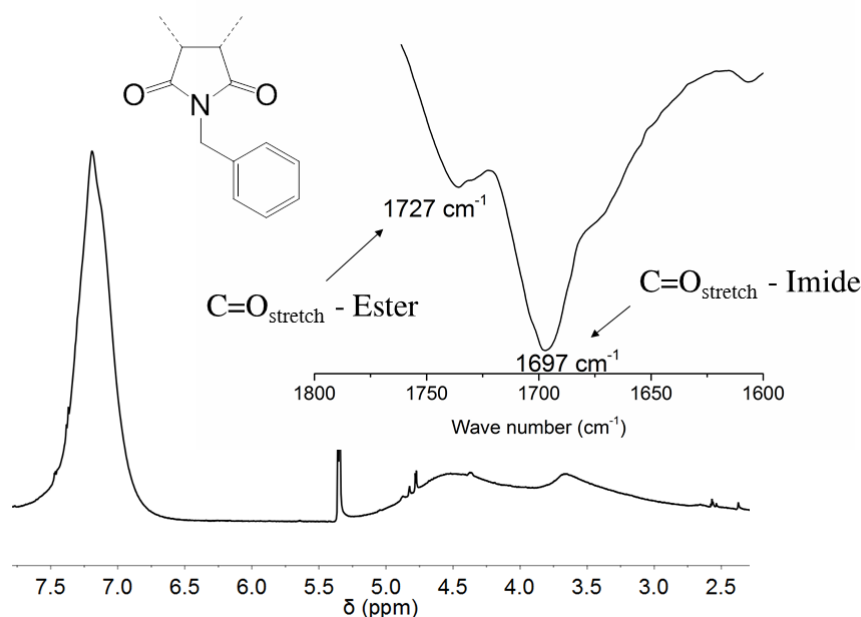
Fig. 3.14.: ^{1}H NMR spectrum of poly(benzyl 2-ylidene-acetate after the reaction with benzyl amine recorded in CDCl3. Section of the FT-IR spectrum showing the expected C=O stretch vibration band representative for a proposed imide structure.

Due to signal overlapping in the ^{1}H NMR, a calculation of the conversion was again impossible but the conversion can be estimated to be significantly higher than 50% according to the IR spectrum. The imide structure is characterized by the FT-IR signal at 1697 cm^{-1}. Again, the feasibility to post-modify **PBnA_C1** with benzylamine is presumably due to tension generated by the densely packed side groups of the C1 polymeric system.

3.1.6. Conclusion

In conclusion, the reaction of stable esters with primary and secondary amines was investigated utilizing C1 and C2 polymers. To the best of my knowledge, this is the first

time that the concept of post-polymerization modification was transferred to functional polymethylenes (C1 polymers). This study provides evidence for the general possibility to functionalize densely packed functional polymethylenes. The product output of C1 and C2 polymeric systems was compared and significant differences were highlighted. In the case of poly(benzyl 2-ylidene-acetate), primary amines tend to predominantly form 5-membered cyclic imides utilizing the stated reaction conditions. In contrast, post-polymerization modification of poly(benzyl acrylate) leads to the well-known amidation. Additionally, the conversions after the same reaction time were higher in case of functional polymethylenes compared to the C2 systems. This finding can probably be attributed to a higher tension of the functional polymethylene structure, resulting from a higher side group density.

3.2. Modification of Functional Polymethylenes via Thiol-ene Chemistry

This chapter is partially adapted from Ref.[80] - *Polym. Chem.*, **2016**, 7, 4525–4530 - with permission from The Royal Society of Chemistry.

The online content can be accessed by using the following URL:

`http://xlink.rsc.org/?DOI=C6PY00818F`

3.2.1. Introduction

The previous study (Chapter 3.1) highlighted the general possibility to post-modify functional polymethylenes.[78] However, poly(benzyl 2-ylidene-acetate) **PBnA_C1** requires relatively harsh reaction conditions and does not allow for facile post-polymerization modification. Hence, the motivation for this subsequent study was the synthesis of suitable monomers and precursor polymers, accessible to a facile, quantitative and controlled post-polymerization modification. In this attempt, allyl 2-diazoacetate with an unsaturated reactive double bond was synthesized. The corresponding functional polymethylene poly(allyl 2-ylidene-acetate) **PAA_C1** was initially synthesized by *Liu* and co-workers.[14] They polymerized allyl 2-diazoacetate with elemental copper and reported the first C1 polymerization of α-diazocarbonyl compounds with transition-metal catalysts. However, they obtained a non-stereoregular **PAA_C1** with rather low molecular weight ($M_w \sim 3000\,\text{gmol}^{-1}$) and did not investigate the capability of post-modifying this polymer. The structural analog C2 polymer poly(allyl acrylate) **PAA_C2** was reported already by *Donati* and *Farina* in 1962.[81] They performed anionic polymerization of allyl acrylate at low temperatures to obtain a crystalline polymer with polyacrylate structure. This polymer was characterized as unstable in air, which tends to crosslink at elevated temperatures via the pendant allyl group.[82] The authors were able to show post-polymerization modification via bromination of the unsaturated bond. In this chapter, I will describe and characterize the first example of a high molecular weight polymethylene bearing allyl side groups at every main chain carbon atom. In addition, the first functional polymethylene suitable for post-polymerization modification via thiol-ene chemistry is presented.

3.2.2. Synthesis and Characterization of Allyl 2-diazoacetate

Allyl 2-diazoacetate has been reported in the literature[14] and was prepared via the synthetic route B depicted in Scheme 1.9. The ^{1}H NMR spectrum exhibits a singlet signal at 4.78 ppm as expected for the backbone proton of a diazo ester (Figure 3.15).

The protons H^d (5.83-602 ppm) and H^e (5.18-5.40 ppm) give rise to multiplets due to vicinal and geminal proton coupling.
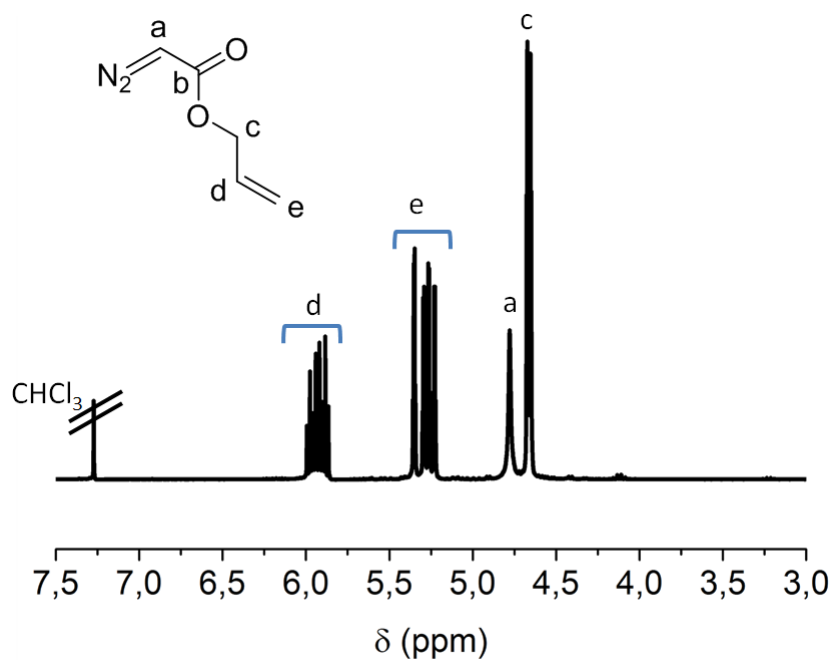
Fig. 3.15.: ^{1}H NMR spectrum of allyl 2-diazoacetate in CDCl$_3$ (300 MHz spectrum).

The ^{13}C NMR spectrum in Figure 3.16 shows a small signal for the backbone carbon atom C^a at 46.2 ppm. The double bond carbon atoms C^d and C^e are observed at 132.1 ppm and 118.2 ppm.
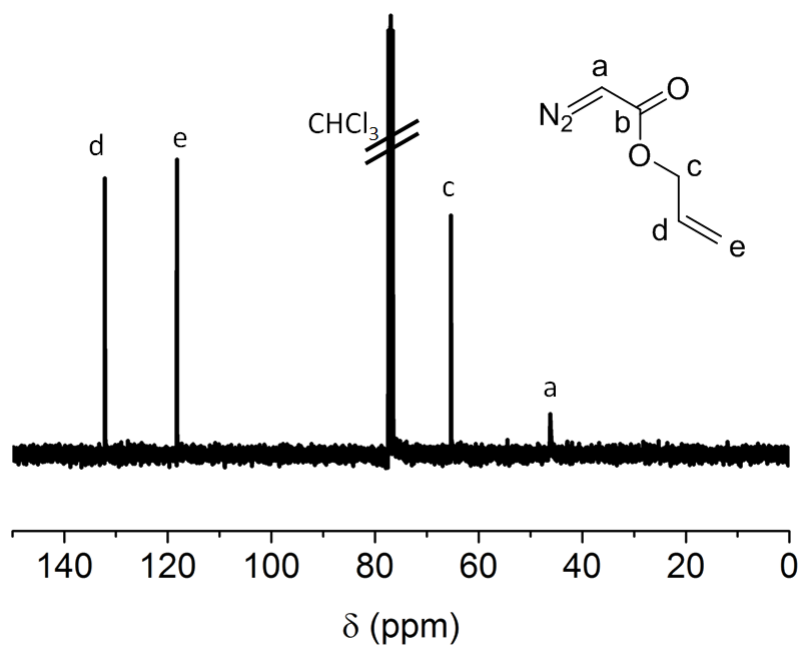
Fig. 3.16.: ^{13}C NMR spectrum of allyl 2-diazoacetate in CDCl$_3$ (75 MHz spectrum).

Chapter 3.1 pointed out the usefulness of IR spectroscopy in the identification of diazo compounds. The FT-IR spectrum of allyl 2-diazoacetate is shown in Figure 3.17 and it exhibits a strong diazo vibration band at $2106\,cm^{-1}$, as well as a C=C vibration at $1648\,cm^{-1}$. Thus, taking all spectral data into account, evidence for a successful synthesis of allyl 2-diazoacetate is provided.
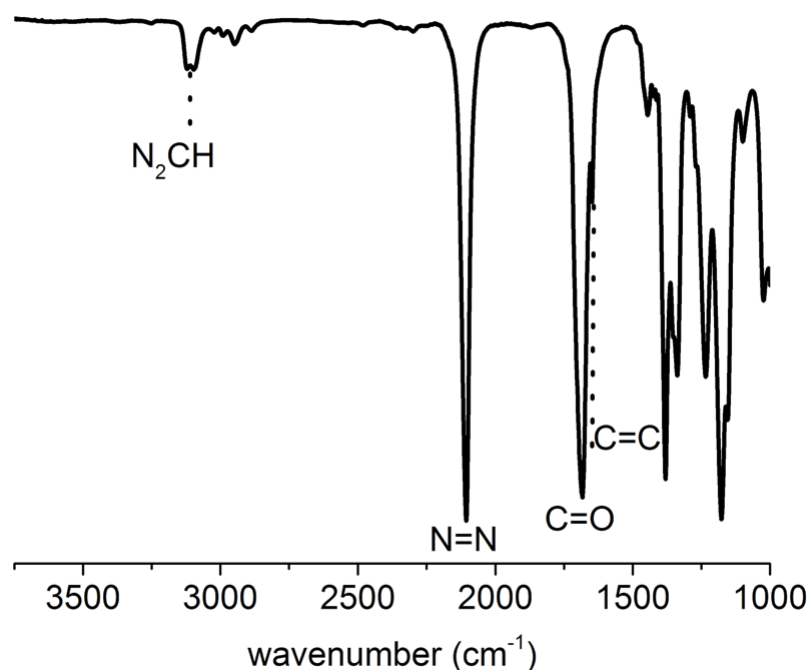
Fig. 3.17.: FT-IR spectrum of allyl 2-diazoacetate.

3.2.3. Synthesis and Characterization of Poly(allyl 2-ylidene-acetate)

The synthesis of poly(allyl 2-ylidene-acetate) **PAA_C1** via rhodium mediated C1 polymerization was inspired by procedures described in the literature.[79] Hence, 2 mol% [(*L*-Prolinate)Rh^{I}(1,5-Dimethyl-1,5-cyclooctadiene)] were utilized as catalyst and allyl 2-diazoacetate was used as monomer (Scheme 3.2).

The C1 polymerization was performed overnight in chloroform, and **PAA_C1** was obtained by repeated rapid precipitation in *n*-hexane and intermediately dissolving the polymer in 1,4-dioxane. Following the last precipitation, **PAA_C1** was lyophilized from 1,4-dioxane to obtain the polymer in good yields up to 49%, similar to the yields of poly(benzyl 2-ylidene-acetate) **PBnA_C1** (50%), but less than the yields obtained for poly(ethyl 2-ylidene-acetate) **PEA_C1** (80%) utilizing the same catalyst.[79] Lyophilization was necessary to maintain a soluble polymer. Quite surprisingly, the double bond did not interfere with the rhodium catalyst or at least it did not show

any binding affinity with the rhodium center. Thus, the catalyst did not get poisoned and the C1 polymerization was not hindered.
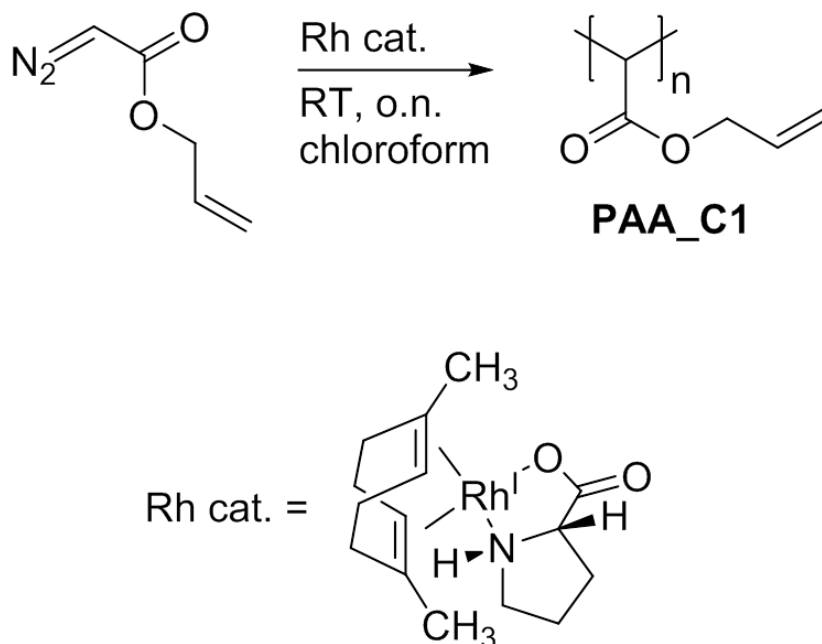
Scheme 3.2.: C1 polymerization of allyl 2-diazoacetate utilizing [(L-prolinate)Rh^I(1,5-dimethyl-1,5-cyclooctadiene)] as catalyst.

A molecular weight distribution (Đ = 2.3) was determined via SEC and an average molecular weight up to $M_n = 54300$ gmol^{-1} was reached. This molecular weight value is significantly higher than the previously reported one by *Liu* and co-workers ($M_w \sim 3000$ gmol^{-1}) via copper catalysis.[14] It is concluded that the rhodium catalyst performs tremendously better in terms of molecular weight and stereoregular control compared to copper powder. The yield of **PAA_C1** was not stated in the original paper; however, the polymer prepared in this study is anticipated to exhibit significantly higher yields. Crucially, the utilized catalyst in this study is acting under homogeneous reaction conditions in contrast to the heterogeneous catalytic copper system. Furthermore, the ligands coordinating to the rhodium center have a significant impact on the molecular weight distribution as has already been reported for other α-diazocarbonyl compounds.[83] In addition, the heterogeneous copper mediated C1 polymerization was solely reported due to the incidental structure determination of functional polymethylenes by *Liu* and co-workers,[14] never due to the overall good polymerization performance in subsequent publications. In contrast to this, the rhodium mediated C1 polymerization of α-diazocarbonyl compounds with [(L-Prolinate)Rh^I(1,5-Dimethyl-1,5-cyclooctadiene)] is a well-established catalytic system.

The chemical structure of **PAA_C1** was fully confirmed by ^{1}H NMR, ^{13}C NMR and IR spectroscopy (Fig. 3.18-3.20). Similar to previously reported functional polymethylenes obtained via this C1 polymerization technique, sharp distinct signals, highlighting a well

ordered microstructure, were recorded in the NMR spectra(Fig. 3.18 and Fig. 3.19).The singlet signals at 170 ppm and 45 ppm in the ^{13}C NMR spectrum suggested the formation of a syndiotactic polymer.[32,35]
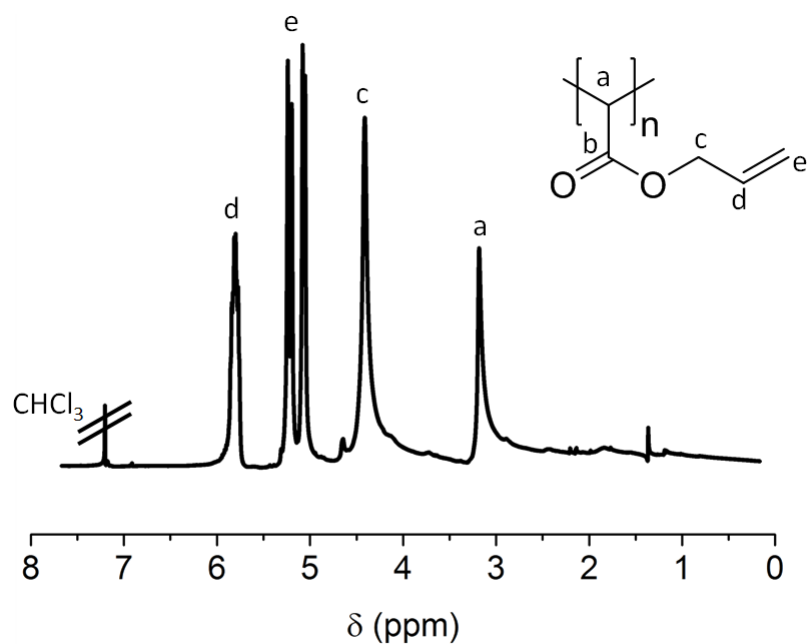
Fig. 3.18.: ^{1}H NMR spectrum of poly(ally 2-ylidene-acetate) in CDCl$_3$.
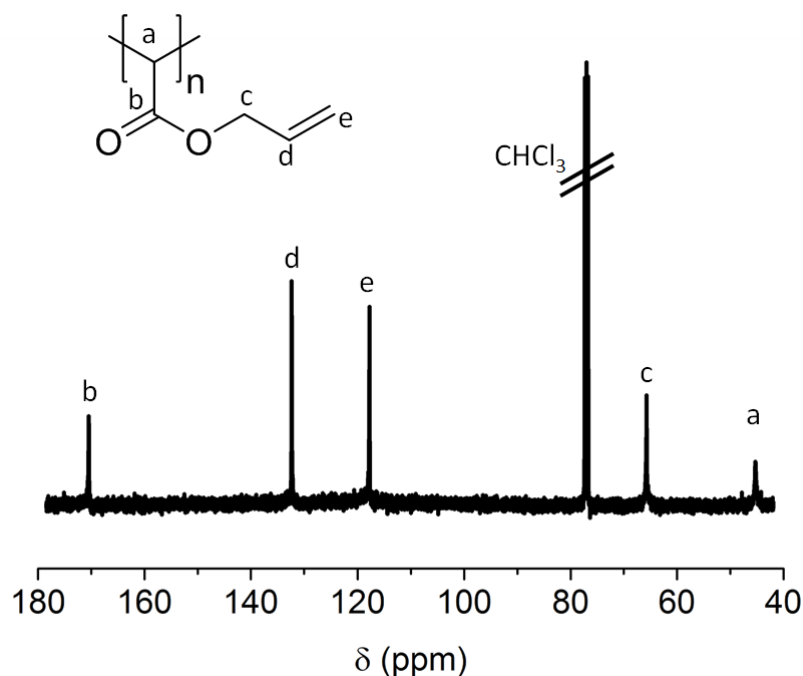
Fig. 3.19.: ^{13}C NMR spectrum of poly(ally 2-ylidene-acetate) in CDCl$_3$.

The carbonyl stretch vibration in the FT-IR spectrum (Fig. 3.20) gives rise to a strong band at 1728 cm^{-1}. Weak bands at 1648 cm^{-1} and 3048 cm^{-1} originate from the double

bond and their respective C=C$_{\text{stretch}}$ vibration as well as the =C-H$_{\text{stretch}}$ vibration. This assignment is supported by the initially conducted bromination of **PAA_C1**, showing the vanished signals upon successful bromination (Appendix Figure A.13).
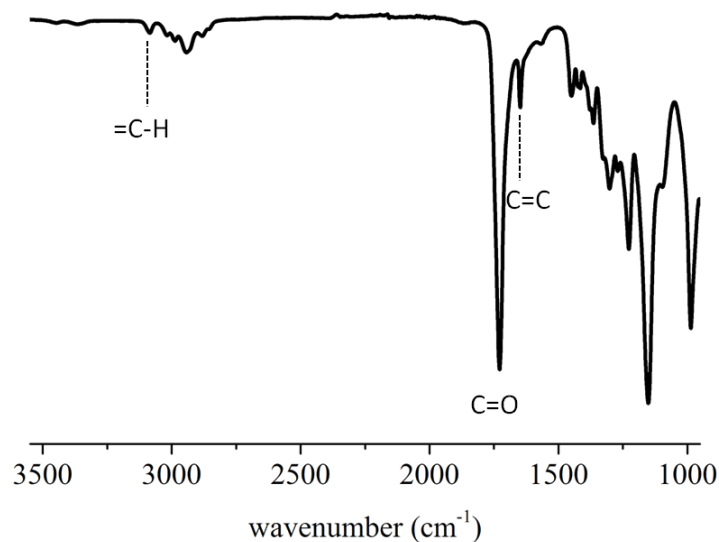
Fig. 3.20.: FT-IR spectrum of poly(ally 2-ylidene-acetate).

The onset temperature of the thermal decomposition (Figure 3.21) was determined at 204 °C and **PAA_C1** showed a rather broad weight loss window compared to **PBnA_C1** and **PEA_C1** with onset temperatures at 253 °C and 346 °C, respectively.
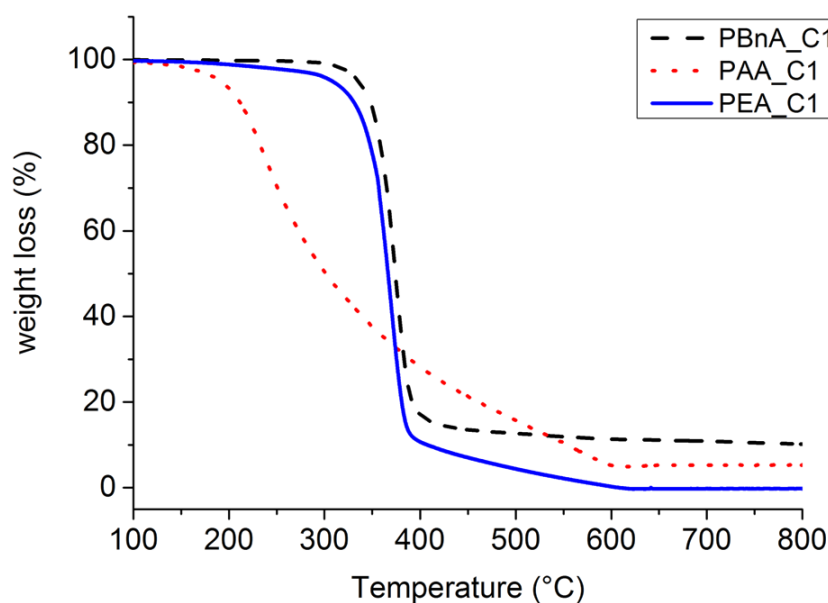
Fig. 3.21.: TGA data showing the weight loss curves of of poly(benzyl 2-ylidene-acetate) **PBnA_C1** (black dashed line), poly(ethyl 2-ylidene-acetate) **PEA_C1** (blue solid line) and poly(ally 2-ylidene-acetate) **PAA_C1** (red dotted line) upon heating at 10 °C per minute under air.

3.2.4. Kinetic Investigation of the C1 Polymerization

The consumption of allyl 2-diazoacetate during the C1 polymerization was tracked via *real-time in situ* FT-IR spectroscopy (Fig. 3.22). Thus, insight into the reaction kinetics of the C1 polymerization was gained. The procedure was inspired by *Xiao* et al. who investigated the C1 polymerization of ethyl 2-diazoacetate with various catalytic systems.[44] Instrument limitations prevented from pursuing the diazo vibration mode, since the optical window only detects up to $2000 \, \text{cm}^{-1}$. Instead, I focused on the shift of the C=O$_{\text{stretch}}$ vibration band upon polymerization. Initially, the carbonyl group gives rise for a peak at $1682 \, \text{cm}^{-1}$, while the newly formed peak at $1728 \, \text{cm}^{-1}$ can be assigned to the carbonyl bond of **PAA_C1**.
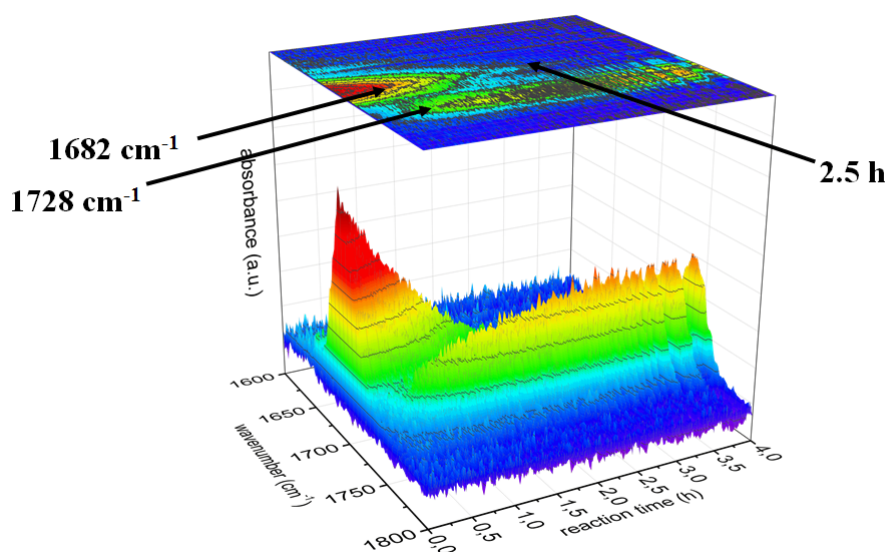
Fig. 3.22.: *Real-time in situ* FT-IR spectra of the polymerization process of allyl 2-diazoacetate pursued for 4 hours.

More than 95% of the monomer were consumed after 2.5 hours as observable in Figure 3.22 and in Figure 3.23A. However, due to the low signal to noise ratio at the advanced stage of the polymerization, the reaction was allowed to proceed for 4 hours in total to assure quantitative conversion of the monomer.

The peak areas at $1682 \, \text{cm}^{-1}$ and $1728 \, \text{cm}^{-1}$ were plotted for each recorded 2D FT-IR spectrum against the reaction time as shown in Figure 3.23A. For a polymerization following first order kinetics, the current concentration c of the monomer should be proportional to e^{-kt}, with k being the reaction rate constant and t being the reaction time.

$$c \propto e^{-kt} \tag{3.1}$$

3. Results and Discussion

The current concentration c is directly expressed by the peak area of each recorded 2D FT-IR spectrum. Equation 3.1 can, therefore, be re-arranged to equation 3.2.

$$ln(\frac{1}{[peak\ area]}) = kt \tag{3.2}$$

Graphical expression of equation 3.2 is shown in Figure 3.23B. The obtained graph for the progression of the monomer peak area was fitted with the linear equation 3.3, and the coefficient of determination ($R^2 = 0.986$) indicates a legitimate linear fit.

$$f(t) = 2.12 \times 10^{-4}t - 2.18 \tag{3.3}$$
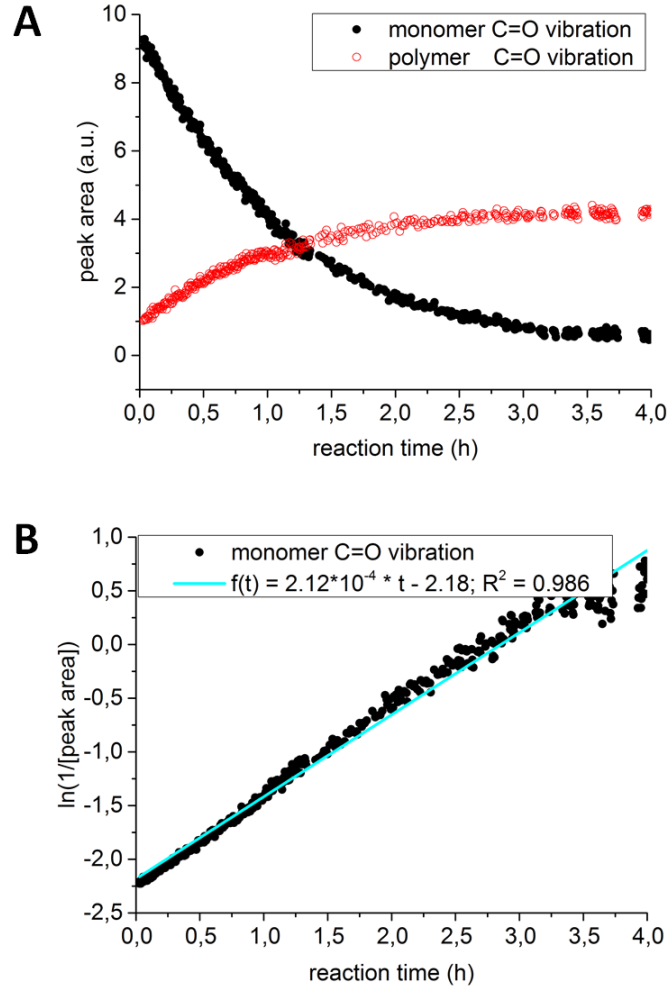
Fig. 3.23.: Illustration of kinetic results. (A) Peak area vs. reaction time; (B) $ln(\frac{1}{[peak\ area]})$ vs. reaction time. Open circles (red) represent the data obtained from polymer formation. Closed circles (black) represent the data obtained from monomer decomposition.

In conclusion, a reaction following first order kinetics is anticipated. In comparison with

the previously reported decomposition of ethyl 2-diazoacetate with [(*L*-Prolinate)Rh$^{\text{I}}$(1,5-cyclooctadiene)], a much faster reaction is observed with allyl 2-diazoacetate.[44] The rate constant k is the slope of equation 3.3 ($k = 2.12 \times 10^{-4} s^{-1}$) and is higher than the one recorded for ethyl 2-diazoacetate ($k = 1.54 \times 10^{-4} s^{-1}$) by *Liu* and co-workers.

3.2.5. Post-Polymerization Modification of Poly(allyl 2-ylidene-acetate)

As briefly stated above, the initial modification of **PAA_C1** to test the reactivity was done with bromine. A quantitative conversion of C=C double bonds was observed by IR spectroscopy (Appendix Figure A.13); however, the obtained product was insoluble in all tested solvents. Next, **PAA_C1** was subject to well-known thiol-ene reactions for allyl group containing polymers.[59,84] A photochemical pathway was chosen as photoinitiated thiol-ene reactions generally require shorter reaction times and lead to higher efficiencies. Furthermore, they are more tolerant to functional groups and backbones. Hence, 2,2-dimethoxy-2-phenylacetophenone (DMPA) was chosen as a photoinitiator for the studies presented here. The obtained conversions for the investigated thiols are listed in Table 3.3 and were determined by ^{1}H NMR spectroscopy. The conversions decreased with the bulkiness of the substituent. The highest conversion (96%) was obtained with 1-mercaptohexane with a linear alkyl chain.

Table 3.3.: Conversions reached of **PAA_C1** modifications via thiol-ene reactions. Conversions were determined via ^{1}H NMR spectroscopy.

Thiol	Conversion (%) of C=C bonds
1-Mercaptohexane	96
tert-Butylmercaptan	82
2-Ethylhexylmercaptan	78
Benzylmercaptan	71

Figure 3.24 shows the recorded ^{1}H NMR and FT-IR spectra of the post-modified **PAA_C1**. The signals characteristic for the unsaturated C=C double bond are highlighted in grey. The ^{1}H NMR of **PAA_C1** exhibits one broad signal for the single proton (-CH=CH$_2$) at 5.81 ppm and a doublet of doublets pattern originating from the =CH_2 group between 4.97-5.37 ppm. For all thiols investigated, these signals decreased significantly after post-polymerization modification. Furthermore, new signals in the alkyl region of the ^{1}H NMR spectrum between 0.75 ppm and 1.90 ppm arose and proved the successful, even though not quantitative conversion, in all cases. Notably, all of the tested hydrophobic thiols remained soluble during the modification process; however, after purification, some of them exhibited substantial crosslinking. This was dependent

on the conversion as well as on the utilized thiol moiety. This crosslinking might be attributed to the same crosslinking that occurred for the pristine polymer that was observed after drying it simply from solution. However, it is also known that thiol-ene reactions may show intramolecular cyclization (refer to Chapter 1.3.2).[62,63]
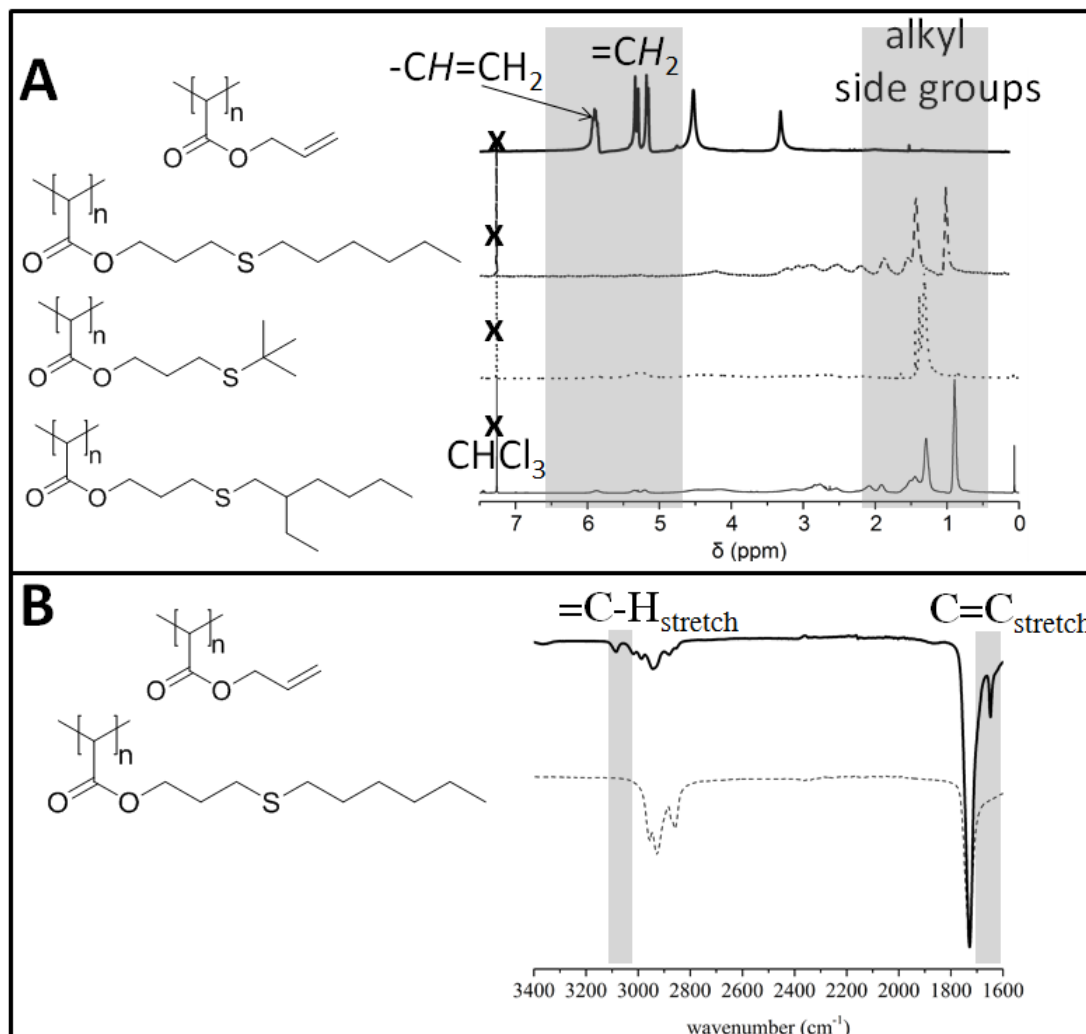
Fig. 3.24.: Spectral data of **PAA_C1** prior and after functionalization via thiol-ene reactions. (**A**) ^{1}H NMR spectra; (**B**) FT-IR spectra.

Utilization of hydrophilic thiol moieties for the post-polymerization modification of **PAA_C1**, such as mercaptoethanol, *N*-acetyl-*L*-cystein or mercaptoacetic acid, led to completely insoluble materials. These products turned insoluble during the course of the reaction, likely due to a change in the polarity and a subsequent precipitation of the polymeric species formed. Again, this insolubility can possibly be assigned to a significant crosslinking via the remaining double bonds after non-quantitative conversion.

Therefore, in addition to the thiol-ene reaction in solution, the surface of **PAA_C1** surface coatings was modified. The inherent self-crosslinking ability of **PAA_C1** was

utilized to form stable thin polymer films, which were subsequently modified with thiols. The thin coated polymer layer was obtained by spin-coating of a 1 wt% solution of **PAA_C1** in chloroform onto a silicon wafer. In order to obtain a stable film, the coating was irradiated with UV-light ($\lambda = 315\text{-}400\,\text{nm}$) for 3 hours. Subsequently, the polymer surface was modified under UV irradiation with the respective thiol dissolved in methanol and additional utilization of DMPA as photo initiator. A simple test to elucidate the successful modification is the measurement of the contact angle. Results of water contact angle measurements are listed in Table 3.4.

Table 3.4.: Changes of the contact angle upon post-polymerization modification utilizing surface thiol-ene reactions. The sample name indicates the thiol used to modify **PAA_C1**.

Sample	Advancing contact angle [°]	Receding contact angle [°]	Hysteresis [°]
PAA_C1	73.5±3.1	24.9±2.6	48.6
Mercaptoethanol	34.6±1.2	9.5±0.3	25.1
N-Acetyl-*L*-cystein	43.3±2.0	11.3±2.3	32.0
Mercaptoacetic acid	50.2±0.8	12.2±0.3	37.9
1-Mercaptohexane	104.1±4.7	45.7±1.0	58.5
Benzylmercaptan	73.4±2.0	26.8±2.5	46.6
1-Mercaptohexane[a]	99.1±5.7	38.0±4.0	61.1
Benzylmercaptan[a]	75.8±1.2	24.0±1.4	51.8

[a] Modification was performed in solution prior to spin-coating.

To account for surface roughness, dynamic advancing and receding contact angles were measured instead of the static sessile drop method. The measurement of the advancing and receding contact angle is beneficial as it provides the maximum and minimum possible droplet contact angles which differ in surfaces with a certain degree of roughness.[85] Furthermore, the experimental advancing contact angle can be regarded as a good approximation of the *Young's* contact angle, which is the mathematically defined contact angle of a drop on an ideal surface.[86] Therefore, the advancing contact angle was utilized for the comparison of the hydrophilic surface properties. The measurement of the advancing and receding contact angle was performed three times for each sample. Advancing contact angle measurements showed a significant decrease upon modification with mercaptoethanol, *N*-Acetyl-*L*-cystein and mercaptoacetic acid. The hydrophobic thiol 1-mercaptohexane shows the anticipated increase of the contact angle, while the modification with benzylmercaptan solely resulted in a small contact angle difference. The latter can probably be attributed to a similar polarity of the aromatic ring and the allyl group. The determined hysteresis suggests a certain degree of roughness in the surfaces. All surface modifications were successfully evidenced by the contact angle measurements and display the wide range of tunable surface

properties. In addition, no significant impact on the contact angle was noticed by different functionalization methods, i.e., if the **PAA_C1** was functionalized in solution and spin-coated afterwards, the same contact angle was determined as for the above described contact angle measurements. The surface properties could be altered between 35 ° and 104 ° with the tested thiols. Hence, functionalization via thiol-ene chemistry might be helpful to alter the surface properties of **PAA_C1** thin films with regard to future application, e.g., on anti-fouling surfaces.

3.2.6. Conclusion

Rhodium mediated C1 polymerization proved to be suitable for the synthesis of high molecular weight poly(allyl 2-ylidene-acetate). The kinetics were recorded via *real-time in situ* FT-IR spectroscopy and the polymerization exhibits first order kinetics. Furthermore, evidence for the suitability of the synthesized functional polymethylene for post-polymerization modification at moderate reaction conditions was provided. Namely, thiol-ene reactions were performed in solution with hydrophobic thiols as well as on the surface of stable polymeric thin films with hydrophobic and hydrophilic thiols. It became clear that there is an ongoing search for functional polymethylenes accessible to a controlled post-polymerization modification. This is mainly due to difficulties in controlling the inherent self-crosslinking ability of poly(allyl 2-ylidene-acetate). However, this drawback was utilized for the preparation of thin film surface coatings and the adjustability of the surface properties in a wide range was demonstrated.

3.3. Modification of Functional Polymethylenes via Oxirane Cleavage

This chapter is partially adapted from Ref.[87] - *Macromolecules*, **2017**, 50, 1415-1421 - with permission from The American Chemical Society.
The online content can be accessed by using the following URL:
`http://pubs.acs.org/doi/abs/10.1021/acs.macromol.6b02465`

3.3.1. Introduction

Chapter 3.2 clearly showed the necessity for an ongoing search for a fully controllable functional polymethylene suitable for subsequent post-polymerization modification. In this regard, epoxides are interesting side groups as they are highly reactive compounds. The three-membered oxirane ring can be easily opened with various nucleophiles. In addition, this cleavage is an addition reaction without the release of any by-product.[51] Glycidyl methacrylate is one of the most common monomers as it can be easily polymerized to poly(glycidyl methacrylate) **PGMA_C2** via free radical polymerization. Furthermore, it has been thoroughly investigated regarding ring-opening modifications with amines and thiols.[68,88] Noteworthy, the analogues C1-polymer has not been described yet.

3.3.2. Synthesis and Characterization of Glycidyl 2-diazoaceteate

The monomer synthesis of glycidyl 2-diazoacetate was performed according to method **A** in Scheme 1.9. A racemic mixture of glycidol was reacted with bromoacetyl bromide to yield glycidyl 2-bromoacetate, which was subsequently utilized for a reaction with *N,N*'ditosylhydrazine in basic medium to yield the monomer in 26%. This yield is in the commonly obtained range for the reactive diazocarbonyl compounds. The structure of glycidyl 2-diazoacetate was fully confirmed by ^{1}H NMR, ^{13}C NMR and IR spectroscopy. To the best of my knowledge, this is the first time that the synthesis of glycidyl 2-diazoacetate has been reported. Detailed spectral information are illustrated in Figures 3.25-3.27. The ^{1}H NMR spectrum (Fig. 3.25) exhibits the commonly observed broad singlet signal at 4.81 ppm, resulting from the N_2CH group. Furthermore it shows the expected splitted signals of H^c between 3.90 - 4.58 ppm and H^e between 2.58-2.92 ppm, originating from diastereotopicity of the chiral molecule.[89]
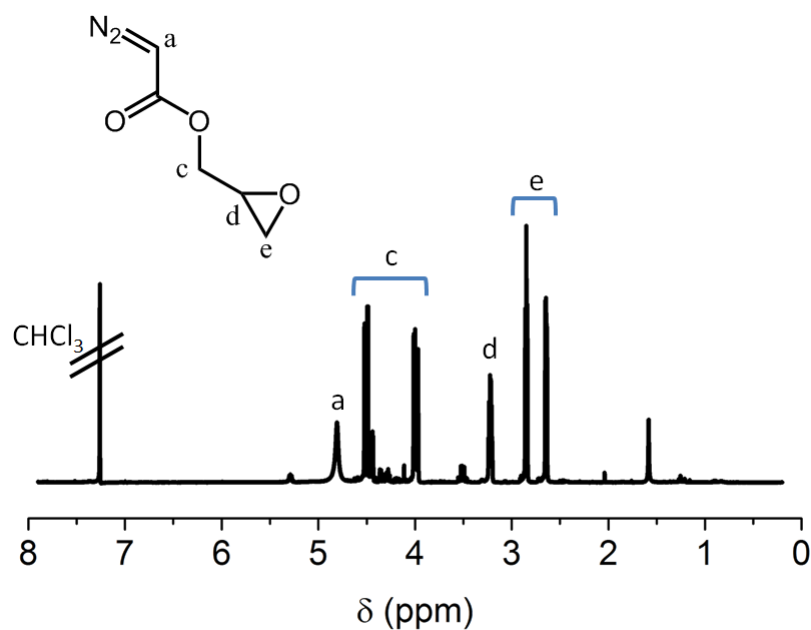
Fig. 3.25.: ^{1}H NMR spectrum of glycidyl 2-diazoacetate in CDCl$_3$.

The carbon atom of the N$_2$CH-group gives rise to a broader signal at 46.3 ppm in the corresponding ^{13}C NMR spectrum of glycidyl 2-diazoacetate (Fig. 3.26).
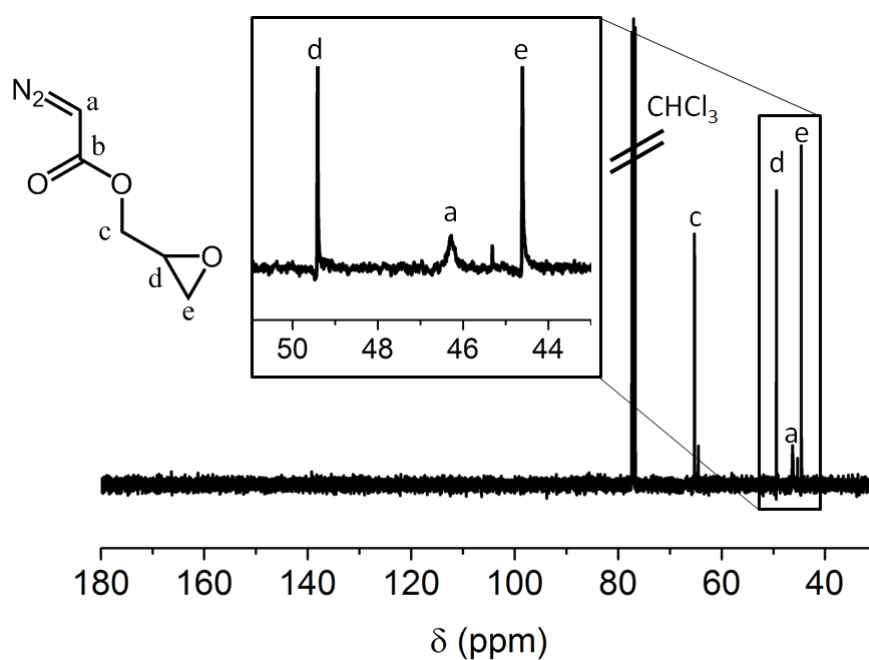
Fig. 3.26.: ^{13}C NMR spectrum of glycidyl 2-diazoacetate in CDCl$_3$.

As usual, the FT-IR spectrum is highly expressive for diazo compounds (Fig. 3.27). The diazo group of glycidyl 2-diazoacetate results in a vibration at 2107 cm^{-1} and the CH vibration next to that group gives rise to a vibration mode at 3104 cm^{-1}. Furthermore,

the oxirane ring results in two distinct signals at 907 and 859 cm^{-1}, these signals are indicative of monosubstituted oxiranes.[90]
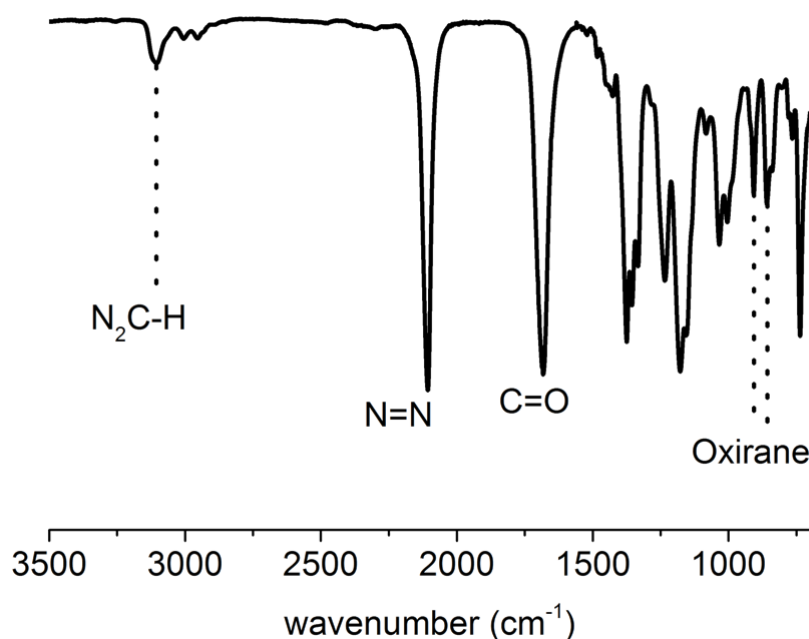
Fig. 3.27.: FT-IR spectrum of glycidyl 2-diazoacetate.

3.3.3. Synthesis and Characterization of Poly(glycidyl 2-ylidene-aceteate) and Poly(glycidyl methacrylate)

Poly(glycidyl methacrylate) **PGMA_C2** was synthesized by FRP of glycidyl methacrylate in tetrahydrofurane at 65 °C, utilizing AIBN as radical initiator. The polymerization was performed for 23 hours. Poly(glycidyl 2-ylidene-acetate) **PGA_C1** was obtained by rhodium mediated C1 polymerization with 2 mol% [(*L*-Prolinate)Rh$^{\mathrm{I}}$(1,5-cyclooctadiene)] in chloroform, following the general procedure published by *Jellema* et al. (Scheme 3.3).[79]

PGA_C1 was obtained in decent yields up to 53% similar to the results for previously reported polymethylenes.[78,80] The number average molecular weights ($M_n = 3900$ gmol^{-1}; $M_w = 9900$ gmol^{-1}) were determined by size exclusion chromatography with dimethylformamide as eluent. However, accurate average molecular weight determination was difficult as the elution peak partially overlaps with a system peak (Figure 3.28). Furthermore, as previously reported for the rhodium mediated polymerization of ethyl 2-diazoacetate with the same catalyst [(*L* prolinate)Rh$^{\mathrm{I}}$(1,5-cyclooctadiene)], several active catalytic species can lead to a bimodal distribution under the applied polymerization conditions.[41]
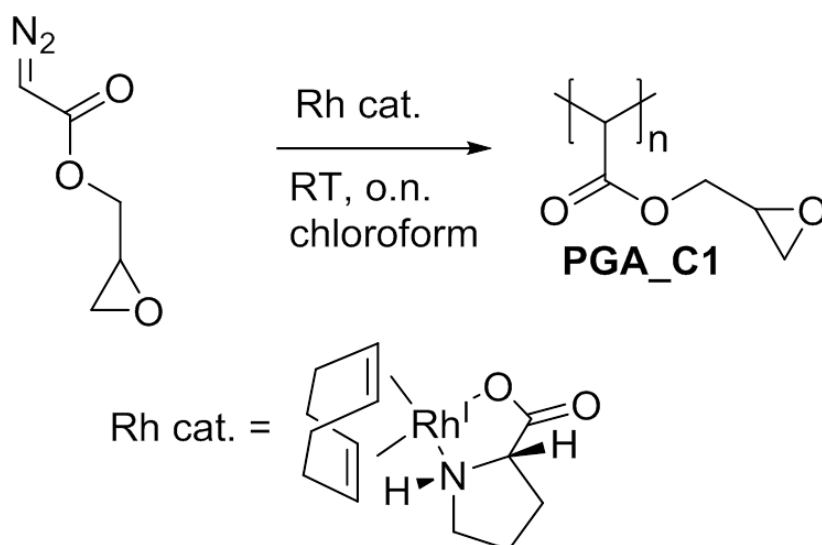
Scheme 3.3.: Rhodium mediated C1 polymerization of glycidyl 2-diazoacetate yielding poly(glycidyl 2-ylidene-acetate).
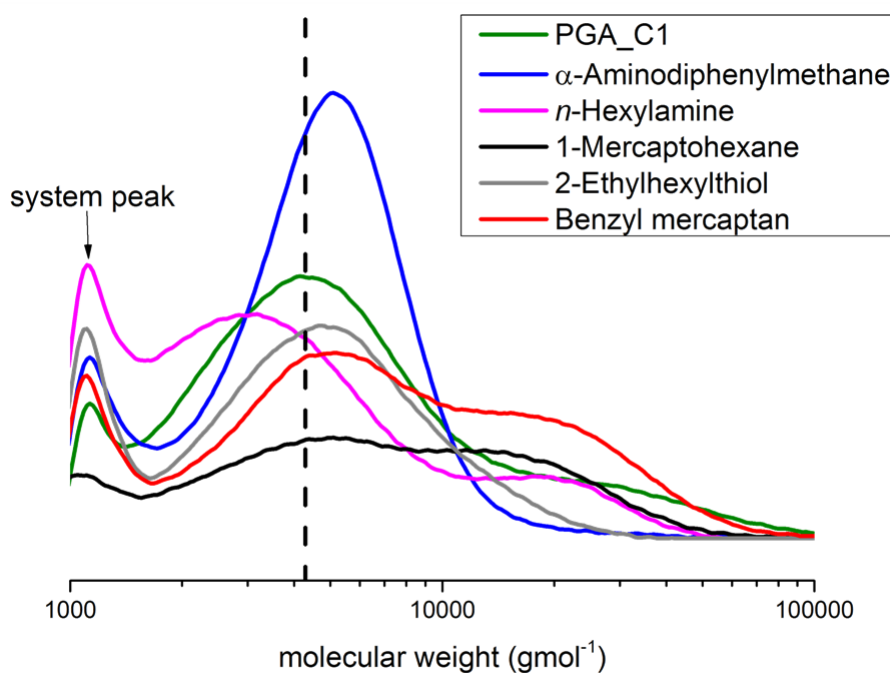
Fig. 3.28.: SEC data of poly(glycidyl 2-ylidene-acetate) before and after functionalization with selected amines and thiols. Dimethylformamide was used as eluent. Purification of the products via dialysis led to a decrease of the peak of low molecular weight material.

Figure 3.29 shows the ^{1}H NMR spectra obtained for the structural investigation of **PGA_C1** and **PGMA_C2**. The recorded spectra show the characteristic chemical shifts for the oxirane ring, with a doublet at 2.73 ppm and a singlet signal at 3.23 ppm. These signals recorded for **PGA_C1** are comparable to the signals obtained from **PGMA_C2**. However, compared to **PGMA_C2** and also compared to previously

reported other functional polymethylenes prepared via rhodium mediated C1 polymerization, conspicuous broader signals are observed for **PGA_C1**. A possible explanation for this might be the utilization of a racemic mixture of glycidol for C1 polymerization, thus resulting in non-stereoregular polymers, despite using a rhodium catalyst as suggested by a reviewer of the submitted manuscript. The chiral epoxide might lead to diastereomeric transition states, hence preventing the stereocontrolled mechanism which leads to syndiotactic functional polymethylenes.
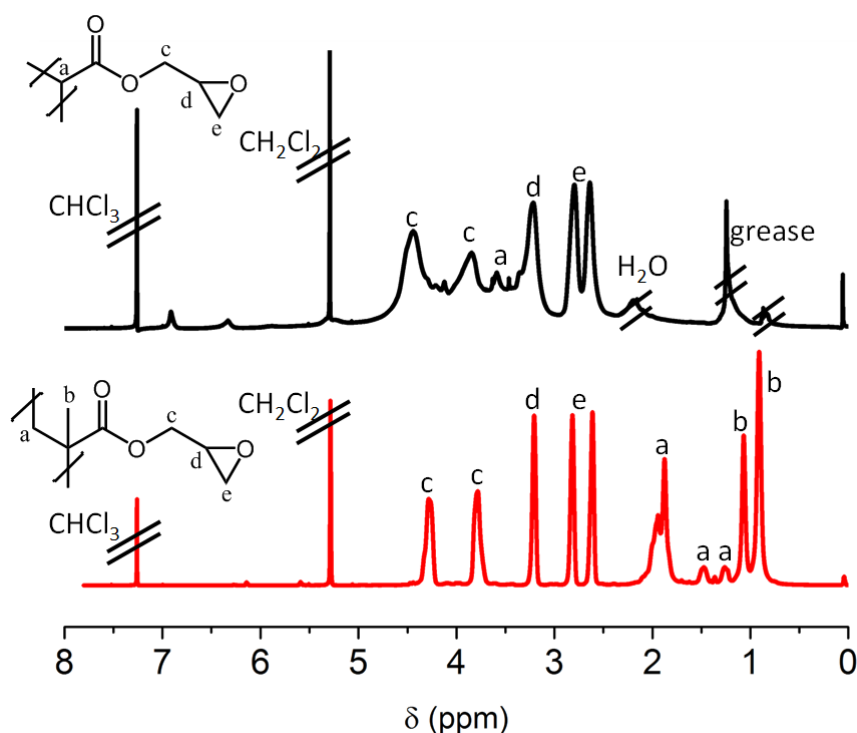
Fig. 3.29.: Comparison of ^{1}H NMR spectra obtained from poly(glycidyl 2-ylidene-acetate) **PGA_C1** (black line) and poly(glycidyl methacrylate) **PGMA_C2** (red line). The spectra were measured in CDCl$_3$.

It is noteworthy that, the ^{13}C NMR spectrum in Figure 3.30 does not show any signal for the backbone carbon C^a, this is due to signal overlapping with the carbon signal of the oxirane ring C^{e}at 44.5 ppm.
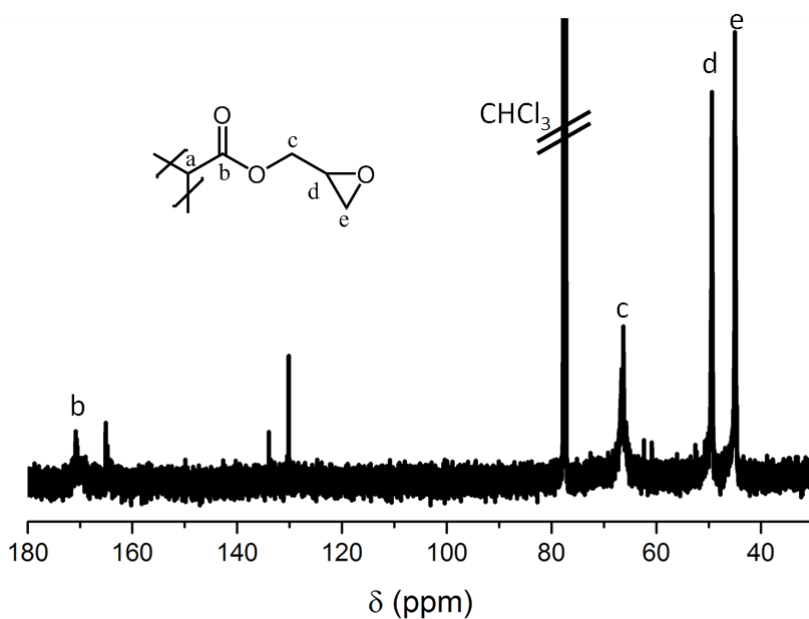
Fig. 3.30.: ^{13}C NMR of poly(glycidyl 2-ylidene-acetate) in CDCl$_3$.

The backbone signal for functional polymethylenes bearing ester side groups is generally observed in the proximity of 45 ppm. The overlap is proven by the ^{1}H-^{13}C HSQC NMR spectrum in Figure 3.31.
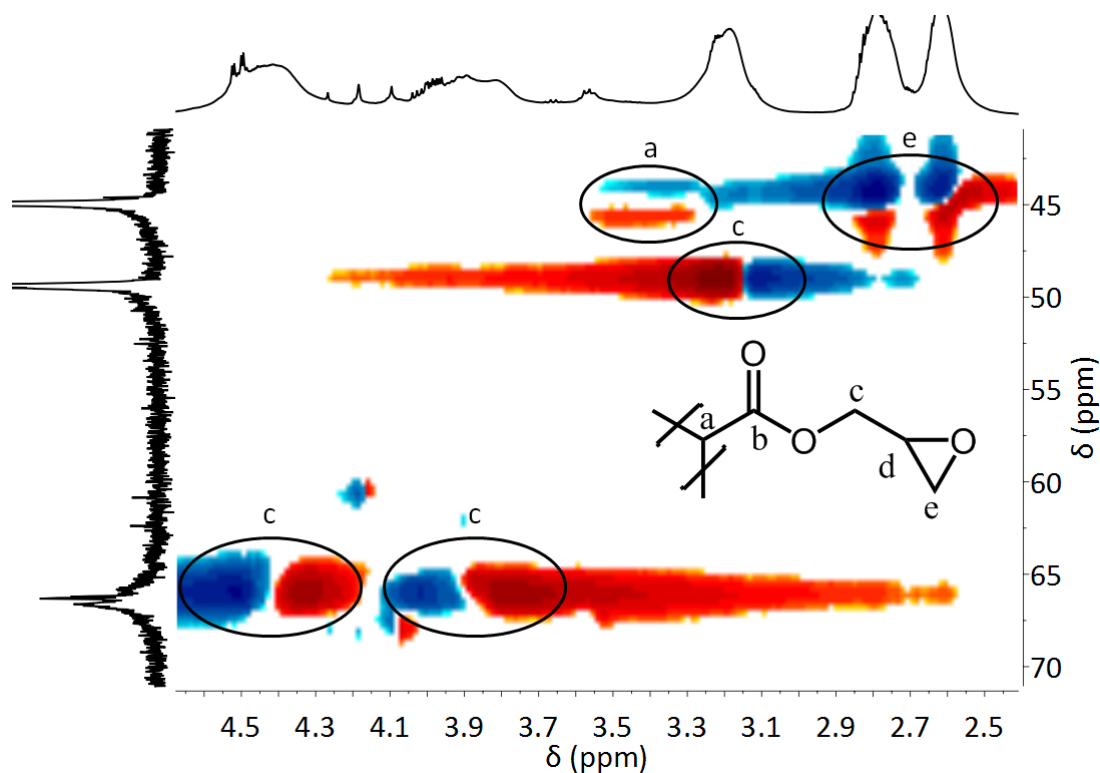
Fig. 3.31.: ^{1}H - ^{13}C HSQC NMR spectrum of poly(glycidyl 2-ylidene-acetate) in CDCl$_3$. This spectrum shows the overlap of the backbone signal C^a with the epoxide signal C^e in the ^{13}C NMR spectrum at 44.5 ppm.

Furthermore, besides the expected signals for the structure of **PGA_C1**, additional signals in the double bond region of the ^{1}H NMR spectrum (Figure 3.29) and ^{13}C NMR spectrum (Figure 3.30) were noted which could not be assigned at this point.

The FT-IR spectrum exhibits a carbonyl stretch vibration mode at $1730\,\text{cm}^{-1}$ and a strong band at $1155\,\text{cm}^{-1}$, characteristic for the C-O ester vibration (Fig. 3.32). Especially the two sharp signals at 905 and $852\,\text{cm}^{-1}$ are indicative of monosubstituted oxirane rings (vide supra).[90]
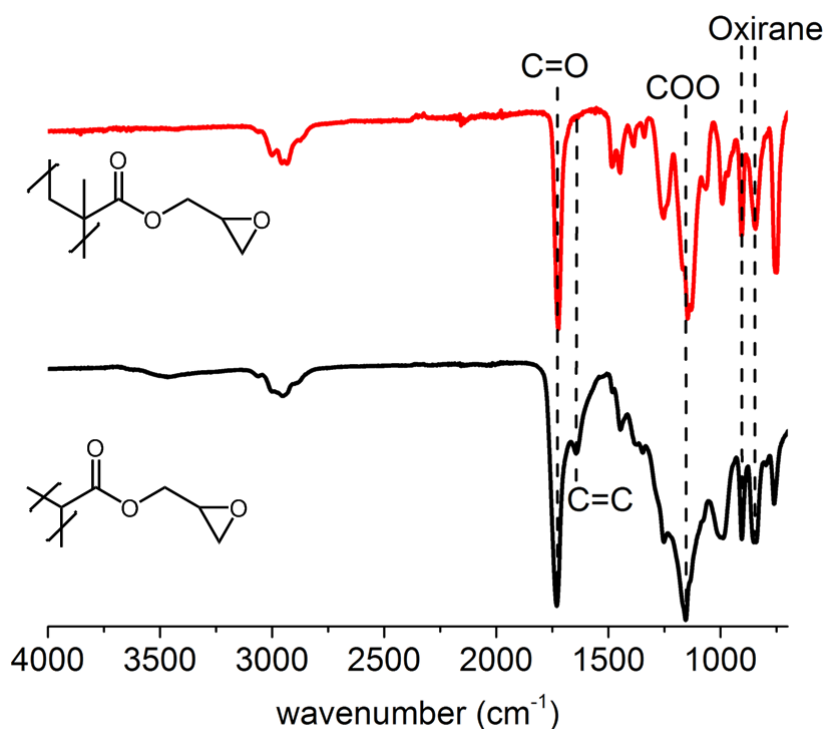
Fig. 3.32.: Comparison of FT-IR spectra obtained for poly(glycidyl methacrylate) **PGMA_C2** (red line) and poly(glycidyl 2-ylidene-acetate) **PGA_C1** (black line).

As shown above, a comparison with the structural analog methacrylate clearly supports the major constitution of a functional polymethylene bearing glycidyl acetate as a polar side group. However, one major difference between the two polymers **PGA_C1** and **PGMA_C2** can be seen in the FT-IR spectra, where it is most pronounced. An additional band for **PGA_C1** occurs at $1644\,\text{cm}^{-1}$ and a small broad band is noticeable at $3061\,\text{cm}^{-1}$. These two bands can be assigned to a C=C double bond. Evidence is given by a decrease of these signals after addition of elemental bromine to a solution of **PGA_C1** in dichloromethane (Fig. A.14). Bromine addition does not only lead to a bromination of the C=C double bonds, but also the oxirane ring is opened, thereby forming halohydrins and explaining the newly formed strong band at $3427\,\text{cm}^{-1}$ assigned to a hydroxy group.[91] Furthermore, a slight broad band in the FT-IR spectrum of

PGA_C1 is already noticeable at $3465\,\text{cm}^{-1}$, suggesting a hydroxy group as well. Taking all the previous signal assignments into account, an additional substructure, due to a partial β-H elimination of the methylene group next to the epoxide ring is proposed. This substructure is anticipated to be formed during the polymerization process and results in a partial cleavage of the ring structure and a related C=C double bond formation. The proposed structure is shown in Scheme 3.4 and the proportion of this double bond containing structure is below $5\,\text{mol}\%$ according to the ^{1}H NMR spectrum.
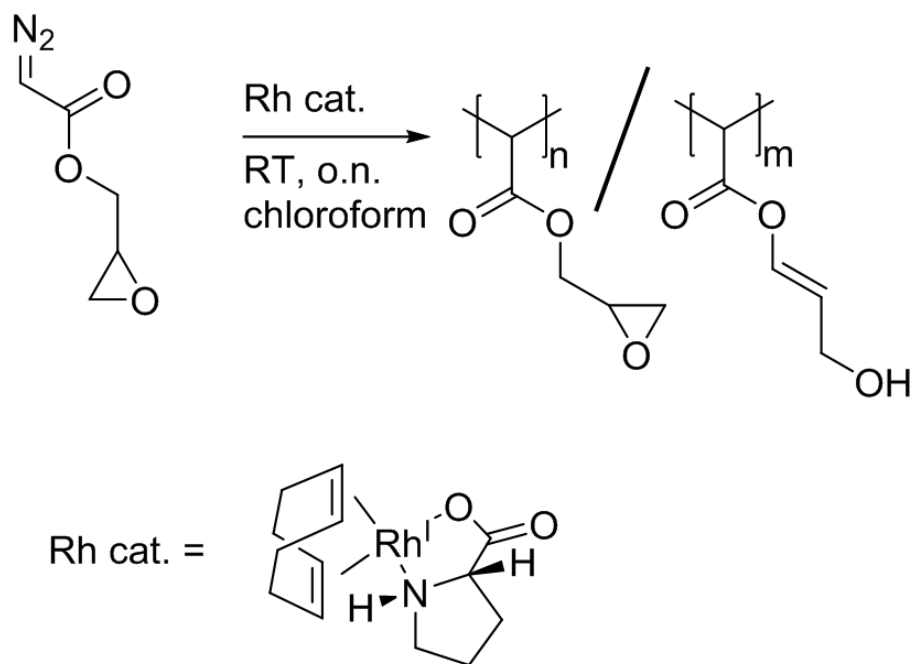
Scheme 3.4.: Partial β-H-elimination of the methylene group next to the epoxide ring of poly(glycidyl 2-ylidene-acetate) during the polymerization process, resulting in a partial cleavage and C=C double bond formation.

Figure 3.33 reveals the two thermal decomposition steps of **PGA_C1** as recorded by thermogravimetric analysis. An onset temperature of $260\,°\text{C}$ was determined for the first weight loss step, the second one occurred at an onset temperature of $457\,°\text{C}$. Again, according to the weight loss curves **PGA_C1** and **PGMA_C2** are similar for the first thermal decomposition at $260\,°\text{C}$, but no second weight loss step is observed for the C2 polymer. At this point, no explanation can be given for this. By utilization of glycidyl acrylate instead of glycidyl methacrylate in future research, it might be possible to elucidate this in more detail.
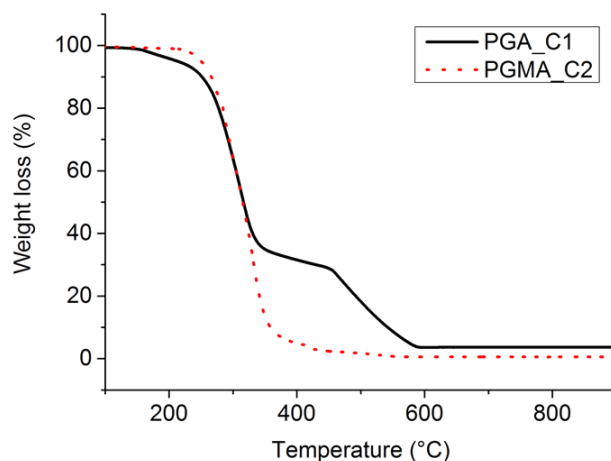
Fig. 3.33.: TGA data of **PGA_C1** (black solid line) and **PGMA_C2** (red dotted line) in comparison. The measurement was done at a heating rate of 10K/min under air.

3.3.4. Post-Polymerization Modification of Poly(glycidyl 2-ylidene-acetate)

Oxirane rings can be easily opened with various nucleophiles, due to a release in ring strain. This addition of nucleophiles enables the attachment of multiple functionalities to the polymer backbone. The reactivity of **PGA_C1** was initially tested by ring-opening under acidic conditions, resulting in a water soluble diol-polymethylene (Fig. 3.34).
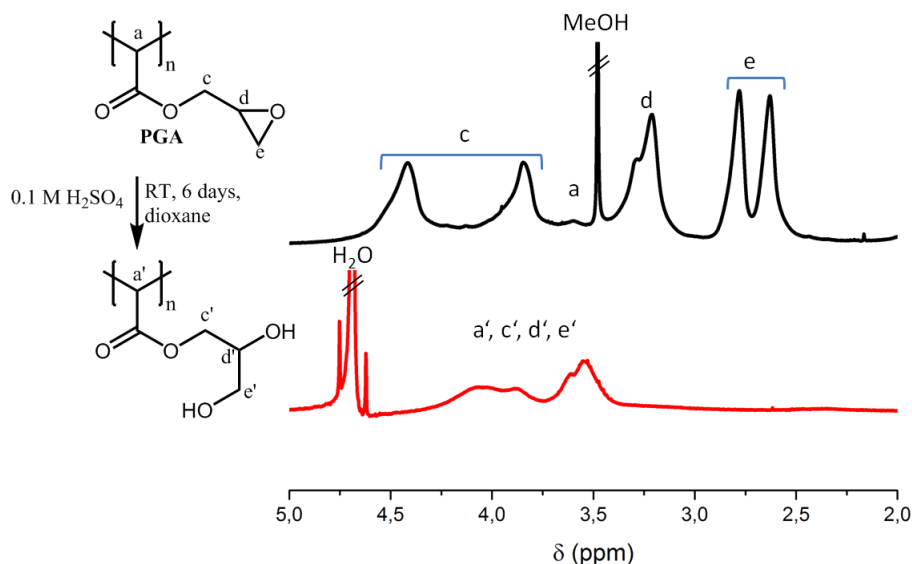
Fig. 3.34.: **PGA_C1** hydrolysis utilizing acidic conditions. ^{1}H NMR spectra prior to (black line) and after (red line) ring opening. The ^{1}H NMR spectrum of **PGA_C1** was measured in deuterated chloroform and the diol functionalized species was dissolved in D_2O for analysis.

This reaction proceeds quantitatively according to the ^{1}H NMR spectrum, as shown by the absence of ring proton signals at 2.73 ppm and 3.23 ppm. Furthermore, new and broad signals at higher ppm values between 3.33 ppm and 4.50 ppm were recorded and the initially split signals of the methylene group (H^c) merge after acidic treatment to a broad peak between 3.75 and 4.50 ppm (H$^{c'}$).

Subsequently, I explored the reaction of **PGA_C1** with various amines and thiols (Scheme 3.5). These results were compared with functionalizations of **PGMA_C2** known from the literature utilizing the same reaction conditions.
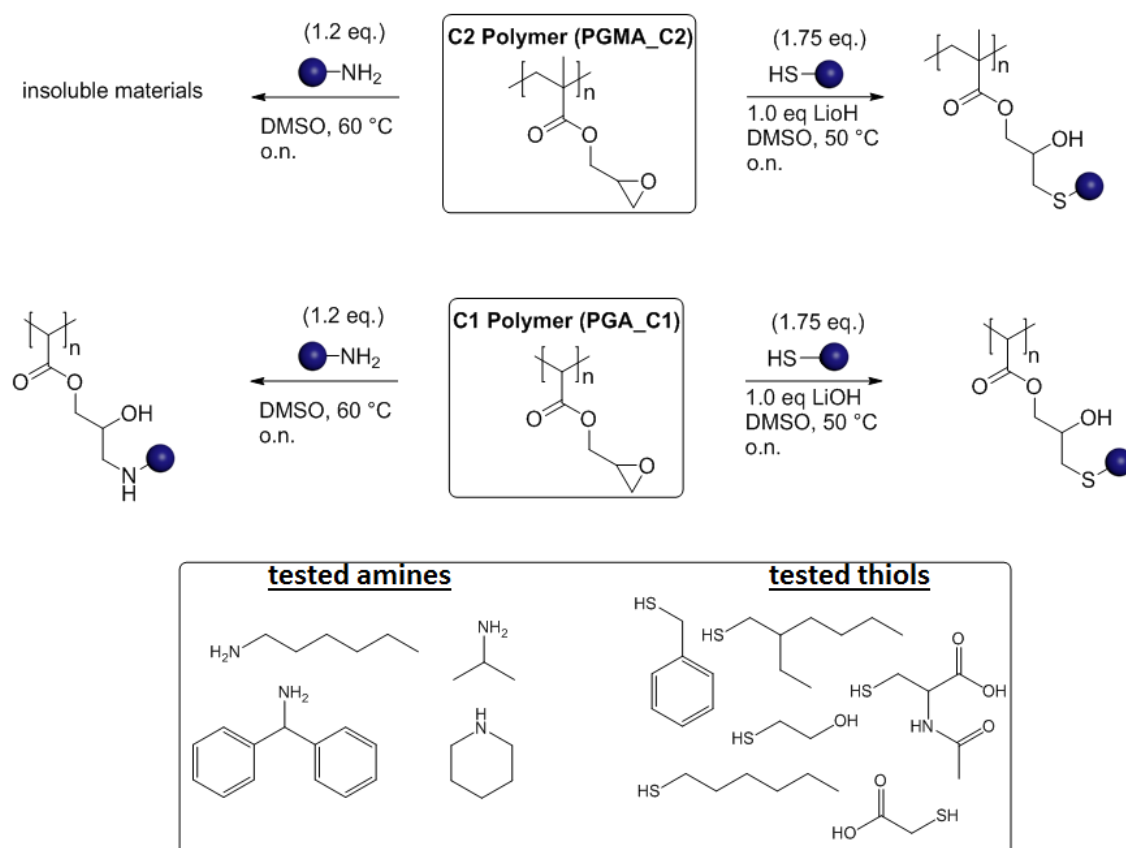
Scheme 3.5.: Amine and thiol ring-opening reactions of poly(glycidyl 2-ylidene-acetate) and poly(glycidyl methacrylate) with various nucleophiles. The thiol ring-opening reactions of poly(glycidyl methacrylate) were solely investigated for benzylmercaptan and 1-mercaptohexane.

Modification with Amines

Previous reports describe the functionalization of **PGMA_C2** with primary amines and the formation of insoluble materials due to intramolecular and intermolecular cross-coupling reactions.[68] In contrast, the functionalization of **PGA_C1** with primary amines did result in soluble materials with almost quantitative conversions according to their investigation by ^{1}H NMR and IR spectroscopy (Fig. 3.35). The accurate calcula-

tion of the conversion proved to be difficult again since the signals overlap in the spectra; however, the conversion was in all cases estimated to be more than 90%. Noteworthy, IR spectroscopy is highly sensitive to functional groups, and some of the functionalized products show a remaining oxirane ring even though NMR showed quantitative conversions (Fig. A.18). Reactions were performed overnight in dimethyl sulfoxide at 60 °C with 1.2 equivalents of the respective amine. Probably, the reason why functionalized **PGA_C1** remained soluble is due to a strong preference of intramolecular reactions over intermolecular cross-coupling reactions. These intramolecular secondary reactions are hard to distinguish from single additions by spectroscopic means; however, as shown by our previous studies, they are likely to occur in C1 polymers.[78] In this study (Chapter 3.1), functionalization of poly(benzyl 2-ylidene-acetate) with primary amines leads to the formation of a cyclic 5-membered imide structure, while no intramolecular reaction was observed for the structural analog C2 polymer poly(benzyl acrylate).

Figure 3.35 exemplary depicts spectral data for **PGA_C1** before and after functionalization with *n*-hexylamine and α-aminodiphenylmethane all other spectral data are part of appendix A.3. The ^{1}H NMR spectra prove the successful ring-opening due to absence of the ring protons at 2.73 ppm and 3.23 ppm. Additionally, the appearance of new signals in the alkyl region (0.63 ppm - 1.63 ppm) of the ^{1}H NMR spectra further supports the functionalization with *n*-hexylamine, while aromatic signals (6.82 ppm - 7.66 ppm) clearly provide evidence for a successful functionalization with α-aminodiphenylmethane.
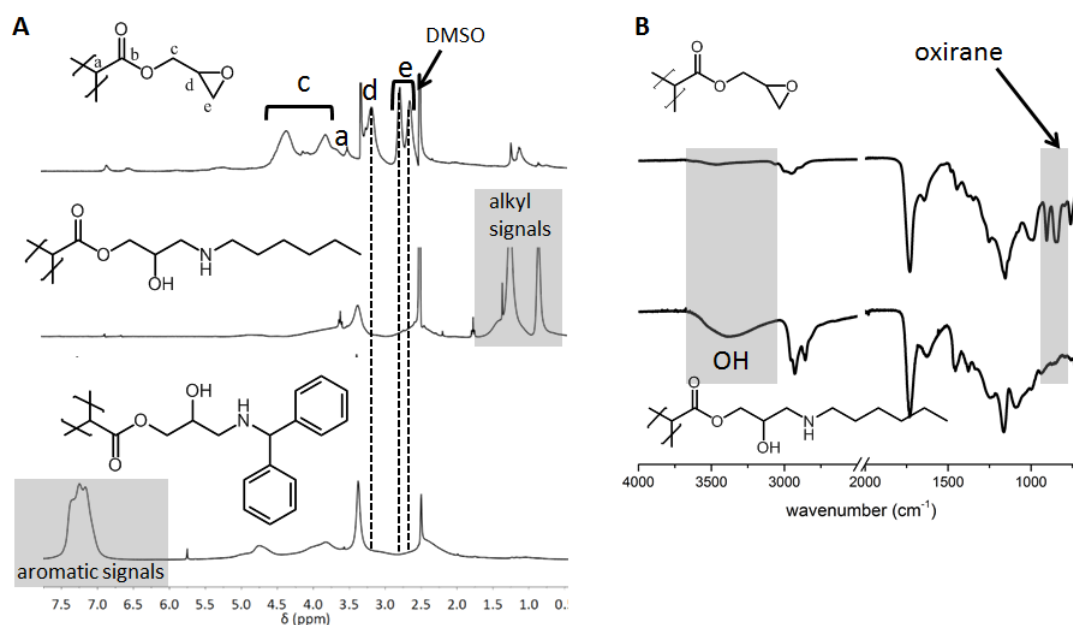
Fig. 3.35.: Analytical data before and after functionalization of poly(glycidyl 2-ylidene-acetate). (**A**) ^{1}H NMR spectra of **PGA_C1** before and after functionalization with *n*-hexylamine and α-aminodiphenylmethane; (**B**) FT-IR spectra showing a successful conversion of **PGA_C1** with *n*-hexylamine.

Further evidence for a successful modification is given by the absence of oxirane vibration bands at 905 and 852 cm^{-1} in the FT-IR spectrum and the appearance of a broad OH vibration band at 3388 cm^{-1}. Especially the successful reaction with α-aminodiphenylmethane was rather unexpected, as it is a sterically demanding amine. Size exclusion chromatography of **PGA_C1** after functionalization with α-aminodiphenylmethane showed an increase in molecular weight, as expected for an addition post-polymerization modification (see Fig. 3.28). However, the molecular weight determined at the peak maximum resulted only in a slight increase from $M_{max} = 4300$ gmol^{-1} to $M_{max} = 5100$ gmol^{-1}. This might be attributed to the high side group density that results in a deviation from a random coil formation due to chain extension. Contrary, an unexpected decrease in molecular weight was observed for *n*-hexylamine ($M_{max} = 3100$ gmol^{-1}) which might indicate the presence of hydrogen bonding and a consequent compression of the particle size which did not take place for the sterically demanding α-aminodiphenylmethane. Piperidine as a secondary amine was also used to elucidate the reactivity of the C1 polymer. It was successfully and quantitatively converted in **PGA_C1** functionalization, highlighting the versatility of this post-polymerization modification approach.

Modification with Thiols

Next, the investigation of **PGA_C1** with various thiols was investigated. The experimental work was inspired by previously reported studies by *Gadwal* et al. and their investigation of **PGMA_C2**.[88] In general, rather harsh reaction conditions were employed, utilizing a stochiometric amount of lithium hydroxide and performing the reaction at 50 °C in dimethyl sulfoxide. The reactions were allowed to proceed overnight to achieve high conversions. Initial experiments with and without base or thiol were performed and clarified the importance of each compound. Thus, data misinterpretations were prevented from the beginning. In the absence of any thiol, by the sole addition of lithium hydroxide in an equimolar quantity (1.0 eq.) to a solution of **PGA_C1** in dimethyl sulfoxide, no ring cleavage was observed during a 22-hour reaction time at 50 °C. In the presence of thiols (1.75 eq.), the same reaction conditions resulted in quantitative conversion. Again, the conversion could only be estimated due to signal overlapping in the ^{1}H NMR spectrum. Estimated conversions for all investigated thiols were found to be more than 90%. Figure 3.36 shows no remaining signals for the bottom spectrum at 2.73 ppm and 3.23 ppm, clearly evidencing a successful quantitative conversion of **PGA_C1** with 2-ethylhexylthiol by ^{1}H NMR spectroscopy. Furthermore, new signals at 0.88 ppm, 1.04 - 1.60 ppm and 2.54 ppm result from the attached alkyl chain protons of 2-ethylhexylthiol. Again, the FT-IR spectrum provides further proof for a successful conversion by the absence of oxirane vibration bands at

905 and 852 cm⁻¹and the newly formed broad OH vibration band at 3450 cm⁻¹.
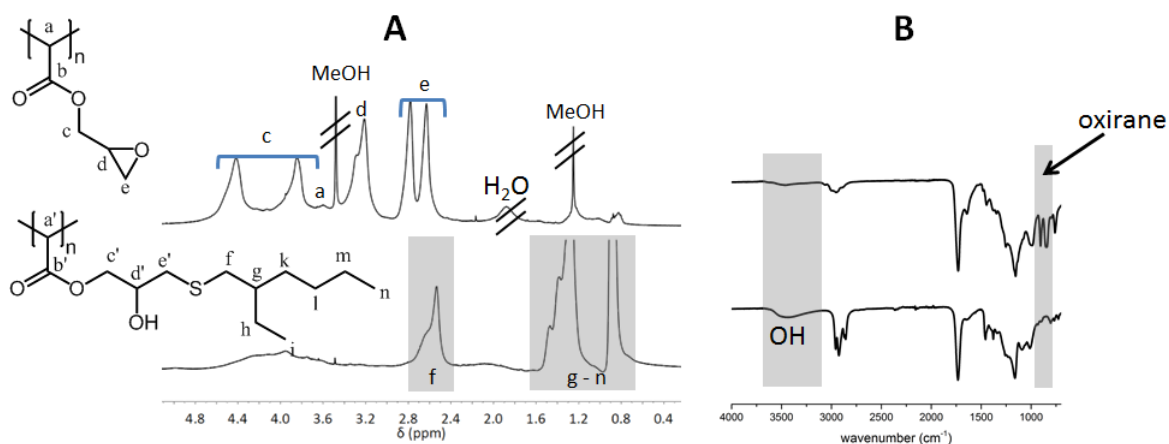
Fig. 3.36.: Post-polymerization modification of poly(glycidyl 2-ylidene-acetate) with 2-ethylhexylthiol. (**A**) ¹H NMR spectrum; (**B**) FT-IR spectrum.

The SEC data after thiol modification showed a slight increase of the peak maxima (Fig. 3.28). However, similar to the case of post-modification with amines, these data underestimate the molecular weight change, since size exclusion chromatography does not account correctly for deviations from a spherical shape and is solely a relative method for molecular weight determination based on calibration with polystyrene standards. No steric limitations were observed for thiol modifications. Furthermore, comparison of the post-polymerization modification results of **PGA_C1** and **PGMA_C2** with 1-mercaptohexane and benzylmercaptan does not reveal differences in the conversion. Both polymers were quantitatively converted and it was concluded that steric hindrance is not an issue which negatively influences thiol promoted oxirane cleavage. Hence, these post-polymerization modifications are broadly applicable due to the solubility of **PGA_C1** in a number of different mid-range organic solvents, such as chloroform and tetrahydrofurane, as well as polar solvents, such as dimethylsulfoxide and *N,N*-dimethylformamide.

3.3.5. Conclusion

The successful synthesis of poly(glycidyl 2-ylidene-acetate) and facile post-polymerization modification via oxirane cleavage of the three-membered ring are presented. Nucleophilic moieties, such as various amines and thiols were utilized for ligation reactions which did not lead to significant disturbances due to steric hindrance of bulky amines or thiols was found. In comparison to poly(glycidyl methacrylate), the modification with primary amines lead to soluble polymers. This was attributed to a predominant occurrence of intramolecular reactions rather than intermolecular cross-coupling reactions as previously

reported for poly(glycidyl methacrylate). Noteworthy, no conversion differences were observed for oxirane ring-opening reactions with thiols for poly(glycidyl methacrylate) and poly(glycidyl 2-ylidene-acetate). Overall, poly(glycidyl 2-ylidene-acetate) proved to be currently the best choice for a broad range of different ligation reactions, thus offering access to a wide range of new functional polymethylenes.

3.4. One Monomer Multiple Polymers

3.4.1. Introduction

Diazocarbonyl compounds are fascinating compounds with frequent use as reactants in organic chemistry as already stated in Chapter 1. Their inherent reactivity can be fine-tuned by alteration of the functionalities. The predominant reaction in most cases is the initial formation of carbenes by loss of nitrogen; however, applying suitable reaction conditions with the right catalysts can result in divergent reactivities. For example, the group of *Liu* and co-workers observed pyrazole formation upon 1,3-dipolar cycloaddition of diazo groups to terminal alkynes.[92] They utilized bisdiazo compounds and bisalkynes, for the formation of polypyrazoles (Scheme 3.6).
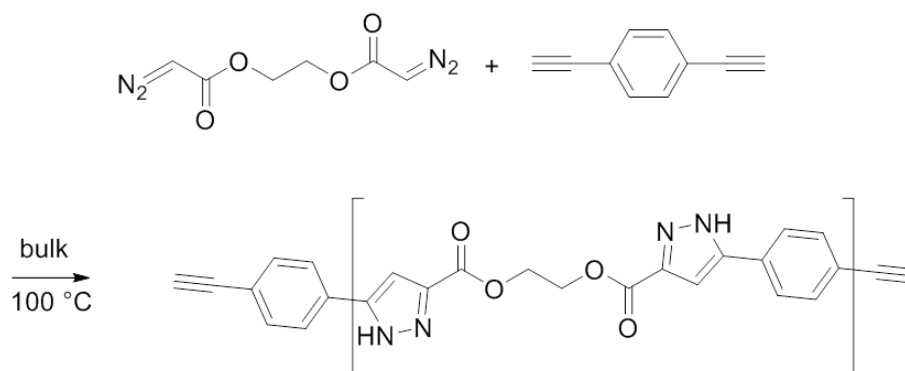
Scheme 3.6.: One example of polypyrazole synthesis by utilization of bisdiazo compounds and bisalkynes. Adapted from reference.[92]

Herein, inspired by *Liu* and co-workers, the utilization of propargyl 2-diazoacetate as monomer for two different polymers is described. Namely, rhodium mediated C1 polymerization led to the formation of the corresponding functional polymethylene, which thermally induced 1,3-dipolar cycloaddition resulted in the formation of a polypyrazole. The latter reaction was already reported by *Shapiro* et al. in 1991 where they observed the formation of oligopyrazoles after longer periods (2 weeks) during storage at 0 °C.[93] However, they did not further characterize the obtained polymer. In addition, by utilizing a single compound bearing both reactive functionalities* in a stochiometric 1:1 ratio, the presented synthesis of a polypyrazole should result in higher molecular weights compared to the approach by *Liu* and co-workers (polypyrazoles in the MW range of 6500 - 9300 gmol^{-1}).[92]

---

*Characteristic of an AB-monomer, i.e. propargyl 2-diazoacetate contains a diazo and an alkyne group.

3.4.2. Synthesis and Characterization of Propargyl 2-diazoacetate

The monomer propargyl 2-diazoacetate can be prepared via both synthetic routes (A & B) as shown in Scheme 1.9; however, since the synthetic effort for route B is less, this route was preferred. The monomer was obtained as a yellow liquid in 34%, comparable to other diazo esters prepared in this work. The inherent high reactivity of α-diazocarbonyl compounds often results in relatively low yields, commonly below 50%. Figures 3.37-3.39 clearly show the successful preparation as evidenced by ^{1}H NMR, ^{13}C NMR and FT-IR spectroscopy.

The small and broad singlet peak at 4.84 ppm in the ^{1}H NMR spectrum (Fig. 3.37) is the commonly observed shape of the proton signal for the N_2=CH- group (compare with Fig. 3.25). The corresponding carbon atom appears at 46.4 ppm in the ^{13}C NMR spectrum (Fig. 3.38) and the C-H vibration of this group can be assigned to the weak band in the FT-IR spectrum at 3177 cm^{-1} (Fig. 3.39). The present methylene group results in signals at 4.78 ppm and 52.2 ppm in the respective NMR spectrum. An additional strong peak arises from the methine group at 2.51 and 75.0 ppm in the respective spectrum.
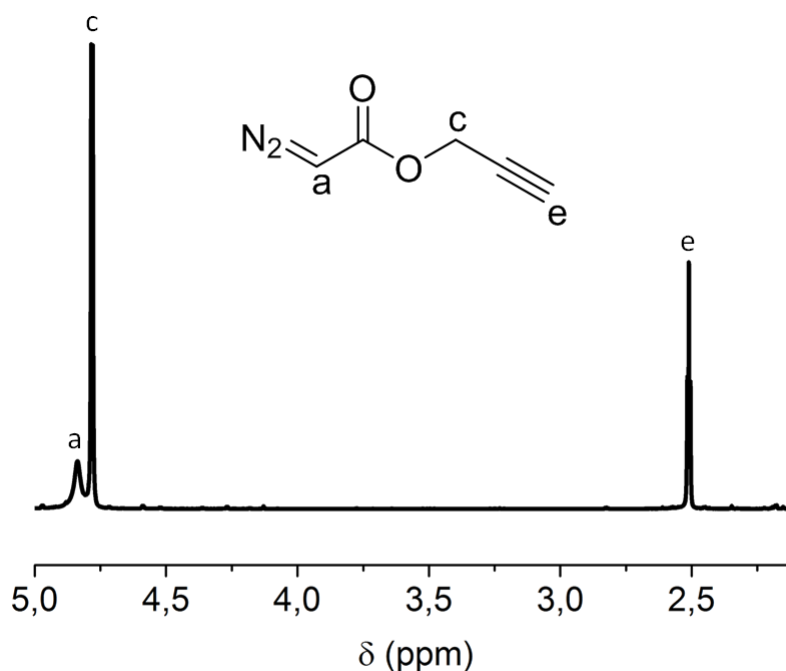
Fig. 3.37.: ^{1}H-NMR spectrum of propargyl 2-diazoacetate measured in deuterated chloroform at 300 MHz.
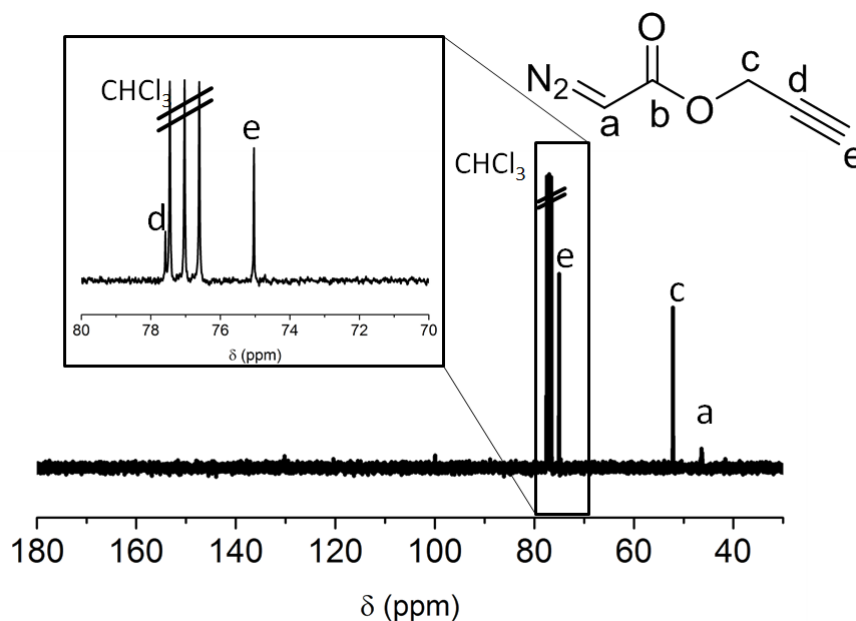
Fig. 3.38.: ^{13}C-NMR spectrum of propargyl 2-diazoacetate measured in deuterated chloroform at 75 MHz.

In addition to the above-mentioned signals, the α-diazocarbonyl compound exhibits a strong diazo vibration band at 2110 cm^{-1}. Furthermore, the proton attached to the C≡C triple bond gives rise to a signal at 3292 cm^{-1}.
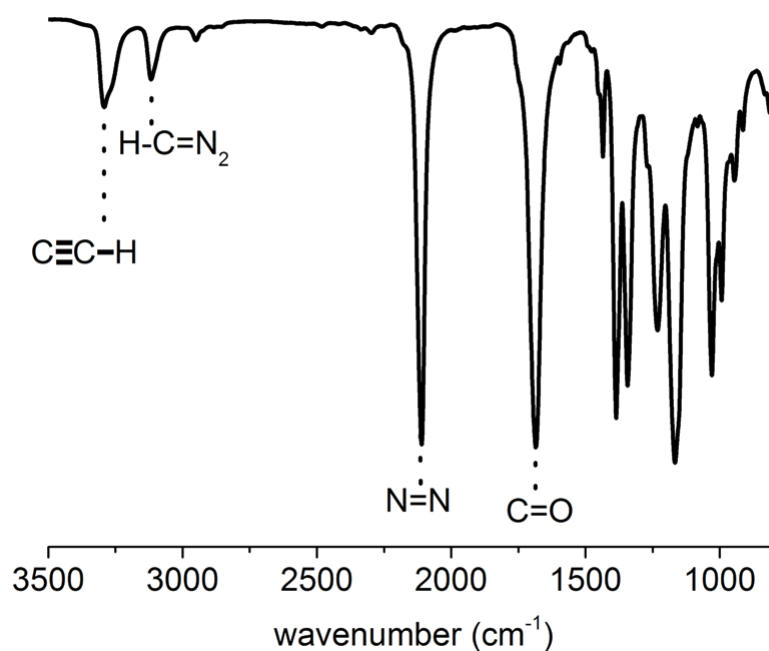
Fig. 3.39.: FT-IR spectrum of propargyl 2-diazoacetate.

Overall, propargyl 2-diazoacetate bears two highly reactive functional groups, namely the diazo group and the alkyne. Due to these functionalities multiple reactions are

triggerable by application of suitable reaction conditions. Two approaches towards the synthesis of a functional polymethylene and a polypyrazole are described in the following.

3.4.3. Synthesis and Characterization of Poly(propargyl 2-ylidene-acetate)

First, propargyl 2-diazoacetate was polymerized via rhodium mediated C1 polymerization, utilizing [(*L*-prolinate)Rh^I(1,5-dimethyl-1,5-cyclooctadiene)] as catalyst and chloroform as solvent (Scheme 3.7).
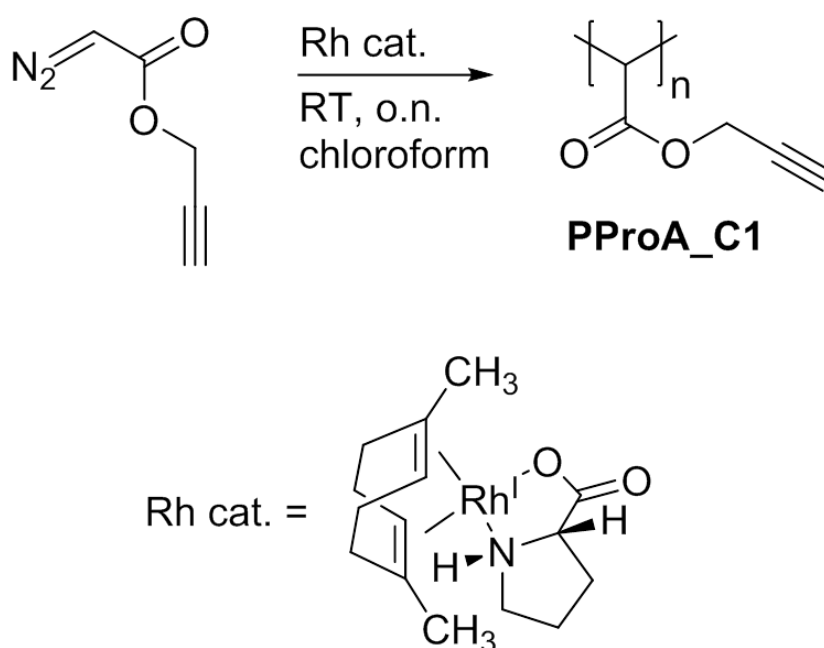
Scheme 3.7.: Rhodium mediated C1 polymerization of propargyl 2-diazoacetate to yield poly(propargyl 2-ylidene-acetate).

The reaction was performed at room temperature in chloroform and proceeded overnight. In contrast to previous C1 polymerizations, the reaction solution turned slightly turbid and the turbid particles were filtered off before further purification. The turbidity is presumably an accompaniment of the highly reactive carbon-carbon triple bond. However, the major fraction is poly(propargyl 2-ylidene-acetate) **PProA_C1**, and the polymer was obtained after rapid precipitation and lyophilization from 1,4-dioxane to prevent crosslinking as already observed for poly(allyl 2-ylidene-acetate).[80] After lyophilization, a soluble polymer with a yield of 22% was obtained. It is likely that the crosslinking can be attributed to similar reasons as observed for poly(allyl 2-ylidene-acetate) and poly(allyl acrylate) which are subject to the discussion in Chapter 3.2 and which bear a highly reactive unsaturated bond, as well.[80,82]

The ^{1}H NMR spectrum of **PProA_C1** in Figure 3.40 still exhibits the methylene and methine group at 4.78 and 2.51 ppm, respectively. .
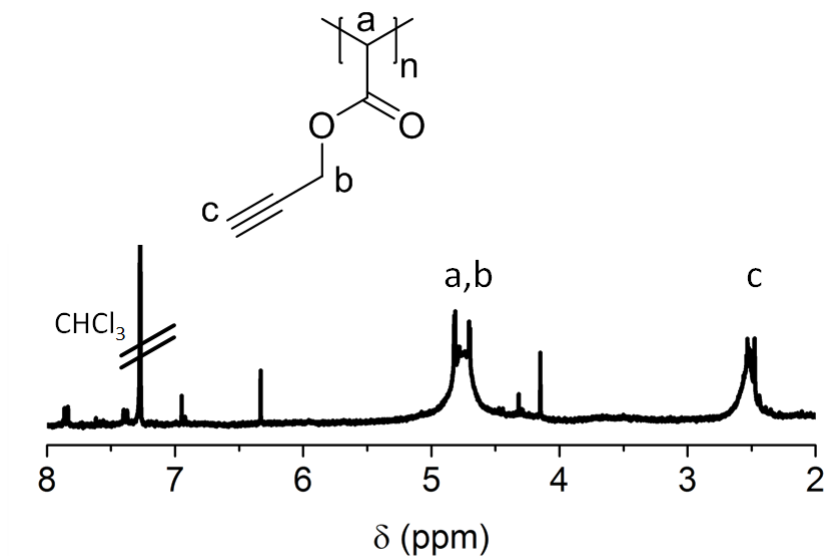
Fig. 3.40.: ^{1}H-NMR spectrum of poly(propargyl 2-ylidene-acetate) measured in deuterated chloroform at 300 MHz.

Furthermore, the N=N$_{stretch}$ vibration, as recorded via FT-IR spectroscopy (Fig. 3.41) at 2110 cm^{-1}, as well as the N$_2$C-H vibration at 3177 cm^{-1} cm^{-1} substantially declined or vanished completely.
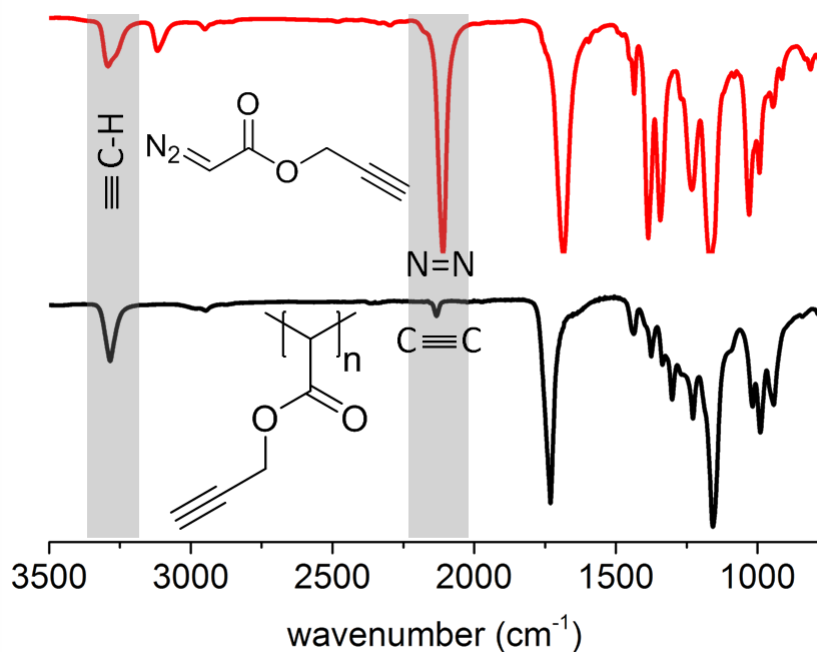
Fig. 3.41.: FT-IR spectrum of poly(propargyl 2-ylidene-acetate) (black line) in comparison to the FT-IR spectrum of the monomer propargyl 2-diazoacetate (red line).

Noteworthy, the remaining weak signal at $2110\,\text{cm}^{-1}$ can also be attributed to the C≡C stretch vibration, thereby, a quantitative conversion as for all previously investigated α-diazocarbonyl compounds is assumed. Additional evidence for a successful C1 polymerization is given by the vibrational band at $3294\,\text{cm}^{-1}$, remaining unaffected by the polymerization and originating from the C-H$_{\text{stretch}}$ vibration of the C≡C triple bond. The spectral data provide evidence for a successful C1 polymerization of novel **PProA_C1**. The recorded molecular weight distribution shows predominantly lower molecular weight chains, while some chains exhibit a molecular weight up to $20{,}000\,\text{g}\,\text{mol}^{-1}$ (Fig. 3.42) .
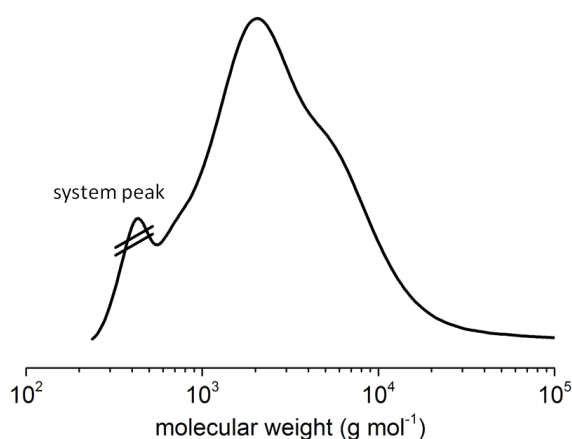
Fig. 3.42.: SEC trace of poly(propargyl 2-ylidene-acetate). Tetrahydrofurane was used as eluent.

A molecular weight of $2100\,\text{gmol}^{-1}$ was determined at the peak maximum.[†]
The TGA weight loss curve of **PProA_C1** is depicted in Figure 3.40 and exhibits an onset of 230 °C. The trend is similar as for **PAA_C1** but rather broad compared to **PEA_C1 and PBnA_C1** (compare with Fig. 3.20).
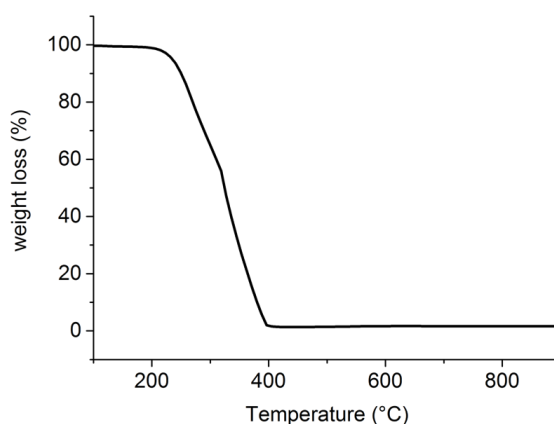
Fig. 3.43.: TGA data of **PProA_C1**. The measurement was done at a heating rate of 10K/min under air.

[†]The signal overlap with the system peak prevents proper determination of M_n and M_w.

3.4.3.1. Post-Polymerization Modification via Azide-Alkyne Reaction

The reactivity of the carbon-carbon triple bond of **PProA_C1** was proven by a successful post-polymerization modification with benzyl azide. Azide-alkyne reactions or *Huisgen* 1,3-dipolar cycloadditions are often used for facile post-polymerization modification of polymers bearing either azide or alkyne functionalities. Clearly, the triple bond proton at 2.53 ppm vanishes in the ^{1}H NMR spectrum, while novel signals in the aromatic region of the chemical shift appear (Fig. 3.44).
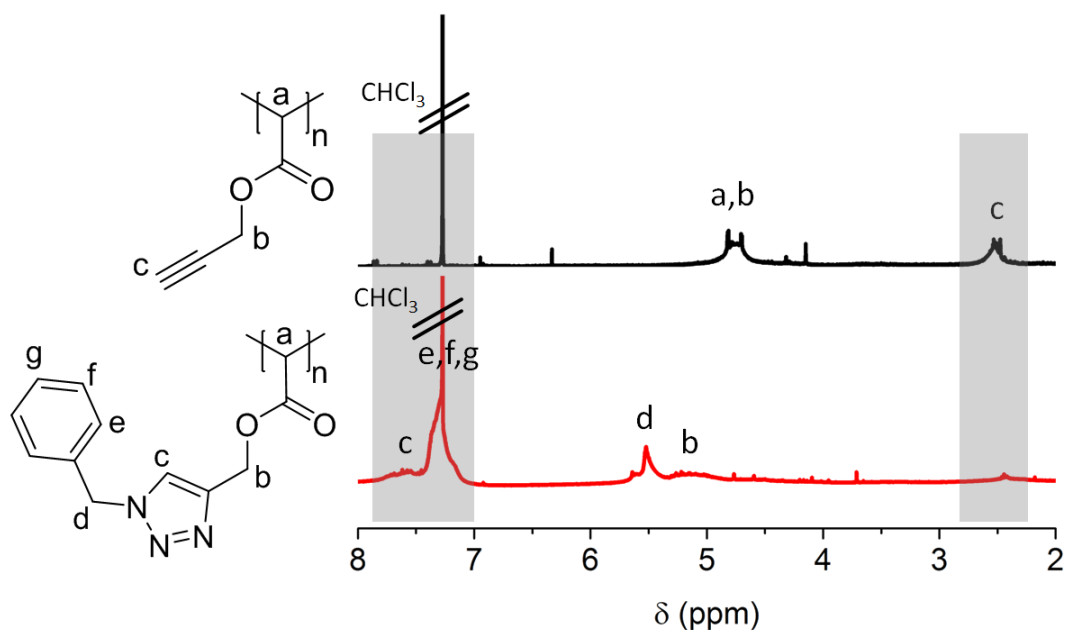
Fig. 3.44.: ^{1}H-NMR spectra recorded for poly(propargyl 2-ylidene-acetate) prior to (black line) and after (red line) functionalization with benzyl azide. NMR spectra were recorded in CDCl$_3$.

These aromatic signals are highlighted in grey and originate from the benzyl group as well as from the formed aromatic 1,2,3-triazole. Further investigation is required in order to explore alkyne-azide cycloadditions in-depth.

3.4.4. Polypyrazole Synthesis and Characterization

In a second polymerization approach, propargyl 2-diazoacetate was subject to a polypyrazole formation at elevated temperatures (100 °C) in bulk state (Scheme 3.8).

As illustrated in Figure 3.45 and Figure 3.46, the spectral data are proof for the proposed synthesis. The proton NMR spectrum (Fig. 3.45) exhibits signals arising from the heteroaromatic ring structure. The proton attached to the nitrogen atom (H^b) appears between 13.49-14.26 ppm and the proton attached to the aromatic carbon atom (H^c)
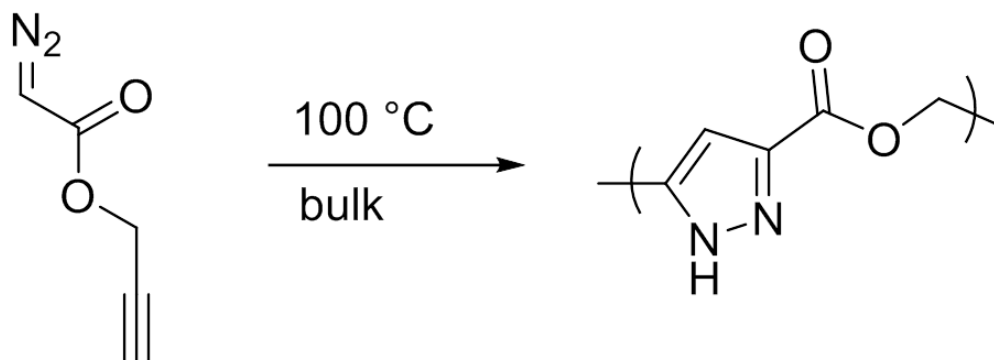
Scheme 3.8.: Bulk polymerization of propargyl 2-diazoacetate at elevated temperatures leads to the formation of a polypyrazole.

appears at 6.88 ppm, thus it is shifted further downfield as the triple bond proton due to electronic reasons arising from the pyrazole formation. Also the signal H^a at 5.32 ppm is slightly shifted to higher ppm values compared to the corresponding monomer signal at 4.78 ppm.
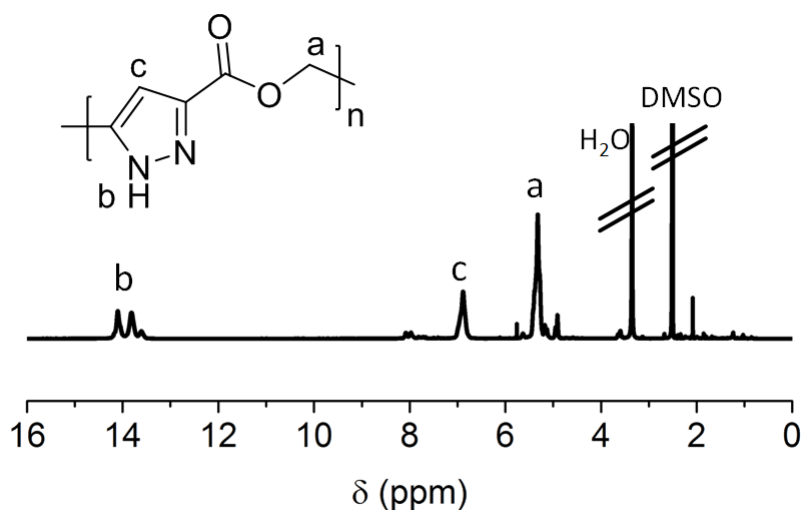
Fig. 3.45.: ^{1}H-NMR spectrum of the synthesized polypyrazole measured in DMSO-d^6 at 300 MHz.

Besides the ^{1}H NMR spectrum, a broad N-H vibration band of the product can be observed in the FT-IR spectrum above 3000 ppm and the N=N bond at 2110 cm^{-1}, being characteristic for the monomer species, vanished almost completely (Fig. 3.46).
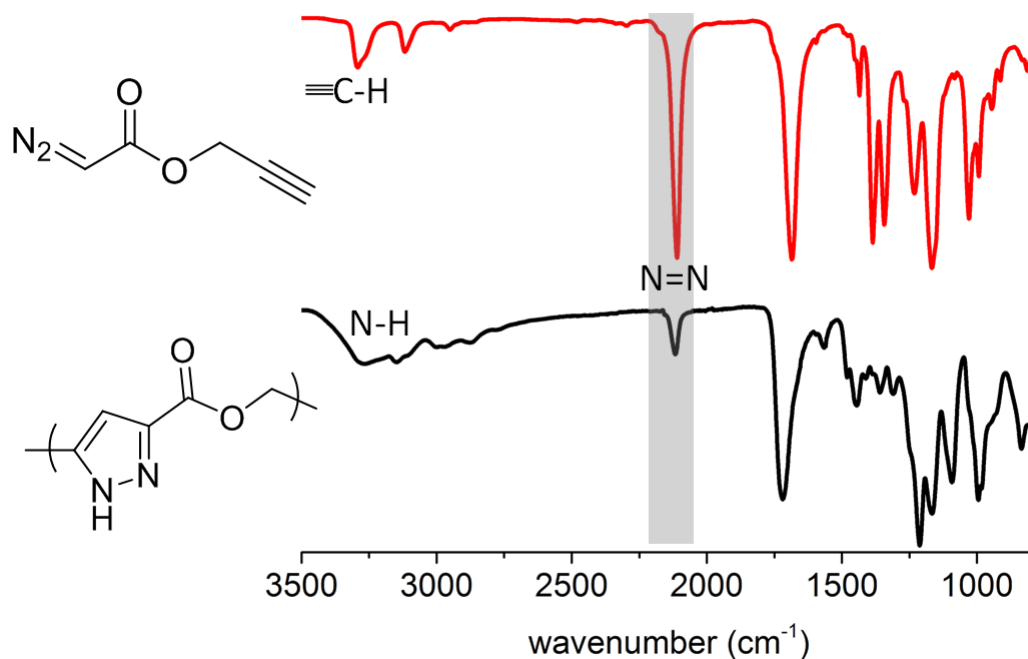
Fig. 3.46.: FT-IR spectra of the synthesized polypyrazole (black line) in comparison to propargyl 2-diazocacetate (red line).

The recorded SEC trace (Fig. 3.47), utilizing dimethylformamide as eluent, illustrates a broad molecular weight distribution (Đ $= 1.86$). The average molecular weights were determined to be $M_n = 5300 \, \text{gmol}^{-1}$ and $M_w = 9800 \, \text{gmol}^{-1}$, thus clearly showing the formation of a polymeric species. Unexpectedly, in comparison with the previously reported polypyrazoles, a similar molecular weight was recorded for the present AB-monomer. This is likely due to the bulk reaction conditions preventing diffusion as a result of solidification at an advanced stage of the reaction.
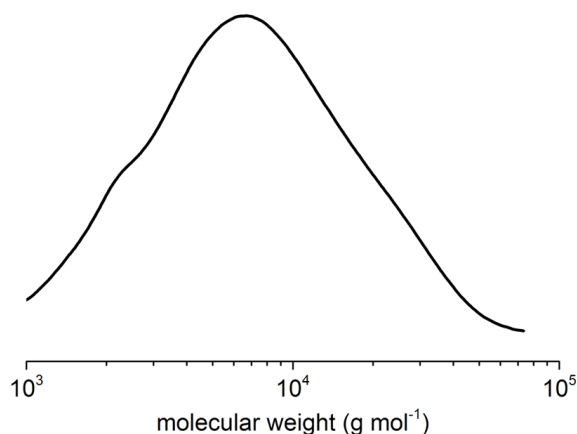
Fig. 3.47.: SEC trace of the synthesized polypyrazole. Dimethylformamide was utilized as eluent.

The weight loss curve in Figure 3.48 was obtained by thermogravimetric analysis and

shows a relatively broad profile with multiple steps, starting to decompose at 245 °C with a complete decomposition at 730 °C.
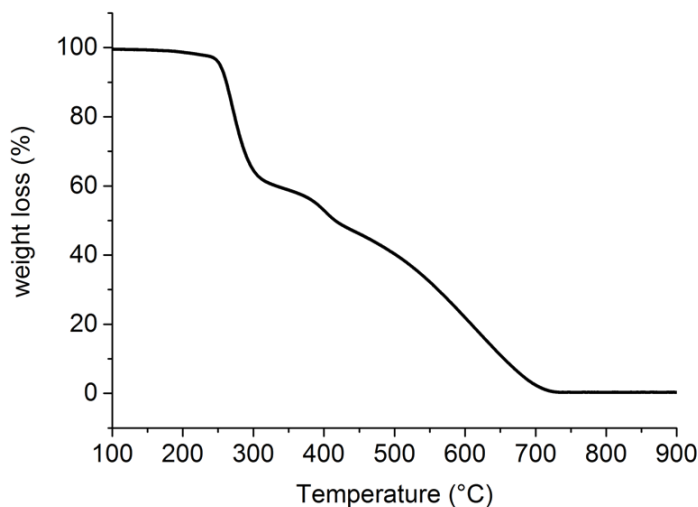
Fig. 3.48.: TGA weight loss curve of the synthesized polypyrazole. The measurement was done at a heating rate of 10K/min under air.

3.4.5. Conclusion

The successful synthesis of two different polymer classes from a single monomer is presented. First of all, rhodium mediated C1 polymerization of propargyl 2-diazoacetate results in poly(propargyl 2-ylidene-acetate). This polymethylene can be post-modified via a *Huisgen* 1,3-dipolar cycloaddition resulting in a 5-membered heterocycle, herein benzyl azide was utilized for post-polymerization modification. Secondly, bulk polymerization of propargyl 2-diazoacetate at elevated temperatures leads to a 1,2-dipolar cycloaddition, thereby forming a polypyrazole. It is known that carbene precursors, such as diazo compounds can also be utilized for manifold other reactions.

3.5. Approach Towards the Synthesis of Dense Bottle-Brush Copolymers

3.5.1. Introduction

One important part for the development of novel polymeric materials for advanced applications is the polymer architecture (Fig. 3.49).[94] Polymer architecture ranges from linear chains to simple branching or more complex AB- or ABC-block copolymers exhibiting various microphase separations. Other structural motifs include graft (also: brush) polymers and star-shaped polymers. Precision control of the polymer architecture can be considered as the driving force towards novel materials for advanced applications. This is the reason why utmost control of the architecture and design of new architectures is a critical goal for polymer chemists.
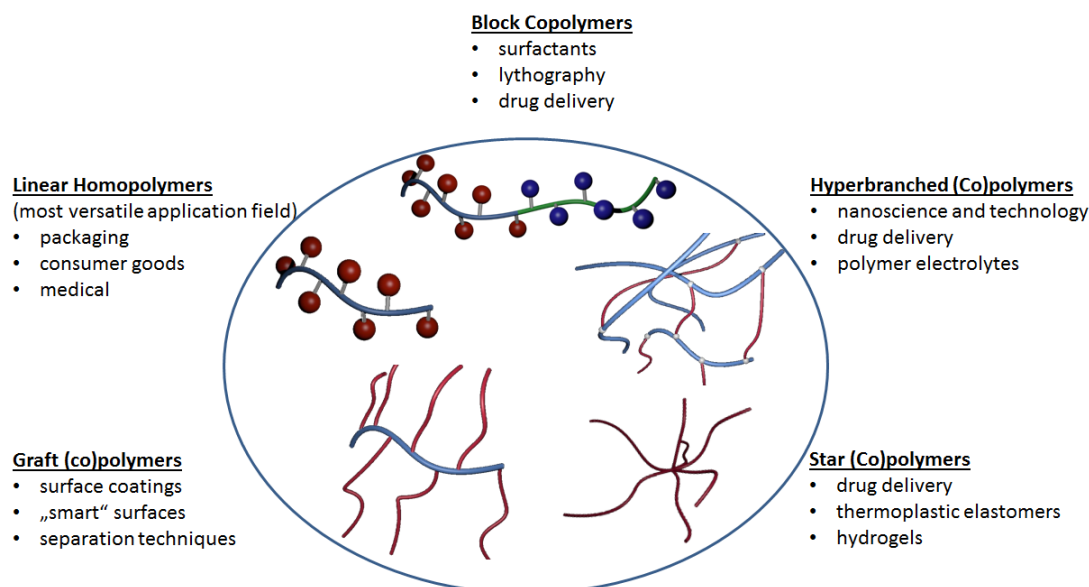
Fig. 3.49.: Depiction of various polymer architectures and examples of their use for applications.

Besides the different applications, the architecture of a polymer has a tremendous influence on the physical properties of a polymeric material, e.g. solubility, transition temperatures, toughness and semicrystallinity. Hence, a good understanding of the influence of polymer architecture on physical properties as well as control of architectural design of polymers is inevitable for new applications.

Bottle-brush copolymers are linear polymers with a very high grafting density of side chain polymers attached to the backbone.[95] These densely functionalized polymers

result in chain extension of the backbone and can be utilized for various purposes, such as templates for nanonparticle synthesis and nanowires.[96,97] Due to the amphiphilic core-shell properties they might also be useful as drug carrier systems, either as cylindrical- or spherical shaped encapsulating species. There are different approaches to prepare brush architectures. Brush copolymers in general can be synthesized by "grafting-from", "grafting-to" and "grafting-through" strategies. "Grafting-from" is beneficial if it comes to structural unity, high grafting density and a high degree of polymerization of the primary chain. It is schematically shown in Figure 3.50.
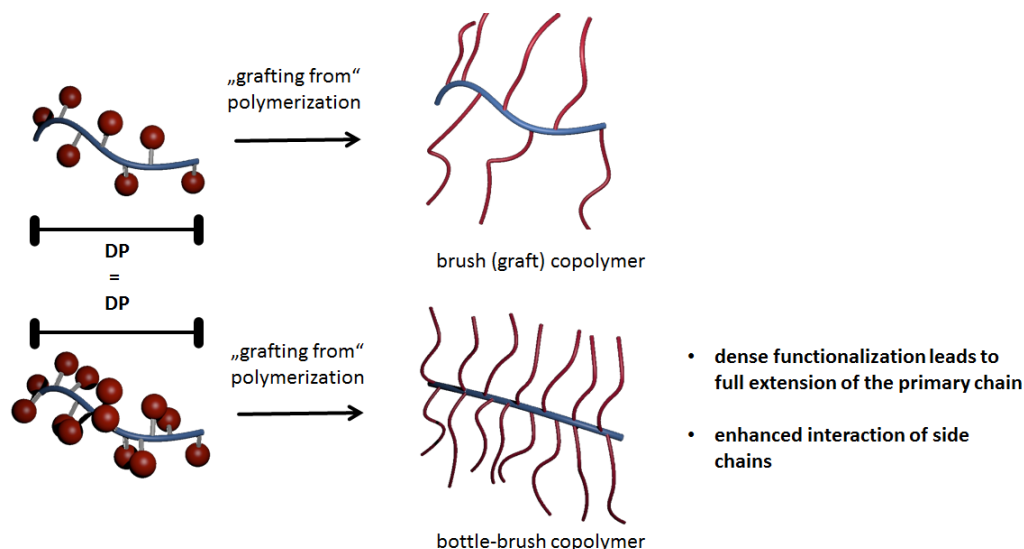
Fig. 3.50.: „Grafting from" approach for two linear polymers with a different side group density but identical degree of polymerization of the polymer backbone.

In comparison, the "grafting-to" concept might result in insufficient conversion of side groups and the "grafting-through" approach is challenging regarding the polymerization of macromonomers. Furthermore, higher molecular weights are sometimes difficult to achieve via the "grafting-through" approach, but also offer a valuable method to control the molecular weight in dependence of the macromonomer length. Yet, it has to be mentioned that the "grafting-through" approach was already shown to be successful for palladium catalyzed C1 polymerization of oligo(ethylene glycols).[29]

The shape of graft polymers depends on the length ratio of backbone and side chain polymers, as well as on the grafting density. A perfect chain extension of the backbone can only be expected if the grafting density is raised to a very high degree, thus, requiring polymers with an inherent dense degree of functional side groups without adjacent spacer groups, ranking functional polymethylenes as ideal candidates. The fundamental idea is to synthesize a functional polymethylene bearing a suitable reactive site for the initiation of a second polymerization in the side chain. In order to fully control the unity of side chains and suppress side reactions, such as crosslinking, atom transfer radical polymerization (ATRP) as grafting-from approach is the method of

choice for a subsequent polymerization. Herin, the first synthesis of a functional polymethylene macroinitiator, namely poly(2-(2-bromoisobutyryloxy)ethyl 2-ylidene-acetate), is described. Furthermore, utilization of this macroinitiator in an initial test ATRP with methyl acrylate is also discussed.

3.5.2. Synthesis and Characterization of 2-(2-Bromoisobutyryloxy)ethyl 2-diazoacetate

A suitable functional monomer for a subsequent C1 macroinitiator synthesis can be obtained by conversion of 2-hydroxyethyl 2-bromoisobutyrate (HEBIB) to the corresponding novel diazo ester. Preparation of HEBIB has been described elsewhere.[98] Both synthetic routes (A & B), according to Scheme 1.9 in Chapter 1, were evaluated for the preparation of 2-(2-bromoisobutyryloxy)ethyl 2-diazoacetate. The requirement of harsh basic conditions within the initially targeted route B was presumably the reason for the failure of this synthetic route. However, the synthesis was accomplished via route A in decent yields up to 29%. The monomer was fully characterized by ^{1}H NMR, ^{13}C NMR and IR spectroscopy and the data are depicted in Figures 3.51-3.53. The ^{1}H NMR spectrum in Figure 3.51 clearly depicts the commonly broadened singlet signal at 4.71 ppm, assigned for the proton next to the diazo group (N$_2$CH). The corresponding carbon signal gives rise for the typical signal at 46.3 ppm in the ^{13}C NMR spectrum, as shown in Figure 3.52.
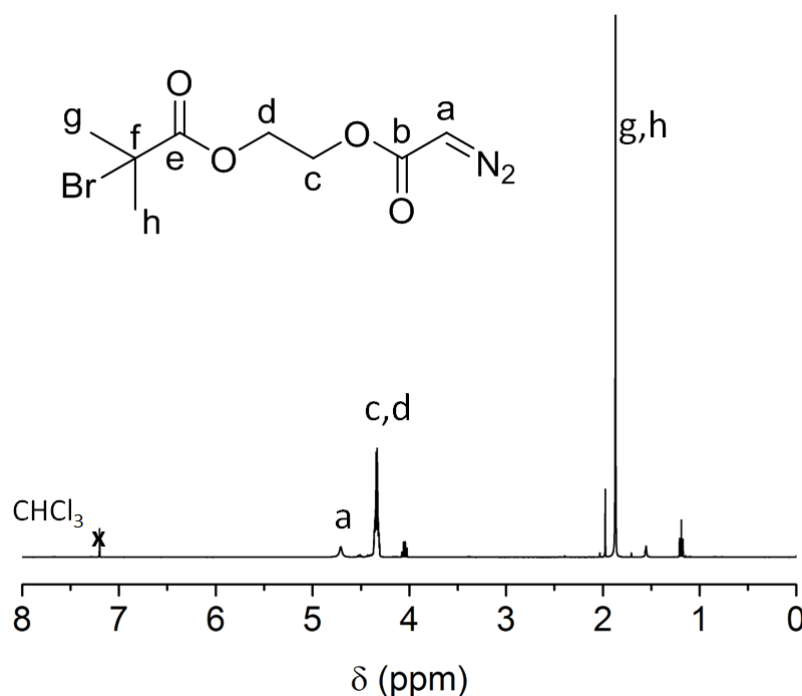
Fig. 3.51.: ^{1}H-NMR spectrum of 2-(2-bromoisobutyryloxy)ethyl 2-diazoacetate measured in deuterated chloroform at 400 MHz.
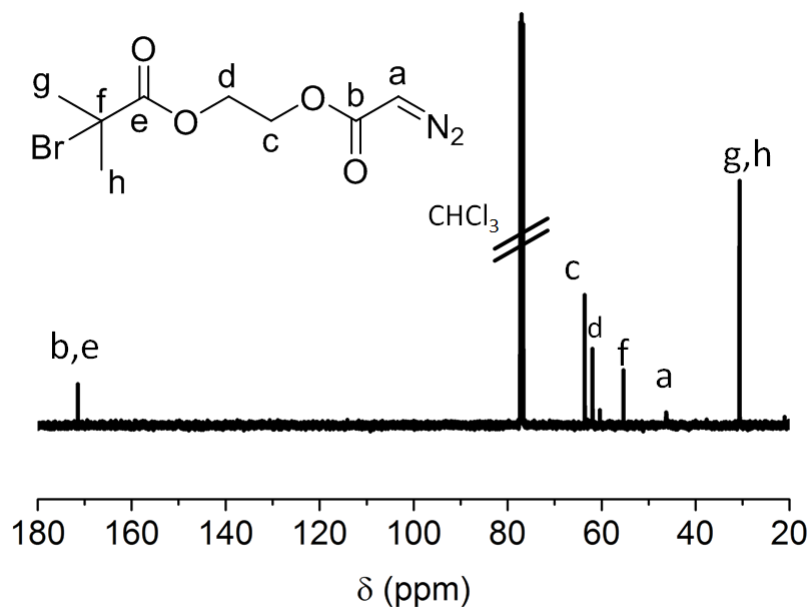
Fig. 3.52.: ^{13}C-NMR spectrum of 2-(2-bromoisobutyryloxy)ethyl 2-diazoacetate measured in deuterated chloroform atz 100 MHz.

In addition to the NMR spectra, the strong vibration band at 2109 cm^{-1} (N$_2$ stretch) and the two bands at 1735 and 1691 cm^{-1} (C=O stretch) in the FT-IR spectrum (Fig. 3.53) gave evidence for the successful synthesis. Furthermore, the vibration of the proton next to the diazo group (N$_2$C-H) can be observed at 3115 cm^{-1}.
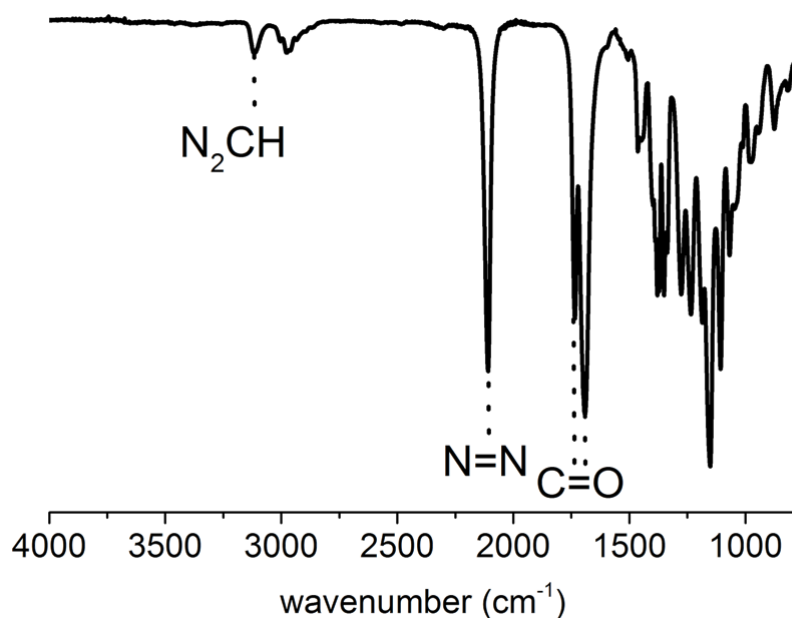
Fig. 3.53.: FT-IR spectrum of 2-(2-bromoisobutyryloxy)ethyl 2-diazoacetate.

3.5.3. Synthesis and Characterization of Poly(2-(2-bromoisobutyryloxy)ethyl 2-ylidene-acetate)

Novel poly(2-(2-bromoisobutyryloxy)ethyl 2-ylidene-acetate) **PBIEA_C1** was synthesized by rhodium mediated C1 polymerization of 2-(2-bromoisobutyryloxy)ethyl 2-diazoacetate with $2\,mol\%$ [(L-prolinate)Rh^I (1,5-cyclooctadiene)] in chloroform, as illustrated in Scheme 3.9. Purification was done by repeated precipitation in n-hexane to yield the brittle polymer in low yields of 11%. Further experiments might increase the yield if the generally better performing catalyst [(L-prolinate)Rh^I (1,5-dimethyl-1,5-cyclooctadiene)] is used.
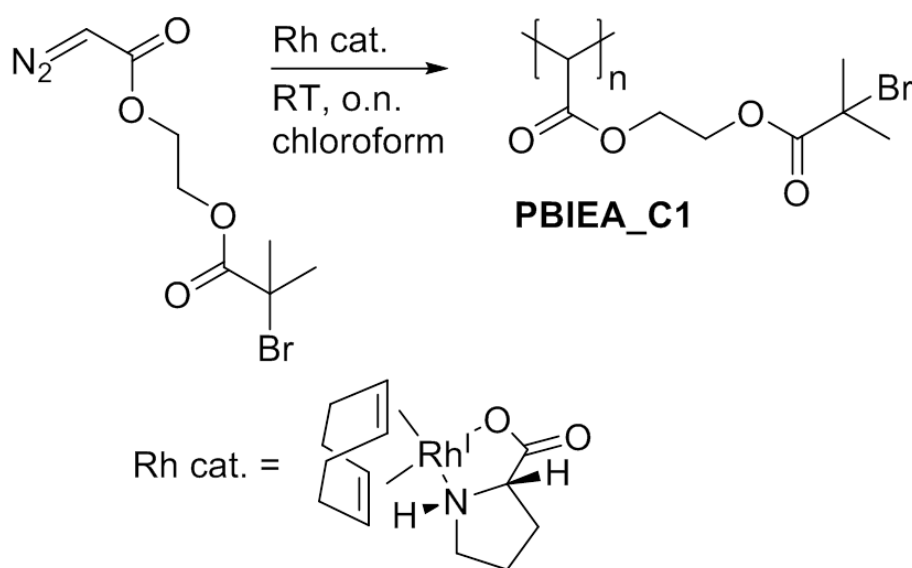
Scheme 3.9.: Rhodium mediated C1 polymerization of 2-(2-bromoisobutyryloxy)ethyl 2-diazoacetate results in poly(2-(2-bromoisobutyryloxy)ethyl 2-ylidene-acetate).

The structural characterization was done by ^{1}H NMR, ^{13}C NMR and IR spectroscopy as illustrated in Figures 3.54-3.56. The upfield shift of the N_2CH-proton, as observed in the ^{1}H NMR spectrum (Fig. 3.54), from $4.71\,ppm$ to $3.25\,ppm$, the backbone proton, is indicative for a successful conversion to functional polymethylenes. Additionally, the methylene groups $H^{c,d}$ and the methyl groups $H^{g,h}$ give rise to strong signals at 4.36 and $1.95\,ppm$, respectively. The corresponding carbon signals were also identified in the ^{13}C NMR spectrum (Fig. 3.55) at 55.5 and $30.7\,ppm$. Again, sharp distinct signals were observed for **PBIEA_C1**, similar as in most of the previously investigated functional polymethylenes and highlighting a well-ordered polymer microstructure.
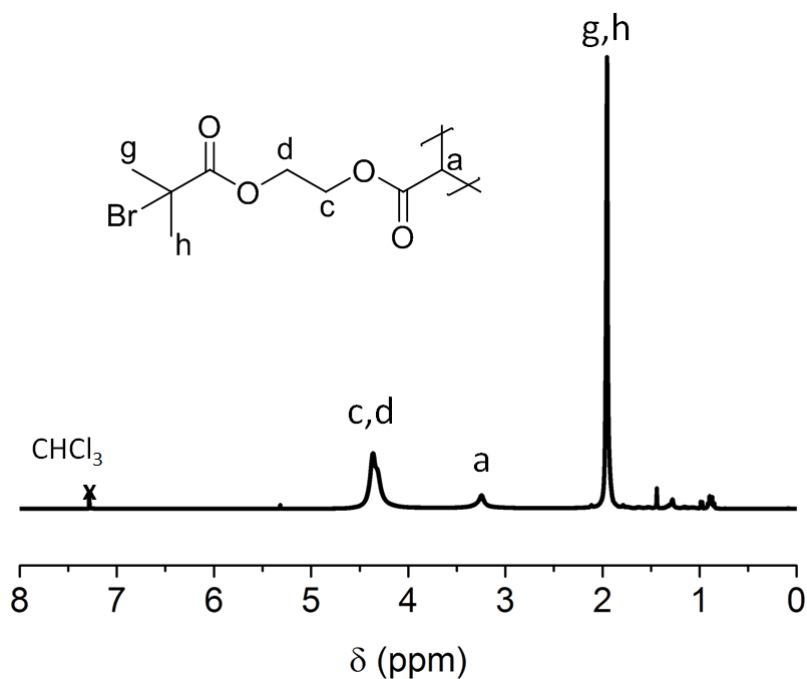
Fig. 3.54.: ^{1}H-NMR spectrum of poly(2-(2-bromoisobutyryloxy)ethyl 2-ylidene-acetate) measured in deuterated chloroform at 400 MHz.
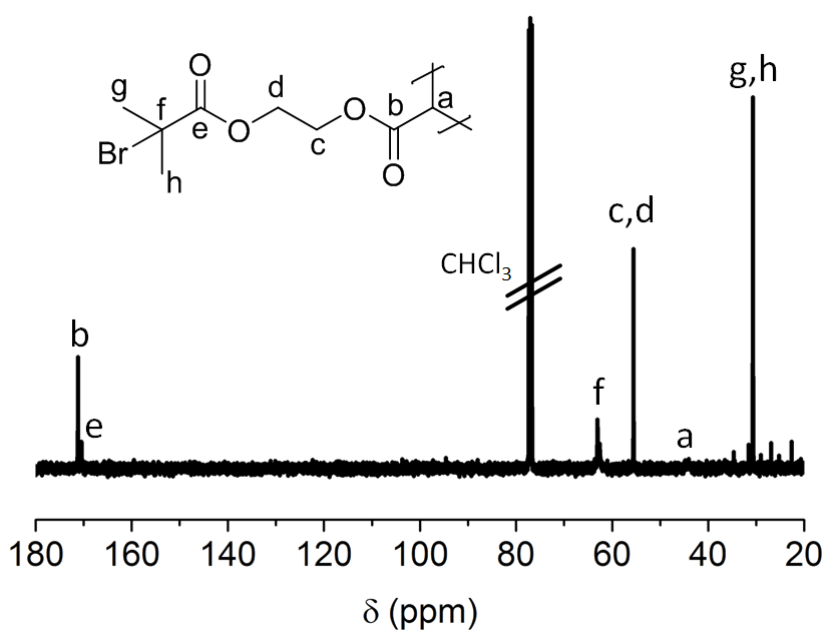
Fig. 3.55.: ^{13}C-NMR spectrum of poly(2-(2-bromoisobutyryloxy)ethyl 2-ylidene-acetate) measured in deuterated chloroform at 100 MHz.

Furthermore, the diazo vibration band in the FT-IR spectrum (Fig. 3.56) at 2109 cm^{-1} vanished after polymerization, while the C=O vibration bands are retained but result in one superimposed signal at 1729 cm^{-1}.
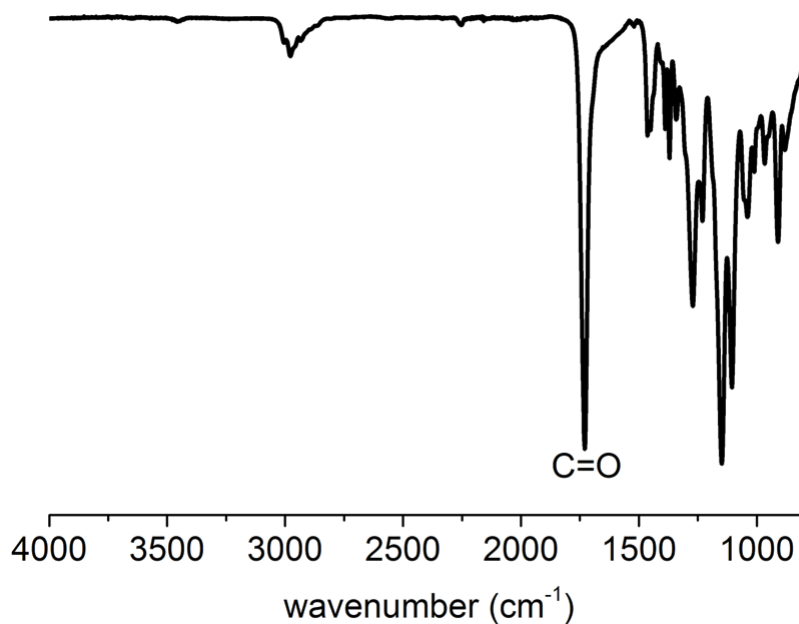
Fig. 3.56.: FT-IR spectrum of poly(2-(2-bromoisobutyryloxy)ethyl 2-ylidene-acetate).

Clearly, the SEC trace in Figure 3.57 reveals the formation of a polymer with $M_n = 30000\,\text{gmol}^{-1}$ ($M_w = 70900\,\text{gmol}^{-1}$) and a relatively broad dispersity $Đ = 2.36$ as commonly observed for the formation of functional polymethylenes via rhodium mediated C1 polymerization.
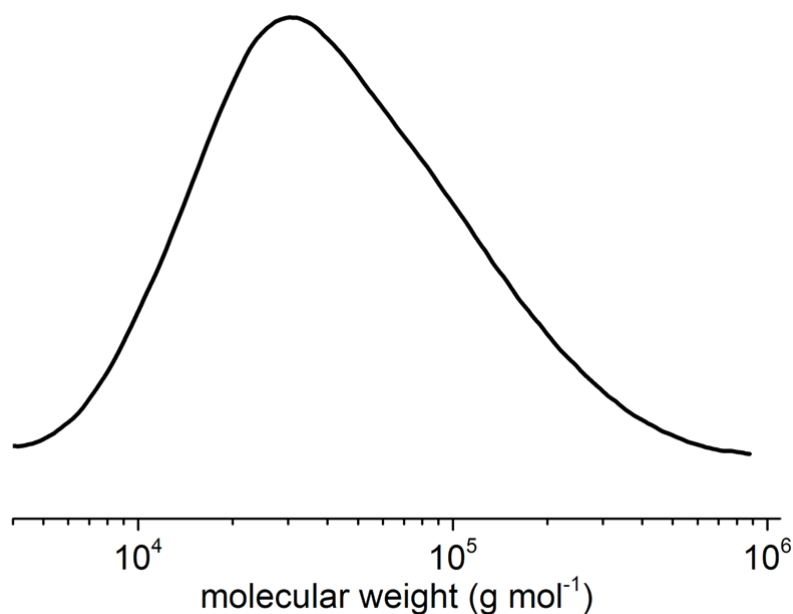
Fig. 3.57.: SEC trace of poly(2-(2-bromoisobutyryloxy)ethyl 2-ylidene-acetate). Tetrahydrofurane was utilized as eluent.

3. Results and Discussion

3.5.3.1. Post-Polymerization Modification via Side Chain ATRP

PBIEA_C1 is, to the best of my knowledge, the first macroinitiator bearing an ATRP initiator at every main chain carbon atom and was successfully synthesized via rhodium mediated C1 polymerization. In a first approach to utilize this macroinitiator for bottle-brush copolymer synthesis via a grafting-from approach, methyl acrylate was subject to a side group initiated atom transfer radical polymerization (ATRP) (Scheme 3.10). The reaction conditions were inspired by *Quin* et al. utilizing a copper bromide catalyst system with 4,4´-dinonyl-2,2´-dipyridyl (dNbpy) as ligand[99] The reaction was performed overnight at 70 °C in 1,4-dioxane. Subsequently, the solvent was evaporated and the residue dissolved in dichloromethane and purified via filtration through a column filled with neutral aluminumoxide. Methyl acrylate was chosen with regard to its relatively small molecular structure, this is probably beneficial regarding space issues originating from the denseley packed side groups of this polymer class.
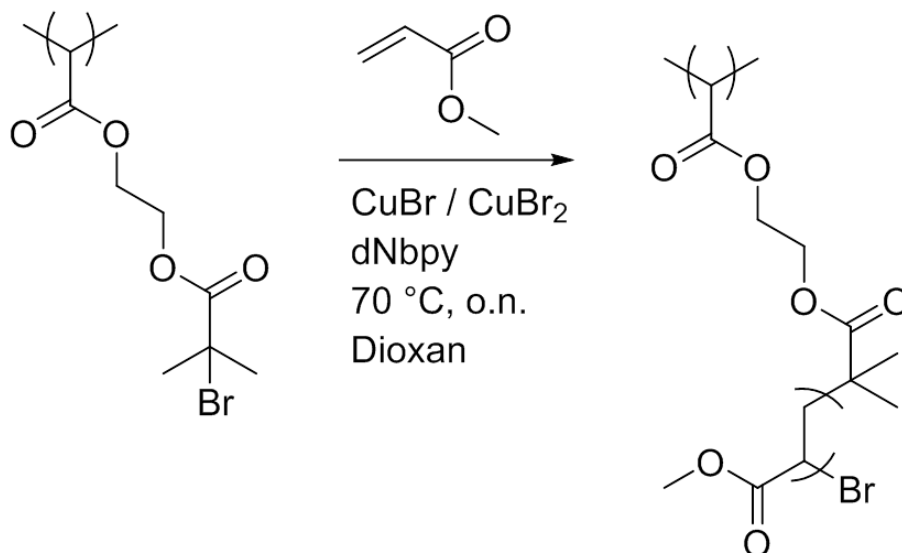
Scheme 3.10.: Poly(2-(2-bromoisobutyryloxy)ethyl 2-ylidene-acetate) can serve as macroinitiator for a subsequent side chain ATRP. This scheme shows the utilization of methyl acrylate as monomer.

The ^{1}H NMR spectrum in Figure 3.58 provides evidence for the successful side chain ATRP with methyl acrylate as the selected monomer. The initial signals of **PBIEA_C1** decline over the course of the reaction (grey marked areas of the spectrum), while large new and broad signals could be identified to emerge from a side chain consisting of methyl acrylate subunits. For example, the proton H^k at 3.67 ppm arises from the methoxy group of the methyl acrylate repeating unit. However, further experiments are required in order to support these initial results, such as the polymerization of various monomers and a comparison with the C2 analog polymer structure.
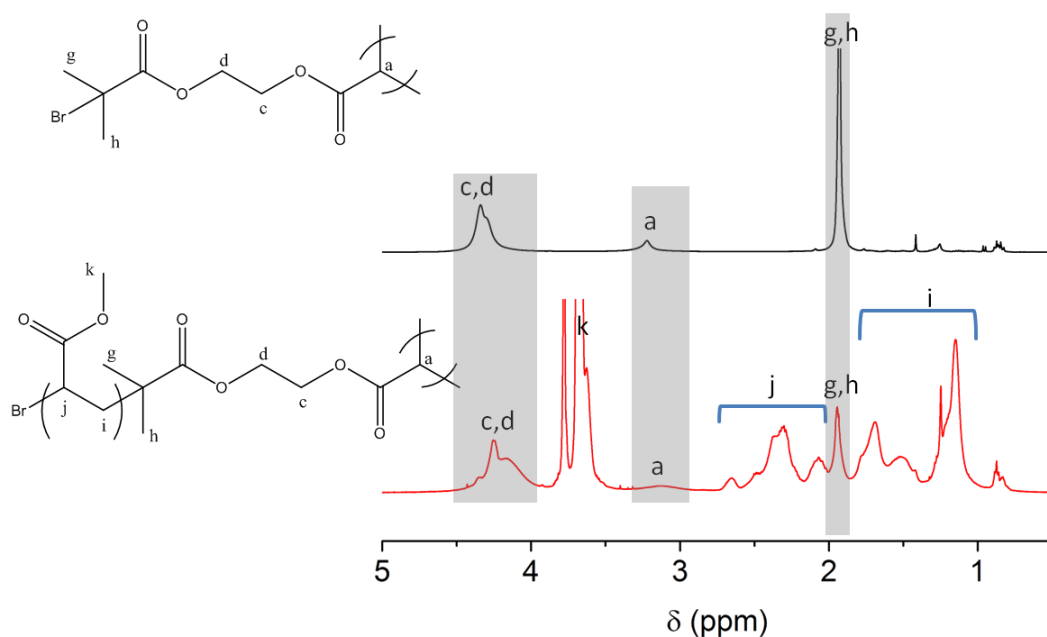
Fig. 3.58.: ^{1}H-NMR spectrum of poly(2-(2-bromoisobutyryloxy)ethyl 2-ylidene-acetate) (black line) in comparison with the spectrum obtained after a grafting-from ATRP with methyl acrylate as monomer (red line). Spectra were recorded in deuterated chloroform at 400 MHz.

A comparison of the SEC traces prior to and after the side chain ATRP is shown in Figure 3.59. As expected, an increase of the molecular weight was observed. The molecular weight determined at the maximum of each curve shifted from 27900 gmol^{-1} to 40900 gmol^{-1}.
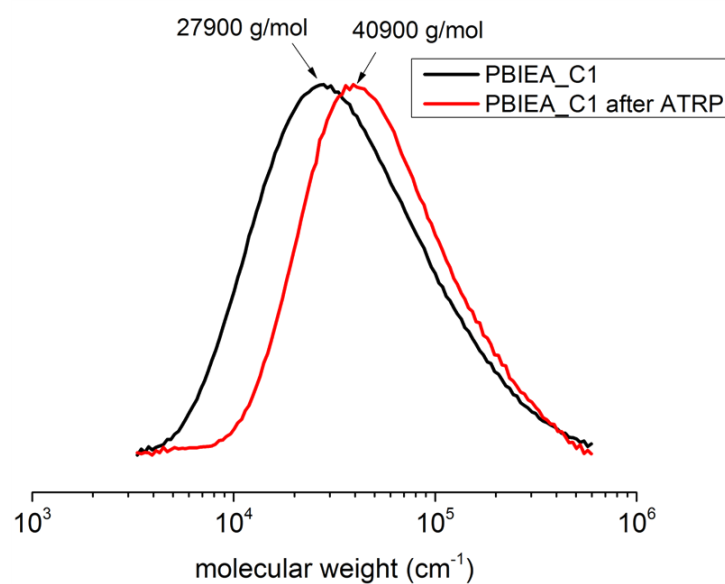
Fig. 3.59.: SEC traces of poly(2-(2-bromoisobutyryloxy)ethyl 2-ylidene-acetate) and the ATRP functionalized polymer utilizing methyl acrylate as a monomer. Chloroform was used as eluent.

Table 3.5 summarizes some of the characteristic polymer results obtained from this measurement.

Table 3.5.: Characteristic polymer data obtained via SEC of poly(2-(2-bromoisobutyryloxy)ethyl 2-ylidene-acetate) and the ATRP functionalized polymer utilizing methyl acrylate as a monomer. Chloroform was used as eluent.

Polymer	M_n (gmol^{-1})	M_w (gmol^{-1})	Đ (M_w/M_n)
PBIEA_C1	24900	59000	2.37
PBIEA_C1 after ATRP with methyl acrylate	34600	77600	2.24

3.5.4. Conclusion

The successful synthesis of the novel ATRP macroinitiator **PBIEA_C1** obtained by rhodium mediated C1 polymerization of 2-(2-bromoisobutyryloxy)ethyl 2-diazoacetate is presented. Following the preparation of poly(2-(2-bromoisobutyryloxy)ethyl 2-ylidene-acetate), various monomers for side chain polymerization can be investigated. This approach for the synthesis of bottle-brush polymers aims for the highest density of side chains, therefore, testing the general possibility to quantitatively initiate the ATRP from every side group is required. Hence, initially the polymerization of small monomers (e.g. methyl methacrylate) was evaluated and has to be further investigated and optimized by alternative feed ratios and different reaction conditions. Next, the well-known polymerization of styrene might follow. Even, if it may not be possible to activate all groups for initiation of a secondary polymerization, the amount of overall started polymerizations, should in any case be higher than with the previously investigated analog C2 polymers. The obtained polymers can be directly compared with the well-known poly(2-(2-bromoisobutyryloxy)ethyl methacrylate) (PBIEM). Thus, a direct insight into the influence of side chain density on the properties of bottle-brush copolymers can be gained.

4. Summary and Outlook

The feasibility of rhodium mediated C1 polymerization to prepare a variety of functional polymethylenes, bearing functionalities suitable for post-polymerization modification, was explored and their performance in subsequent ligation reactions was investigated. Differences and similarities of functional polymethylenes and their analog functional polyethylene structures were revealed. Scheme 4.1 illustrates the selected functional polymethylene scaffolds **1-5** that were synthesized and investigated.
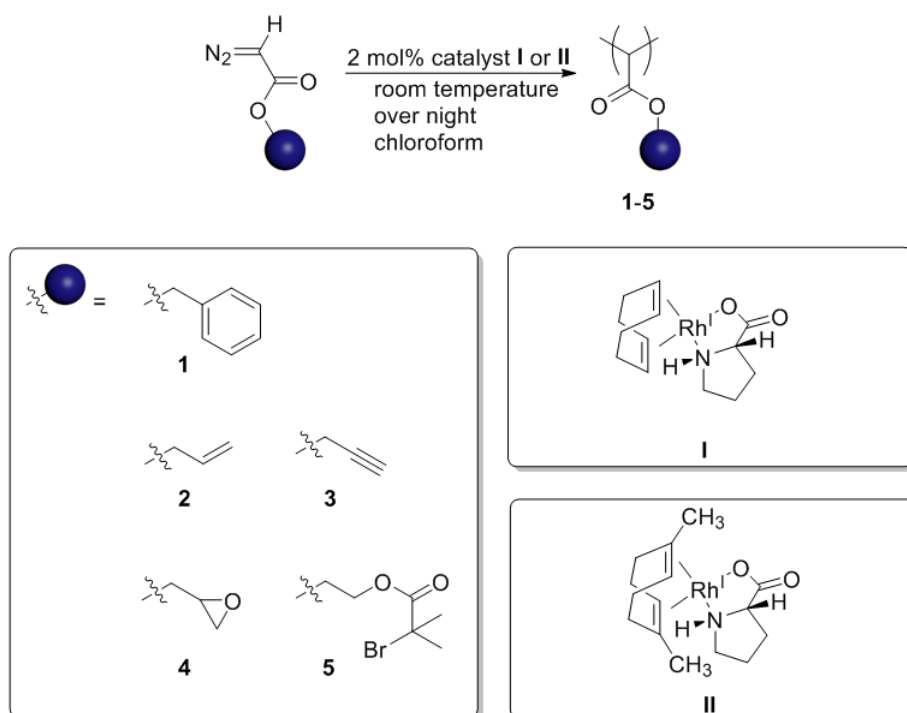
Scheme 4.1.: Selected functional polymethylenes **1-5**, prepared via rhodium mediated C1 polymerization with catalysts **I** and **II** and investigated regarding post-polymerization modifications.

In a first attempt, the general possibility to functionalize polymers with a high density of side groups was elucidated. Specifically, poly(benzyl 2-ylidene-acetate) **1**, a benchmark functional polymethylene bearing a non-reactive ester side group, was selected for a comparative study with the structural analog poly(benzyl acrylate). Both polymers were subject to ligation reactions with primary and secondary amines under equal reaction conditions. Interestingly, this study highlighted the influence of densely packed side groups on the obtained product materials. Initially, amidation was expected to occur for both polymers; however, a predominant imide formation took place upon reaction of **1** with primary amines. Additionally, higher conversions with primary amines were observed for the functional polymethylene **1** compared to poly(benzyl acrylate). This finding was proposed to result from a higher tension of the functional

polymethylenes due to higher side group density, resulting in an increased reactivity. In conclusion, this study gave first evidence that the side group density of polymers is indeed effecting post-polymerization modification results.

Even unprotected carbon-carbon double- and triple bond containing α-diazocarbonyl compounds, i.e. allyl 2-diazoacetate and propargyl 2-diazoacetate, could be successfully polymerized via rhodium mediated C1 polymerization to yield poly(allyl 2-ylidene-acetate) **2** and poly(propargyl 2-ylidene-acetate) **3**. This is especially interesting, as the diene ligands 1,5-cyclooctadiene and 1,5-dimethyl-1,5-cyclooctadiene of complex **I** and **II** are known for their strong binding to the rhodium center and this complex is maintained throughout the polymerization. The cleavage of the *L*-prolinate ligand of catalysts **I** and **II** in the catalyst activation mechanism would result in free space for the monomer or oligomer double bond to complex the catalyst and prevent a polymerization; however, this was neither observed for the polymerization of allyl 2-diazoacetate nor for propargyl 2-diazoacetate. Another intriguing finding in the investigation of **2** and **3** is the fact, that they remain soluble in solution but are readily crosslinked upon drying, presumably via their unsaturated bonds as previously reported for poly(ally acrylate). Both polymers **2** and **3** require lyophilization from a 1,4-dioxane solution in order to prevent crosslinking.

The post-polymerization modification of **2** was achieved by thiol-ene reactions; however these reactions remained difficult to control due to the mentioned self-crosslink ability. Successful thiol-ene reactions with hydrophobic thiols in solution were demonstrated; in contrast, hydrophilic thiols led to completely insoluble materials. Noteworthy, the self-crosslinking process could be utilized to form stable polymeric films, which were subsequently modified with thiols via the remaining double bonds and enabled adjustment of the wettability over a wide range (35-104 degree). Additionally, the polymerization kinetics of **2** were investigated and determined to be of first order. Poly(allyl 2-ylidene-acetate) **2** represents the first functional polymethylene suitable for a facile post-polymerization modification utilizing moderate reaction conditions.

The functional polymethylene **3** was subject to a successful azide-alkyne 1,3-dipolar cycloaddition with benzyl azide. However, in order to fully provide evidence for the capability to utilize azide-alkyne cycloadditions on functional polymethylenes, further experiments with other azides are required. In addition to C1 polymerization, propargyl 2-diazoacetate was utilized as AB-monomer leading to the formation of a polypyrazole at elevated temperatures via a 1,3-dipolar cycloaddition of the diazo group with the terminal alkyne.

The currently best performing functional polymethylene, regarding the feasibility of post-polymerization modifications, is poly(glycidyl 2-ylidene-acetate) **4**. The successful knowledge transfer from ligation reactions performed on poly(glycidyl methacrylate) to **4** was shown. Thus, it was possible to open the three-membered ring of **4** with

amines as well as thiols with quantitative conversions. Even bulky substituents, such as α-aminodiphenylmethane were easily introduced by post-polymerization modification. Consequently, the bulkiness of functional groups is not that much of a limitation for functional polymethylenes as initially expected, neither for their preparation via C1 polymerization nor for a subsequent post-polymerization modification. Additionally, it was noticed that primary amines did not lead to gelation as known for poly(glycidyl methacrylate) under identical reaction conditions. This was proposed to result from a predominant occurrence of intramolecular secondary reactions, due to high functional side group density of **4**, rather than intermolecular cross-coupling reactions as observed for poly(glycidyl methacrylate).

The synthesis of poly(2-(2-bromoisobutyryloxy)ethyl 2-ylidene-acetate) **5** represents the first ATRP macroinitiator with a polymethylene scaffold. This study demonstrates the general feasibility to conduct ATRP in the side chain of functional polymethylenes by a successful conversion with the small monomer species methyl acrylate.

Overall, a variety of functional polymethylenes suitable for post-polymerization modifications was successfully prepared and investigated regarding their ligation reactions. This project enables facile access to a multitude of functional polymethylene scaffolds that are currently not accessible via other approaches. The subsequent research on functional polymethylenes will include the in-depth characterization of the material properties as well as the ongoing development of bottle-brush copolymers via the synthesized macroinitiator.

5. Experimental Part

5.1. Methods and Materials

All chemicals were commercially available and used as received without further purification unless otherwise stated. Yields refer to isolated and purified products. [(L-Prolinate)Rh^I(1,5-cyclooctadiene)] and [(L-Prolinate)Rh^I(1,5-dimethyl-1,5-cyclooctadiene)] were prepared as described in the literature.[83] ^{1}H and ^{13}C nuclear magnetic resonance (NMR) spectra were recorded on a Bruker 300 or 400 MHz FT-NMR spectrometer in deuterated solvents. Fourier transform infrared (FT-IR) spectroscopy was measured on a Thermo Scientific Nicolet iS10. Measurements were conducted with an attenuated total reflectance (ATR) attachment. Real-time in situ FT-IR measurements were performed with a ReactIR™ 45 m from Mettler Toledo, equipped with a DiComp™ probe and a silver halide fiber AgX 6 mm × 2 m, capable of covering a wavenumber region of 2000–650 cm^{-1}, using a MCT detector. Size exclusion chromatography (SEC) data were obtained from different setups calibrated with linear polystyrene standards with various molecular weights:

1. Intelligent pump JASCO PU-980, RI detector SFD RI 2000, Linear 5 μm column MZ-Gel SDplus. Chloroform or tetrahydrofurane were used as eluents.

2. FLOM Intelligent Pump Al-12-13, SFD RI 2000 detector, one guard column PLgel 10 μm and two PLgel 10 lm MIXED-B columns. Tetrahydrofurane was used as eluent.

3. SpectraSYSTEM P1000 isocratic pump, LaChrom RI-Detector L-7490, two precolumns 50x8 mm (100 Å, 50 Å) and a linear column 300x800 mm (5 μm) MZ-Gel SDplus. Dimethylformamide containing 0.01 mol/L LiBr was used as eluent.

Chromatographica V1.0.25 was utilized as software for SEC data evaluation. Thermogravimetric Analysis (TGA) was performed on a Mettler Toledo TGA 1 Star System under air at 10 °C min^{-1}. Differential scanning calorimetry was done on a DSC 1 Star System. Contact angle measurements were performed with a Data-physics OCA 25 apparatus. For static light scattering (SLS) analysis an ALV/CSG-3 Compact Goniometer was used together with an ALV/LSE-5003 Multiple Tau Digital correlator. Measurements of the refractive index increments were conducted on a DnDc-2010 differential refractometer.

5.2. Synthesis of Basic Chemicals

Synthesis of Tosyl azide
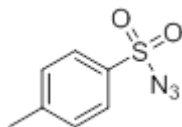
The synthesis of tosyl azide was done by charging an Erlenmeyer flask with sodium azide (19.51 g, 300 mmol, 1.1 eq.) in 50 mL water and 50 mL acetone. Subsequently, the solution was poured into a second Erlenmeyer flask containing a solution of tosyl chloride (51.46 g, 270 mmol, 1.0 eq.) in 250 mL acetone. The solution was stirred at room temperature for 4 hours. Afterwards, the solution was poured in 150 mL water and the organic layer was separated from the aqueous phase, affording the crude product. For purification the crude product was washed twice with water. The product was dried with sodium sulfate and placed under high vacuum to afford the product as a colorless liquid.

Yield: 38.20 g (194 mmol, 72%)

^{1}H-NMR (300 MHz, CDCl$_3$):
δ = 7.85 (d, 2H, CH$_{ar}$), 7.41 (d, 2H, CH$_{ar}$), 2.49 (s, 3H, CH$_3$) ppm.

^{13}C-NMR (75 MHz, CDCl$_3$):
δ = 146.2 (C$_{ar}$), 135.5 (C$_{ar}$), 130.3 (CH$_{ar}$), 127.5 (CH$_{ar}$), 21.8 (CH$_3$) ppm.

FT-IR (ATR):
$\tilde{\nu}$ = 2121, 1595, 1495, 1367, 1162, 1084, 813, 744 cm^{-1}.

The analytical data are in good agreement with the literature.[100]

5. Experimental Part

Synthesis of *N,N*-Ditosylhydrazine
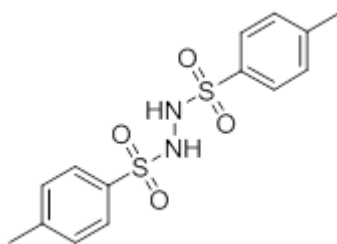
The synthesis of *N,N*-Ditosylhydrazine was done by charging a round bottom flask with p-toluenesulfonyl hydrazide (33.95 g, 182 mmol, 1.0 eq.) and tosyl chloride (52.17 g, 274 mmol, 1.5 eq.). After the addition of 150 mL dichloromethane, the suspension was stirred at room temperature for 1.5 hours, while pyridine (22 mL, 273 mmol, 1.5 eq.) was added dropwise. The suspension first turned homogeneous and yellow and a colorless precipitate formed after several minutes.Subsequently, the reaction was quenched by the addition of 250 mL water and 350 mL diethyl ether. After cooling in an ice bath, the precipitate was filtered off and washed with diethyl ether. For purification, the crude product was recrystallized from methanol to yield the product as colorless needles.

Yield: 44.19 g (130 mmol, 71%)

^{1}H-NMR (300 MHz, DMSO-d^6):
δ = 9.61 (s, 2H, NH), 7.67 (d, 4H, CH$_{ar}$), 7.38 (d, 4H, CH$_{ar}$), 2.39 (s, 6H, CH$_3$) ppm.

^{13}C-NMR (75 MHz, DMSO-d^6):
δ = 143.9 (2C, C$_{ar}$), 136.0 (2C, C$_{ar}$), 129.9 (4C, CH$_{ar}$), 128.2 (4C, CH$_{ar}$), 21.5 (2C, CH$_3$) ppm.

The analytical data are in good agreement with the literature.[50]

Synthesis of 2-Hydroxyethyl 2-bromoisobutyrate (HEBIB)
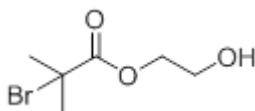
The synthesis of 2-hydroxyethyl 2-bromoisobutyrate was done by dropwise addition of α-bromoisobutyryl bromide (20 mL, 162 mmol, 1.0 Eq.) to a cooled (0 °C) mixture of ethyleneglycol (150 mL, 2.68 mmol, 16.5 Eq.) and triethylamine (22.5 mL, 162 mmol, 1.0 Eq.). Subsequently, the reaction was heated to 60 °C and stirred overnight. Afterwards, the reaction was cooled and quenched with 300 mL water. For purification, the solution was extracted three times with dichloromethane and the combined organic phases were washed with water and dried with magnesium sulfate. The product was obtained as colorless liquid.

Yield: 19.56 g (124 mmol, 77%)

¹H-NMR (400 MHz, CDCl₃):
δ = 4.25 (m, 2H, COOCH₂), 3.81k (m, 2H, CH₂OH), 1.89 (s, 6H, CH₃) ppm.

FT-IR (ATR):
$\tilde{\nu}$ = 3443, 2977, 1733, 1271, 1159, 1107 cm⁻¹.

The analytical data are in good agreement with the literature.[101]

Synthesis of Benzyl azide
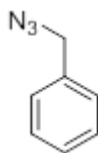
The synthesis of benzyl azide was done by stirring benzyl bromide (2 mL, 16.8 mmol, 1.0 eq.) and sodium azide (1.65 g, 25.4 mmol, 1.5 eq.) in 40 mL dimethylsulfoxide at room temperature for 1 hour. Subsequently, water was slowly added (Attention: Reaction mixture gets warm!) and the solution was extracted three times with diethyl ether after cooling back to room temperature. For further purification, the combined organic phases were washed twice with brine and dried with magnesium sulfate and placed under high vacuum.

¹H-NMR (300 MHz, CDCl₃):
δ = 7.30-7.46 (m, 5H, CH$_{ar}$), 4.36 (2H, CH₂) ppm.

FT-IR (ATR):
$\tilde{\nu}$ = 2090 (N₃), 1253, 736, 697 cm⁻¹.

5.3. Monomer Synthesis

Synthesis of Benzyl 2-diazoacetate
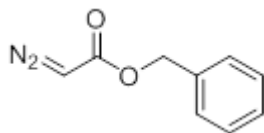
Step A: Benzyl alcohol (21.73 g, 200 mmol, 1.0 eq.) and 2,2,6-tri- methyl-4H-1,3-dioxin-4-one (28.59 g, 200 mmol, 1.0 eq.) were heated at reflux in 50 mL toluene. After 20 hours, the solvent was removed and the residue was used in the next step without further purification.

Step B: The residue containing benzyl acetoacetate (37.20 g, 1.9 mmol, 1.0 eq.) was dissolved in 100 mL acetonitrile and triethylamine (29 mL, 2.1 mmol, 1.1 eq.) was added. Next, a solution of tosylazide (35.77 g, 2.5 mmol, 1.3 eq.) in 150 mL acetonitrile was added dropwise. The resulting reaction mixture was stirred for 16 hours, followed by addition of lithium hydroxide (9.27 g, 3.9 mmol, 2.0 eq.) in 170 mL distilled water. The mixture was finally stirred for 4 hours, filtrated, and extracted three times with diethylether. The combined organic phases were washed with brine and dried with magnesium sulfate, followed by solvent removal. The obtained residue was purified by column chromatography utilizing a mixture of petrol ether and ethyl acetate (4:1; v/v). The product was obtained as yellow liquid.

Yield: 15.34 g (0.87 mmol, 45%)
TLC: $R_f = 0.8$ (petrol ether / ethyl acetate, 4:1 v/v)

^{1}H-NMR (300 MHz, CDCl$_3$):
δ = 7.37 (s, 5H, CH$_{ar}$), 5.22 (s, 2H, CH$_2$), 4.81 (br. s, 1H, CH) ppm.

^{13}C-NMR (75 MHz, CDCl$_3$):
δ = 135.9 (C$_{ar}$), 128.6 (CH$_{ar}$),128.3 (CH$_{ar}$), 128.2 (CH$_{ar}$), 66.5 (CH$_2$), 46.4 (CH) ppm.

FT-IR (ATR):
$\tilde{\nu}$ = 2106, 1683, 1386, 1351, 1171, 1003, 737, 696 cm^{-1}.

5. Experimental Part

Synthesis of Allyl 2-diazoacetate
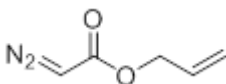
Step A: Allyl alcohol (10.30 g, 0.18 mol, 1.0 eq.) and 2,2,6-trimethyl- 4H-1,3-dioxin-4-one (25.23 g, 0.18 mol, 1.0 eq.) were heated to reflux in 50 mL toluene. After 17 hours, the solvent was removed and the residue was used in the next step without further purification.

Step B: The residue containing allyl acetoacetate (22.33 g, 0.16 mol, 1.0 eq.) was dissolved in 100 mL acetonitrile, and triethylamine (24 mL, 0.17 mol, 1.1 eq.) was added. Next, a solution of tosyl azide (29.02 g, 0.20 mol, 1.3 eq.) in 150 mL acetonitrile was added dropwise. The resulting reaction mixture was stirred for 17 hours, followed by addition of lithium hydroxide (11.27 g, 0.47 mol, 3.0 eq.) in 100 mL distilled water. The mixture was finally stirred for 5 hours, filtered and extracted three times with diethylether. The combined organic phases were washed with water and dried with magnesium sulfate, followed by solvent removal. The obtained residue was purified by column chromatography (petrol ether/ethyl acetate (10 : 1). The product was obtained as yellow liquid.

Yield: 7.39 g (58.6 mmol, 37%)

TLC: $R_f = 0.4$ (petrol ether / ethyl acetate, 10:1 v/v)

^{1}H-NMR (300 MHz, CDCl$_3$):
δ = 5.84–6.02 (m, 1H, CHCH$_2$), 5.20–5.38 (m, 2H, CHCH$_2$), 4.78 (br. s, 1H, CH), 4.63–4.70 (m, 2H, CH$_2$) ppm.

^{13}C-NMR (75 MHz, CDCl$_3$):
δ = 132.1 (CHCH$_2$), 118.2 (CHCH$_2$), 46.2 (CH) ppm.

FT-IR (ATR):
$\tilde{\nu}$ = 2106, 1682, 1381, 1338, 1234, 1177, 1024, 990, 933, 739 cm^{-1}.

Synthesis of (±)-Glycidyl 2-diazoacetate
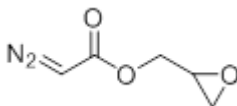
Step A: (±)-Glycidol (8.0 mL, 8.94 g, 0.12 mol, 1.0 eq.) and sodium bicarbonate (31.39 g, 0.36 mol, 3.0 eq.) were dissolved in 400 mL acetonitrile and cooled to 0 °C. Afterwards, bromoacetyl bromide (16.0 mL, 37.18 g, 0.18 mol, 1.5 eq.) was added dropwise and the

solution was stirred at 0 °C for 15 min. Subsequently, the reaction mixture was quenched with 150 mL water and filtrated. The residual solution was extracted three times with dichloromethane. The combined organic phases were washed with brine and dried with magnesium sulfate, followed by solvent removal. The residue was dried in high vacuum and used in the next step without further purification.

Step B: A round bottom flask was charged with (±)-glycidyl 2-bromoacetate (10.98 g, 0.06 mol, 1.0 eq.), *N,N'*-ditosylhydrazine (38.30 g, 0.11 mol, 2.0 eq.) and 200 mL tetrahydrofurane. After cooling to 0 °C, 1,8-diazabicyclo[5.4.0]undec-7-ene (42 mL, 42.88 g, 0.28 mol, 5 eq.) was added dropwise and the solution was kept in an ice bath while stirring it for 20 minutes. Afterwards, the solution was quenched with 150 mL saturated sodium bicarbonate and extracted three times with diethyl ether. Subsequently, the combined organic phases were washed with brine and dried with magnesium sulfate. The remaining residue was purified by column chromatography after evaporation of all volatiles utilizing dichloromethane as eluent. The product was obtained as yellow liquid.

Yield: 2.12 g (15.0 mmol, 26%)

TLC: $R_f = 0.3$ (dichloromethane)

^{1}H-NMR (400 MHz, CDCl$_3$):
δ = 4.81 (br. s, 1H, CH$_2$COO), 4.51 (dd, 1H, J = 12.3 Hz, J = 3.0 Hz, OCH$_2$), 3.99 (dd, 1H, J = 12.3 Hz, J = 6.3 Hz, OCH$_2$), 3.22 (m, 1H, OCH$_2$CH), 2.85 (dd, 1H, J = 4.7 Hz, J = 4.3 Hz, OCH$_2$CHCH$_2$), 2.64 (dd, 1H, J = 4.7 Hz, J = 2.6 Hz, OCH$_2$CHCH$_2$) ppm.

^{13}C-NMR (100 MHz, CDCl$_3$):
δ = 65.2 (OCH$_2$), 49.4 (OCH$_2$CH), 46.3 (CH) 44.6 (OCH$_2$CHCH$_2$) ppm.

FT-IR (ATR):
$\tilde{\nu}$ = 3104, 2107, 1683, 1375, 1178, 907, 859, 736 cm^{-1}.

Synthesis of Propargyl 2-diazoacetate
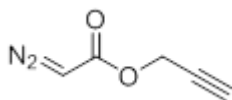
Step A: The synthesis of propargyl acetoacetate was done by charging a round bottom flask with propargyl alcohol (8.41 g, 150 mmol, 1.0 eq.) and 2,2,6-trimethyl-4H-1,3-dioxin-4-one (21.30 g, 150 mmol, 1.0 eq.) in 50 mL toluene. The reaction was heated overnight under reflux conditions. Subsequently, the solvent was evaporated and the crude product was used for the synthesis of propargyl 2-diazoacetate without further purification and analysis.

Step B: The synthesis of propargyl 2-diazoacetate was done by dropwise addition of

tosyl azide (25.41 g, 179 mmol, 1.3 eq.) in 30 mL acetonitrile to a solution of 80 mL acetonitrile containing propargyl acetoacetate (19.17 g, 137 mmol, 1.0 eq.) and triethylamine (21 mL, 151 mmol, 1.1 eq.). The reaction mixture was stirred overnight at room temperature. Subsequently, lithium hydroxide (9.86 g, 412 mmol, 3.0 eq.) in 100 mL water was added and the mixture was stirred for an additional four hours at room temperature. Afterwards, the crude product was extracted three times with diethyl ether and the combined organic phases were washed with water and dried over magnesium sulfate. For further purification, the residue after solvent evaporation was purified by column chromatography with dichloromethane as eluent. The product was obtained as a yellow liquid.

$$\begin{array}{ll} \textbf{Yield:} & 5.82\,\text{g (46.9 mmol, 34\%)} \\ \textbf{TLC:} & R_f = 0.71 \text{ (dichloromethane)} \end{array}$$

^{1}H-NMR (300 MHz, CDCl$_3$):
δ = 4.84 (s, 1H, N$_2$CH), 4.78 (d, 2H, CH$_2$), 2.51 (t, 1H, CH) ppm.

^{13}C-NMR (75 MHz, CDCl$_3$):
δ = 46.4 (N$_2$CH), 52.2 (CH$_2$), 75.0 (CH), 77.6 (C) ppm.

FT-IR (ATR):
$\tilde{\nu}$ = 3292, 3177, 2110, 1686, 1386, 1344, 1232, 1167, 1030 cm^{-1}.

Synthesis of 2-(2-Bromoisobutyryloxy)ethyl 2-diazoacetate
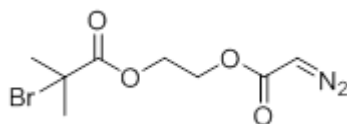
Step A: The synthesis of 2-(2-bromoisobutyryloxy)ethyl 2-bromoacetate was done by dissolving 2-hydroxyethyl 2-bromoisobutyrate (9.20 g, 43.6 mmol, 1.0 eq.) and sodium bicarbonate (11.0 g, 131 mmol, 3.0 eq.) in 200 mL acetonitrile and cooling the solution to 0 °C. Dropwise addition of bromoacetyl bromide (6.0 mL, 69.1 mmol, 1.5 eq.) leads towards a yellow reaction mixture. After stirring the reaction mixture for 1 hours at 0 °C, the reaction was quenched by addition of water. The solution was extracted three times with dichloromethane and washed once with brine. The combined organic phases were dried with magnesium sulfate, the solvent was evaporated and the residue placed under high vacuum. The crude product was not further analyzed.

Step B: The synthesis of 2-(2-bromoisobutyryloxy)ethyl 2-diazoacetate was done by dissolving 2-(2-bromoisobutyryloxy)ethyl 2-bromoacetate (10.56 g, 31.8 mmol, 1.0 eq.)

and *N,N'*-ditosylhydrazine (21.68 g, 63.6 mmol, 2.0 eq.) in 150 mL tetrahydrofurane and cooling the solution to 0 °C. Subsequently, 1,8-Diazabicyclo(5.4.0)undec-7-ene (DBU) (23.8 mL, 159 mmol, 5.0 eq.) were added dropwise. The reaction mixture was stirred at 0 °C for 15 min and quenched with 100 mL saturated sodium bicarbonate solution. The crude product was extracted with diethylether (3x) and the combined organic phases were washed once with brine. The combined organic phases were dried with magnesium sulfate. For further purification, the residue after solvent evaporation was purified by column chromatography with petrol ether / ethyl acetate (4:1 v/v) as eluent. The product was obtained as a yellow liquid.

$$\textbf{Yield:} \quad 2.56\,\text{g (9.17 mmol, 29\%)}$$
$$\textbf{TLC:} \quad R_f = 0.53 \text{ (petrol ether / ethyl acetate, 4:1 v/v)}$$

^{1}H-NMR (400 MHz, CDCl$_3$):

δ = 4.71 (s, 1H, N$_2$CH), 4.34 (m, 4H, CH$_2$), 1.87 (s, 6H, CH$_3$) ppm.

^{13}C-NMR (100 MHz, CDCl$_3$):
δ = 171.5 (2C, C=O), 63.6 (C, CH$_2$), 62.0 (C, CH$_2$), 55.4 (1C, C(CH$_3$)$_2$), 46.3 (1C, N$_2$CH), 30.7 (2C, CH$_3$) ppm.

FT-IR (ATR):
$\tilde{\nu}$ = 3115, 2109, 1735, 1691, 1151, 1107 cm^{-1}.

5.4. Polymerizations of α-Diazocarbonyl Compounds

Synthesis of Poly(benzyl 2-ylidene-acetate)
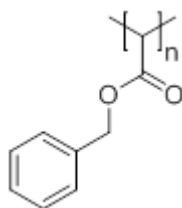
Benzyl 2-diazoacetate (2.48 g, 14.10 mmol, 50 eq.) and [(*L*-prolinate)Rh$^{\text{I}}$(1,5-dimethyl-1,5-cyclooctadiene)] (0.10 g, 0.28 mmol, 1.0 eq.) were separately dissolved in 7.5 mL chloroform each. The catalyst solution was rapidly added to the monomer solution and the resulting reaction solution was stirred for 22 hours at room temperature. The product was obtained as a colorless solid after repeated precipitation in methanol.

$$\textbf{Yield:} \quad 1.22\,\text{g (58\%)}$$

¹H-NMR (300 MHz, CDCl₃):

δ = 6.92–7.25 (m, 5H, CH$_{ar}$), 4.73 (br. s, 2H, CH$_2$), 3.60 (br. s, 1H, CH) ppm.

¹³C-NMR (75 MHz, CDCl₃):

δ = 170.9 (COO), 135.7 (C$_{ar}$), 128.1 (CH$_{ar}$), 66.8 (CH$_2$), 45.1 (CH) ppm.

FT-IR (ATR):

$\tilde{\nu}$ = 1727, 1155, 981, 733, 694 cm^{-1}.

Synthesis of Poly(allyl 2-ylidene-acetate) (PAA)
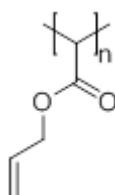
Allyl 2-diazoacetate (7.39 g, 57.9 mmol, 50 eq.) and [(*L*-prolinate)Rh^{I}(1,5-dimethyl-1,5-cyclooctadiene)] (0.41 g, 1.2 mmol, 1.0 eq.) were separately dissolved in 30 mL chloroform each. The catalyst solution was rapidly added to the monomer solution and the resulting reaction solution was stirred for 18 hours at room temperature. Rapid precipitation in *n*-hexane and changing the solvent to 1,4-dioxane was followed by lyophilization.The product was obtained as a colorless solid.

Yield: 2.78 g (49%)

¹H-NMR (300 MHz, CDCl₃):

δ = 5.81 (m, 1H, CHCH$_2$), 5.15 (dd, J = 60.6 Hz, J = 13.9 Hz, 2H, CHCH$_2$), 4.41 (s, 2H, CH$_2$), 3.18 (s, 1H, CH) ppm.

¹³C-NMR (75 MHz, CDCl₃):

δ = 170.5 (COO), 132.4 (CHCH$_2$), 117.8 (CHCH$_2$), 65.8 (CH$_2$), 45.3 (CH) ppm.

FT-IR (ATR):

$\tilde{\nu}$ = 1728, 1227, 1151, 986, 924 cm^{-1}.

5. *Experimental Part*

Synthesis of Poly(glycidyl 2-ylidene-acetate) (PGA)
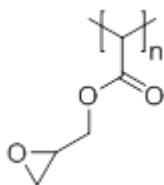
($\pm$)-Glycidyl 2-diazoacetate (3.01 g, 21.1 mmol, 50 eq.) and [(L-prolinate)Rh$^{\mathrm{I}}$(1,5-cyclooctadiene)] (0.14 g, 0.4 mmol, 1.0 eq.) were separately dissolved in 12 mL chloroform each. The catalyst solution was rapidly added to the monomer solution and the resulting reaction solution was stirred for 17 hours at room temperature. The polymer was purified by precipitation in n-hexane for three times. The product was obtained as a yellow solid.

Yield: 1.29 g (53%)

^{1}H-NMR (400 MHz, CDCl$_3$):
δ = 4.13 (d, 2H, OCH$_2$), 3.60 (s, 1H, CHCOO), 3.21 (br. s, 1H, CHCH$_2$), 2.71 (d, 2H, OCH$_2$CHCH$_2$) ppm.

^{13}C-NMR (100 MHz, CDCl$_3$):
δ = 170.4 (COO), 66.2 (CH$_2$), 48.9 (OCH$_2$CH), 44.5 (OCH$_2$CHCH$_2$) ppm.

FT-IR (ATR):
$\tilde{\nu}$ = 3465, 2952, 1730, 1644, 1447, 1253, 1155, 988, 905, 852, 762 cm^{-1}.

Synthesis of Poly(propargyl 2-ylidene-acetate)
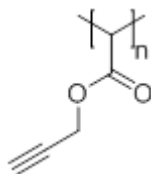
The synthesis of poly(propargyl 2-ylidene-acetate) is done by dissolving [(L-prolinate)Rh$^{\mathrm{I}}$ (1,5-dimethyl-1,5-cyclooctadiene)] (83.7 mg, 0.24 mmol, 1.0 eq.) in 10 mL chloroform, followed by fast addition of a solution of propargyl 2-diazoacetate (1.47 g, 11.9 mmol, 50 eq.) in 10 mL chloroform. After starting the reaction, gas evolution could be observed. The yellow reaction mixture was stirred overnight and turned to a red turbid mixture. Purification was done by filtration and rapid precipitation (1x) in petrol ether. The product was lyophilized from 1,4-dioxane to afford the product as a colorless solid.

Yield: 242 mg (22%)

¹H-NMR (300 MHz, CDCl₃):
δ = 4.77 (m, 3H, CH₂, CH), 2.53 (s, 1H, CH) ppm.

FT-IR (ATR):
$\tilde{\nu}$ = 3284, 2951, 1734, 1155, 992 cm⁻¹.

Synthesis of a Polypyrazol
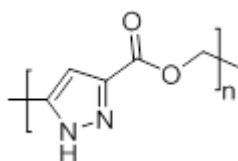
The polypyrazole synthesis was done in bulk by heating 254.1 mg propargyl 2-diazoacetate to 100 °C for 1.5 hours (Note: The reaction proceeds within minutes, but was allowed to proceed for a longer time frame for quantitative conversion). Subsequently, the product was analyzed without further purification.

¹H-NMR (300 MHz, DMSO-d⁶):

δ = 13.49-14.26 (m, 1H, NH), 6.88 (CH$_{ar}$), 5.32 (m, 2H, CH₂) ppm.

FT-IR (ATR):
$\tilde{\nu}$ = 3259, 2118, 1717, 1210, 1164, 1089, 994, 981, 774 cm⁻¹.

Synthesis of Poly(2-(2-Bromoisobutyryloxy)ethyl 2-ylidene-acetate)
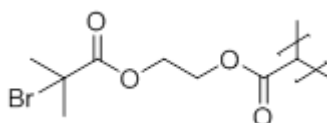
The synthesis of poly(2-(2-bromoisobutyryloxy)ethyl 2-ylidene-acetate) was done by dissolving [(*L*-prolinate)Rhᴵ (1,5-cyclooctadiene)] (26.1 mg, 0.08 mmol, 1.0 eq.) in 7.5 mL chloroform, followed by rapid addition of a solution of 2-(2-bromoisobutyryloxy)ethyl 2-diazoacetate (1.13 g, 4.07 mmol, 50 eq.) in 7.5 mL chloroform. The reaction was stirred at room temperature overnight. Purification was done by precipitating three times in *n*-hexane to afford a yellow solid.

Yield: 111 mg (11%)

¹H-NMR (400 MHz, CDCl₃):

δ = 4.36 (s, 4H, CH₂), 3.25 (s, 1H, CH), 1.95 (s, 6H, CH₃) ppm.

¹³C-NMR (100 MHz, CDCl₃):
δ = 171 (1C, C=O), 170 (1C, C=O), 63 (1C, C(CH₃)Br), 56 (2C, CH₂), 44 (1C, CH), 31 (2C, CH₃) ppm.

FT-IR (ATR):
ν̃ = 2978, 1729, 1148, 1105 cm⁻¹.

5.5. Free Radical Polymerizations

Synthesis of Poly(benzyl acrylate)
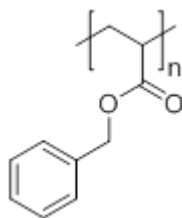
Polymerization was conducted by free radical polymerization of benzyl acrylate (3.51 g, 21.6 mmol, 1.0 eq.) with azobisisobutyronitrile (0.03 g, 0.21 mmol, 0.01 eq.) (AIBN) as initiator in 20 mL 1,4-dioxane at 95 °C. The polymer was purified by repeated precipitation into methanol and obtained as a colorless solid.

Yield: 2.42 g (69%)

¹H-NMR (300 MHz, CDCl₃):
δ = 7.25 (br. d, J = 4.6 Hz, 5H, CH$_{ar}$), 4.96 (s, 2H, CH₂), 2.36 (s, 1H,CH), 1.24–2.02 (m, 2H, CH₂CH) ppm.

¹³C-NMR (75 MHz, CDCl₃):
δ = 174.2 (COO), 135.8 (C$_{ar}$), 128.5 (CH$_{ar}$), 128.1 (CH$_{ar}$), 66.4 (CH₂), 41.3 (CH), 35.0 (CH₂CH) ppm.

FT-IR (ATR):
ν̃ = 1727, 1455, 1151, 735, 695 cm⁻¹.

Synthesis of Poly(glycidyl methacrylate) (PGMA)
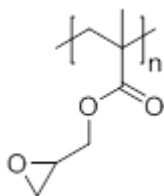
Glycidyl methacrylate (2.0 mL, 2.14 g, 15 mmol, 100 eq.) was heated with azobisisobuty-ronitrile (27.5 mg, 1.0 eq.) at 65 °C in 20 mL tetrahydrofuran under inert condition for 18 hours. Purification was done by repeated precipitation in methanol. The product was obtained as a colorless solid.

Yield: 1.56 g (73%)

^{1}H-NMR (400 MHz, CDCl$_3$):
δ = 3.99 (d, 1H, OCH$_2$), 3.16 (s, 1H, OCH$_2$CH), 2.68 (d, 2H, OCH$_2$CHCH$_2$), 1.12-2.12 (m, 2H, CH$_2$), 0.73-1.13 (m, 3H, CH$_3$) ppm.

^{13}C-NMR (100 MHz, CDCl$_3$):
δ = 176.3-177.8 (COO), 65.8-66.6 (OCH$_2$), 52-55 (CH$_2$), 49.1-49.5 (OCH$_2$CH), 44.9-45.7 (OCH$_2$CHCH$_2$), 16.9-19.8 (CH$_3$) ppm.

FT-IR (ATR):
$\tilde{\nu}$ = 2935, 1723, 1484,1447, 1254, 1146, 906, 844, 749 cm^{-1}.

5.6. Post-Polymerization Modifications

Post-Polymerization Modifications of Poly(benzyl 2-ylidene-acetate) and Poly(benzyl acrylate)

All post-polymerization modifications were conducted for a reaction time of 17 hours at 120 °C. Purification was done by dialysis against methanol/dichloromethane (1:1, v/v).

General Procedure Using Acyl Transfer Reagents:

A round bottom flask was charged with 1.0 eq. of poly(benzyl 2-ylidene-acetate) or poly(benzyl acrylate) dissolved in anisole, 1.0 eq. 1,2,4-triazole (Tz), 3.0 eq. 1,8-diazabicyclo[5.4.0]undec-7-ene (DBU), and 3.0 eq. of amine.

General Procedure Using Bulk Conditions:

A round bottom flask was charged with 1.0 eq. of polymer poly(benzyl 2-ylidene-acetate) or poly(benzyl acrylate) and 25 eq. of amine.

5. Experimental Part

General Procedures for Post-Polymerization Modifications of Poly(allyl 2-ylidene-acetate)

In solution

Post-polymerization modifications of PAA_C1 (1.0 eq.) were conducted overnight with 10.0 eq. of the respective thiol. The reactions were initiated by UVA-irradiation utilizing 0.1 eq. 2,2-dimethoxy-2-phenylacetophenone (DMPA) as a radical photo-initiator. Purification was performed via repeated precipitation with *n*-hexane using dichloromethane as a solvent.

Of thin films

44.9 mg of PAA_C1 were dissolved in 3 mL chloroform and the solution was spin-coated on a silicon wafer at 6000 rpm for 20 seconds. The obtained coated wafer was irradiated with UVA light ($\lambda = 315$–400 nm) overnight to crosslink the films. Subsequently, the films were submerged in a solution of the respective thiol (20 wt%) and 10 mg 2,2-dimethoxy-2-phenylacetophenone (DMPA) in 5 mL methanol. Afterwards, the film was irradiated with UVA light overnight.Washing the film successively with water, acetone and dichloromethane resulted in a functionalized PAA_C1 film.

Post-polymerization Modifications of Poly(glycidyl 2-ylidene-acetate) and Poly(glycidyl methacrylate)

Hydrolysis of PGA_C1:
Hydrolysis of PGA_C1 was conducted by adopting a published procedure[102] by dropwise addition of 5 mL sulfuric acid (0.1 M aqueous solution) to a solution of 49.5 mg polymer in 5 mL dioxane. The solution was stirred for 6 days at room temperature. Subsequently, the solution was neutralized with sodium carbonate and dialyzed against water (MWCO: 6 kD).

General Procedure for Post-Polymerization Modification of PGA_C1 with Nucleophiles:
Post-polymerization modification conditions were adapted from the work of *Gadwal* et al.[88] and *McEwan* et al.[68]

With amines:
Post-polymerization modifications of PGA_C1 (1.0 eq.) with amines was conducted overnight with 1.2 eq. of the respective amine in deuterated DMSO-d^6. The reactions were stirred at 60 °C for 24 hours. Dialysis with a mixture of methanol and dichloromethane (1:1, v/v) was used for purification.

With thiols:
Post-polymerization modifications of PGA_C1 (1.0 eq.) with thiols was conducted

overnight with 1.75 eq. of the respective thiol and 1.0 eq. of lithium hydroxide in DMSO. The reactions were stirred at 50 °C for 24 hours. Dialysis with a mixture of methanol and dichloromethane (1:1, v/v) was used for purification.

Post-Polymerization Modification of Poly(propargyl 2-ylidene-acetate) with Benzyl azide
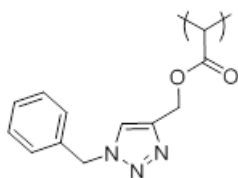
Post-polymerization modification of poly(propargyl 2-ylidene-acetate) with benzyl azide was done by dissolving poly(propargyl 2-ylidene-acetate) (53 mg, 1.0 eq.) and benzyl azide (0.4 mL, 3.31 mmol, 6.0 eq.) in 40 mL dimethylsulfoxide. The reaction mixture was heated to 90 °C overnight and subsequently cooled down to room temperature and precipitated in petrol ether.

Post-Polymerization modification of Poly(2-(2-bromoisobutyryloxy)ethyl 2-ylidene-acetate) with Methyl Acrylate via ATRP
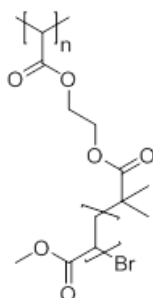
Post-polymerization modification of poly(2-(2-bromoisobutyryloxy)ethyl 2-ylidene-acetate) with methyl acrylate via ATRP was inspired by reference.[99] Poly(2-(2-bromoisobutyryloxy)ethyl 2-ylidene-acetate) (61.6 mg, 1.0 eq.), copper(I) bromide (18.0 mg, 0.12 mmol, 0.5 eq.), copper(II) bromide (1.6 mg, 0.006 mmol, 0.03 eq.),4,4´-dinonyl-2,2´-dipyridyl (42.7 mg, 0.25 mmol, 1.0 eq.) and methyl acrylate (2.2 mL, 24.5 mmol, 100 eq.) were dissolved under Schlenk conditions in dry 1,4-dioxane. Subsequently, the reaction mixture was heated to 70 °C overnight. A colorless precipitate and a green solution were formed. The solvent was evaporated and the residue dissolved in dichloromethane and filtered twice through a short column filled with neutral aluminum oxide.

6. Bibliography

[1] H. Staudinger, *Rubber Chem. Technol.* **1939**, *12*, 117–118.

[2] B. Adhikari, A. K. Sen in *Macromolecular Engineering. Precise Synthesis, Materials Properties, Applications 1st ed.*, K. Matyjaszewski, Y. Gnanou, L. Leibler (Eds.), Wiley-VCH Verlag GmbH & Co. KGaA, Weinheim, **2007**, chapter 13, pp. 2493–2539.

[3] M. Ebrahimi, F. Rosei, *Nat. Photon.* **2016**, *10*, 434–436.

[4] S. Lecommandoux, É. Garanger, *C. R. Chimie* **2016**, *19*, 143–147.

[5] L. S. Boffa, B. M. Novak, *Chem. Rev.* **2000**, *100*, 1479–1494.

[6] P. Nesvadba in *Encyclopedia of Radicals in Chemistry, Biology and Materials*, **2012**, pp. 1–36.

[7] N. G. Gaylord, *J. Macromol. Sci. Polymer Rev.* **1975**, *13*, 235–261.

[8] E. Jellema, A. L. Jongerius, J. N. H. Reek, B. de Bruin, *Chem. Soc. Rev.* **2010**, *39*, 1706–1723.

[9] M. Klapper, C. Hamciuc, R. Dyllick-Brenzinger, K. Müllen, *Angew. Chem. Int. Ed.* **2003**, *42*, 4687–4690.

[10] N. M. G. Franssen, J. N. H. Reek, B. de Bruin, *Chem. Soc. Rev.* **2013**, *42*, 5809–5832.

[11] H. v. Pechmann, *Ber. Dtsch. Chem. Ges.* **1898**, *31*, 2640–2646.

[12] K. J. Shea, J. W. Walker, H. Zhu, M. Paz, G. Jef, *JACS* **1997**, *119*, 9049–9050.

[13] H. Shimomoto, E. Itoh, T. Itoh, E. Ihara, N. Hoshikawa, N. Hasegawa, *Macromolecules* **2014**, *47*, 4169–4177.

[14] L. Liu, Y. Song, H. Li, *Polym. Int.* **2002**, *51*, 1047–1049.

[15] E. Ihara, *J. Synth. Org. Chem Jpn.* **2008**, *66*, 358–367.

[16] J. Luo, K. J. Shea, *Acc. Chem. Res.* **2010**, *43*, 1420–1433.

[17] N. Hadjichristidis, Z. Zhang, H. Zhao, Y. Gnanou, *Chem. Commun.* **2015**, *51*, 9936–9938.

[18] J. J. Tufariello, L. T. C. Lee, *JACS* **1966**, *88*, 4757–4759.

[19] J. J. Tufariello, L. T. C. Lee, P. Wojtkowski, *JACS* **1967**, *89*, 6804–6805.

[20] X.-Z. Zhou, K. J. Shea, *JACS* **2000**, *122*, 11515–11516.

[21] A. G. Nasini, G. Saini, L. Trossarelli, *Pure Appl. Chem.* **1961**, *4*, 255–270.

[22] A. Loose, *J. Prakt. Chem.* **1909**, *79*, 505–510.

[23] M. Imoto, T. Nakaya, *J. Macromol. Sci. Polymer Rev.* **1972**, *7*, 1–48.

[24] E. Ihara, N. Haida, M. Iio, K. Inoue, *Macromolecules* **2002**, *36*, 36–41.

[25] E. Ihara, M. Fujioka, N. Haida, T. Itoh, K. Inoue, *Macromolecules* **2005**, *38*, 2101–2108.

[26] E. Ihara, M. Kida, M. Fujioka, N. Haida, T. Itoh, K. Inoue, À. C, *J. Polym. Sci., Part A: Polym. Chem.* **2007**, *45*, 1536–1545.

[27] E. Ihara, Y. Ishiguro, N. Yoshida, T. Hiraren, T. Itoh, K. Inoue, *Macromolecules* **2009**, *42*, 8608–8610.

[28] E. Ihara, H. Takahashi, M. Akazawa, T. Itoh, K. Inoue, *Macromolecules* **2011**, *44*, 3287–3292.

[29] H. Shimomoto, K. Shimizu, C. Takeda, M. Kikuchi, T. Kudo, H. Mukai, T. Itoh, E. Ihara, N. Hoshikawa, A. Koiwai, N. Hasegawa, *Polym. Chem.* **2015**, *6*, 8124–8131.

[30] D. G. H. Hetterscheid, C. Hendriksen, W. I. Dzik, J. M. M. Smits, E. R. H. van Eck, A. E. Rowan, V. Busico, M. Vacatello, V. Van Axel Castelli, A. Segre, E. Jellema, T. G. Bloemberg, B. de Bruin, *JACS* **2006**, *128*, 9746–9752.

[31] M. Tokita, K. Shikinaka, T. Hoshino, K. Fujii, J. Mikami, N. Koshimizu, K. Sakajiri, S. Kang, J. Watanabe, K. Shigehara, *Polymer* **2013**, *54*, 995–998.

[32] N. Koshimizu, Y. Aizawa, K. Sakajiri, K. Shikinaka, K. Shigehara, S. Kang, M. Tokita, *Macromolecules* **2015**, *48*, 3653–3661.

[33] E. Ihara, T. Itoh, H. Shimomoto, *Macromol. Symp.* **2015**, *349*, 57–64.

[34] H. Shimomoto, H. Asano, T. Itoh, E. Ihara, *Polym. Chem.* **2015**, *6*, 4709–4714.

[35] E. Jellema, P. H. M. Budzelaar, J. N. H. Reek, B. de Bruin, *JACS* **2007**, *129*, 11631–11641.

[36] A. F. Noels, *Angew. Chem. Int. Ed.* **2007**, *46*, 1208–1210.

[37] N. M. G. Franssen, B. Ensing, M. Hegde, T. J. Dingemans, B. Norder, S. J. Picken, G. O. R. Alberda van Ekenstein, E. R. H. van Eck, J. a. a. W. Elemans, M. Vis, J. N. H. Reek, B. de Bruin, *Chem. Eur. J.* **2013**, *19*, 11577–11589.

[38] M. Finger, J. N. H. Reek, B. de Bruin, *Organometallics* **2011**, *30*, 1094–1101.

[39] M. Finger, M. Lutz, J. N. H. Reek, B. de Bruin, *Eur. J. Inorg. Chem.* **2012**, *2012*, 1437–1444.

[40] A. J. C. Walters, O. Troeppner, I. Ivanović-Burmazović, C. Tejel, M. P. del Río, J. N. H. Reek, B. de Bruin, *Angew. Chem. Int. Ed.* **2012**, *51*, 5247–5251.

[41] A. J. C. Walters, E. Jellema, M. Finger, P. Aarnoutse, J. M. M. Smits, J. N. H. Reek, B. de Bruin, *ACS Catal.* **2012**, *2*, 246–260.

[42] N. M. G. Franssen, M. Finger, J. N. H. Reek, B. de Bruin, *Dalton Trans.* **2013**, *42*, 4139–4152.

[43] A. J. C. Walters, Ph.D. thesis, University of Amsterdam (UvA), **2013**.

[44] L. Xiao, F. Li, Y. Li, X. Jia, L. Liu, *RSC Adv.* **2014**, *4*, 41848–41855.

[45] T. Curtius, *Ber. Dtsch. Chem. Ges.* **1883**, *16*, 2230–2231.

[46] H. Zollinger, *Diazo Chemistry I - Aromatic and Heteroaromatic Compounds*, VCH Verlagsgesellschaft, VCH Publishers, Weinheim - New York - Basel - Cambridge - Tokyo, **1994**.

[47] H. Zollinger, *Diazo Chemistry II: Aliphatic, inorganic and organometallic compounds*, VCH Verlagsgesellschaft, VCH Publishers, Weinheim - New York - Basel - Cambridge - Tokyo, **1995**.

[48] M. Regitz, G. Maas, *Diazo Compounds - Properties and Synthesis*, Academic Press, Inc., London, **1986**.

[49] G.-Y. Li, C.-M. Che, *Org. Lett.* **2004**, *6*, 1621–1623.

[50] T. Toma, J. Shimokawa, T. Fukuyama, *Org. Lett.* **2007**, *9*, 3195–3197.

[51] H. C. Kolb, M. G. Finn, K. B. Sharpless, *Angew. Chem. Int. Ed.* **2001**, *40*, 2004–2021.

[52] K. A. Günay, P. Théato, H.-A. Klok in *Functional Polymers by Post-Polymerization Modification: Concepts, Guidelines, and Applications 1st ed.*, P. Theato, H.-A. Klok (Eds.), Wiley-VCH Verlag GmbH & Co. KGaA, Weinheim, **2013**, chapter 1, pp. 1–44.

[53] R. Huisgen in *Proc. Chem. Soc.*, pp. 357–369.

[54] L. Liang, D. Astruc, *Coord. Chem. Rev.* **2011**, *255*, 2933–2945.

[55] D. Fournier, R. Hoogenboom, U. S. Schubert, *Chem. Soc. Rev.* **2007**, *36*, 1369–1380.

[56] A. Scarpaci, C. Cabanetos, E. Blart, V. Montembaul, L. Fontaine, V. Rodriguez, F. Odobel, *J. Polym. Sci., Part A: Polym. Chem.* **2009**, *47*, 5652–5660.

[57] B. S. Sumerlin, N. V. Tsarevsky, G. Louche, R. Y. Lee, K. Matyjaszewski, *Macromolecules* **2005**, *38*, 7540–7545.

[58] T. Posner, *Chem. Ber.* **1905**, *38*, 646–657.

[59] N. K. Singha, H. Schlaad in *Functional Polymers by Post-Polymerization Modification: Concepts, Guidelines, and Applications*, P. Théato, H.-A. Klok (Eds.),

6. Bibliography

Wiley-VCH Verlag GmbH & Co. KGaA, Weinheim, Germany, **2013**, chapter 3, pp. 65–86.

[60] L. M. Campos, K. L. Killops, R. Sakai, J. M. J. Paulusse, D. Damiron, E. Drockenmuller, B. W. Messmore, C. J. Hawker, *Macromolecules* **2008**, *41*, 7063–7070.

[61] D. P. Nair, M. Podgórski, S. Chatani, T. Gong, W. Xi, C. R. Fenoli, C. N. Bowman, *Chem. Mater.* **2014**, *26*, 724–744.

[62] J. Justynska, Z. Hordyjewicz, H. Schlaad, *Polymer* **2005**, *46*, 12057–12064.

[63] A. Gress, A. Völkel, H. Schlaad, *Macromolecules* **2007**, *40*, 7928–7933.

[64] J. P. Pascault, R. J. J. Williams in *Epoxy Polymers: New Materials and Innovations*, J. P. Pascault, R. J. J. Williams (Eds.), Wiley-VCH Verlag GmbH & Co. KGaA, Weinheim, Germany, **2010**, chapter 1, pp. 1–12.

[65] T. Hino, T. Endo, *J. Polym. Sci. Part A: Polym. Chem.* **2004**, *42*, 2166–2170.

[66] M. Gervais, A. L. Brocas, G. Cendejas, A. Deffieux, S. Carlotti, *Macromolecules* **2010**, *43*, 1778–1784.

[67] B. Schulte, a. Walther, H. Keul, M. Moller, *Macromolecules* **2014**, *47*, 1633–1645.

[68] K. a. McEwan, S. Slavin, E. Tunnah, D. M. Haddleton, *Polym. Chem.* **2013**, *4*, 2608–2614.

[69] P. Ferruti, A. Bettelli, A. Feré, *Polymer* **1972**, *13*, 462–464.

[70] H. G. Batz, G. Franzmann, H. Ringsdorf, *Angew. Chem. Int. Ed.* **1972**, *11*, 1103–1104.

[71] A. Godwin, M. Hartenstein, A. H. E. Müller, S. Brocchini, *Angew. Chem., Int. Ed.* **2001**, *40*, 594–597.

[72] M. Eberhardt, R. Mruk, R. Zentel, P. Théato, *Eur. Polym. J.* **2005**, *41*, 1569–1575.

[73] Y. Liu, L. X. Wang, C. Y. Pan, *Macromolecules* **1999**, *32*, 8301–8305.

[74] N. Metz, P. Théato, *Eur. Polym. J.* **2007**, *43*, 1202–1209.

[75] X. Yang, V. B. Birman, *Org. Lett.* **2009**, *11*, 1499–502.

[76] R. Kakuchi, K. Wongsanoh, V. P. Hoven, P. Theato, *J. Polym. Sci., Part A: Polym. Chem.* **2014**, *52*, 1353–1358.

[77] I. B. Kim, R. Phillips, U. H. F. Bunz, *Macromolecules* **2007**, *40*, 5290–5293.

[78] T. Krappitz, P. Theato, *J. Polym. Sci. Pol. Chem.* **2016**, *54*, 686–691.

[79] E. Jellema, A. L. Jongerius, G. A. van Ekenstein, S. D. Mookhoek, T. J. Dingemans, E. M. Reingruber, A. Chojnacka, P. J. Schoenmakers, R. Sprenkels, E. R. H. van Eck, J. N. H. Reek, B. de Bruin, *Macromolecules* **2010**, *43*, 8892–8903.

[80] T. Krappitz, D. Brauer, P. Theato, *Polym. Chem.* **2016**, *7*, 4525–4530.

[81] M. Donati, M. Farina, *Macromol. Chem. Phys.* **1963**, *60*, 233–235.

[82] G. F. D'Alelio, T. R. Hoffend, *J. Polym. Sci., Part A: Polym. Chem.* **1967**, *5*, 323–337.

[83] E. Jellema, A. L. Jongerius, A. J. C. Walters, J. M. M. Smits, J. N. H. Reek, B. de Bruin, *Organometallics* **2010**, *29*, 2823–2826.

[84] C. E. Hoyle, C. N. Bowman, *Angew. Chem. Int. Ed.* **2010**, *49*, 1540–1573.

[85] L. Gao, T. J. McCarthy, *Langmuir* **2006**, *22*, 6234–6237.

[86] Y. Yuan, T. R. Lee in *Surface Science Techniques*, G. Bracco, B. Holst (Eds.), Springer Berlin Heidelberg, **2013**, pp. 3–34.

[87] T. Krappitz, P. Feibusch, C. Aroonsirichock, V. P. Hoven, P. Theato, *Macromolecules* **2017**, *50*, 1415–1421.

[88] I. Gadwal, M. C. Stuparu, A. Khan, *Polym. Chem.* **2015**, *6*, 1393–1404.

[89] E. Helms, N. Arpaia, M. Widener, *J. Chem. Educ.* **2007**, *84*, 1328–1330.

[90] D. L. Pavia, G. M. Lampman, G. S. Kriz, *Introduction to Spectroscopy 3rd ed.*, Thomson Learning, **2001**.

[91] H. Sharghi, Z. Pazirae, K. Niknam, *Bull. Korean Chem. Soc.* **2002**, *23*, 1611–1615.

[92] L. Xiao, S. Cai, Q. Liu, L. Liao, X. Guo, Y. Li, X. Jia, F. Li, L. Liu, *Polym. Chem.* **2014**, *5*, 607–613.

[93] E. A. Shapiro, A. B. Dyatkin, O. M. Nefedov, *Russ. Chem. Bull.* **1991**, *40*, 934–939.

[94] K. Matyjaszewski, *Polym. Int.* **2003**, *52*, 1559–1565.

[95] R. Verduzco, X. Li, S. L. Pesek, G. E. Stein, *Chem. Soc. Rev.* **2015**, *44*, 2405–2420.

[96] M. Zhang, C. Estournès, W. Bietsch, A. H. E. Müller, *Adv. Funct. Mater.* **2004**, *14*, 871–882.

[97] R. Djalali, S. Y. Li, M. Schmidt, *Macromolecules* **2002**, *35*, 4282–4288.

[98] L. Ren, J. Zhang, C. G. Hardy, D. Doxie, B. Fleming, C. Tang, *Macromolecules* **2012**, *45*, 2267–2275.

[99] S. Qin, K. Matyjaszewski, H. Xu, S. S. Sheiko, *Macromolecules* **2003**, *36*, 605–612.

[100] M. Presset, D. Mailhol, Y. Coquerel, J. Rodriguez, *Synthesis* **2011**, *2011*, 2549–2552.

6. Bibliography

[101] L. Ren, J. Zhang, C. G. Hardy, D. Doxie, B. Fleming, C. Tang, *Macromolecules* **2012**, *45*, 2267–2275.

[102] C. S. Gudipati, M. B. H. Tan, H. Hussain, Y. Liu, C. He, T. P. Davis, *Macromol. Rapid Commun.* **2008**, *29*, 1902–1907.

A. Available Supporting Informations

A.1. Supporting Information for Chapter 3.1

The supporting information for chapter 3.1 is partially adapted from Ref.[78] - *J. Polym. Sci. Pol. Chem.*, **2016**, 54, 686–691 - with permission from Wiley Periodicals, Inc. The online content can be accessed by using the following URL:

http://doi.wiley.com/10.1002/pola.27891

^{13}C NMR Spectrum and SEC trace of Poly(benzyl 2-ylidene-acetate) (PBnA_C1) Functionalized with *n*-Hexylamine
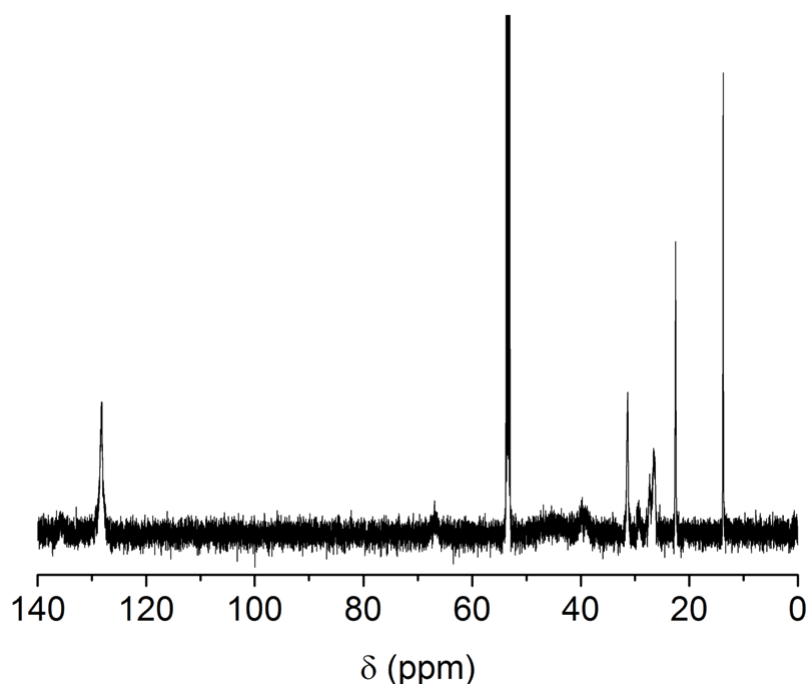
Fig. A.1.: ^{13}C NMR spectrum of poly(benzyl 2-ylidene-acetate) **PBnA_C1** functionalized with *n*-hexylamine. The spectrum was measured in CD_2Cl_2 (150 MHz spectrum).
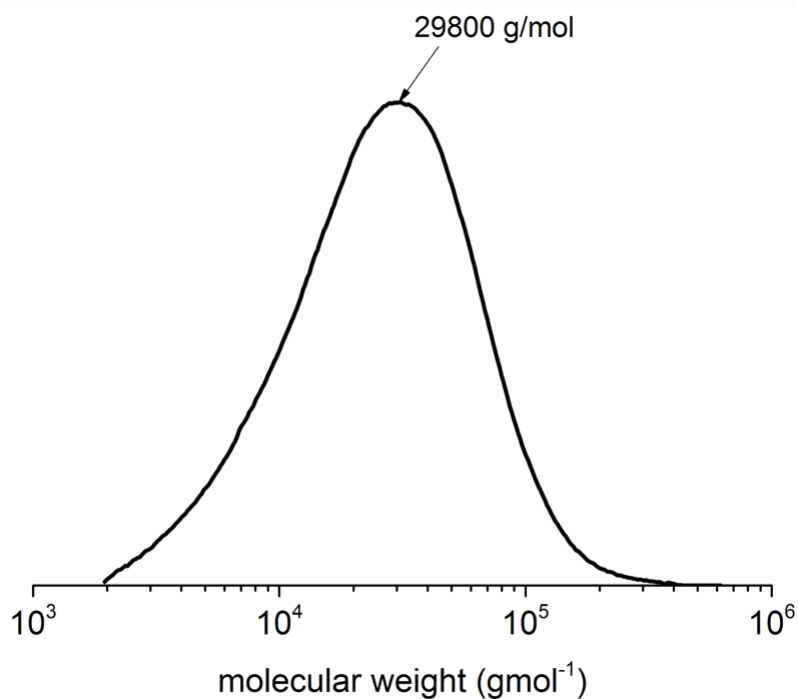
Fig. A.2.: SEC trace of poly(benzyl 2-ylidene acetate) **PBnA_C1** functionalized with *n*-hexylamine. Eluent: THF.

^{1}H and ^{13}C NMR Spectra of Poly(benzyl 2-ylidene-acetate) (PBnA_C1) Functionalized with Piperidine
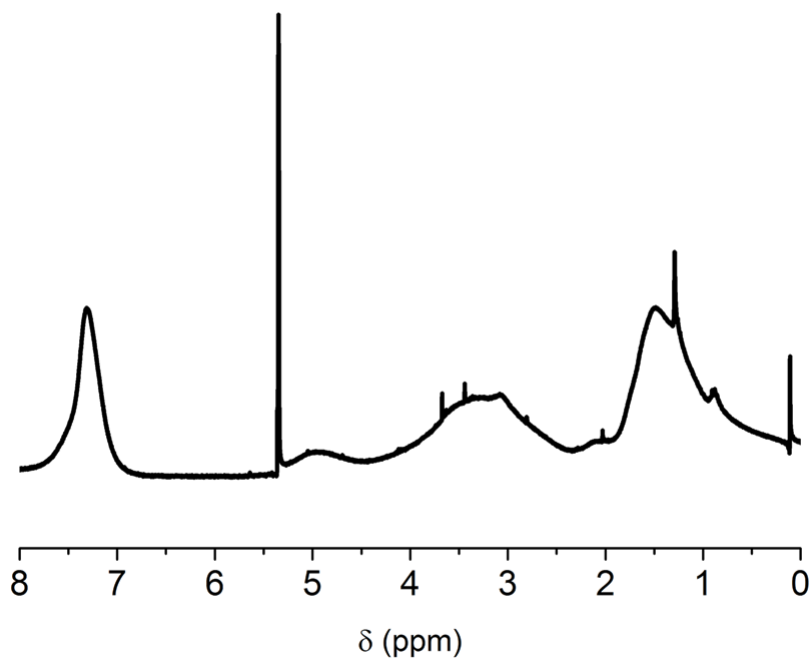
Fig. A.3.: ^{1}H NMR spectrum of poly(benzyl 2-ylidene-acetate) **PBnA_C1** functionalized with piperidine. The spectrum was measured in CD_2Cl_2 (600 MHz spectrum).
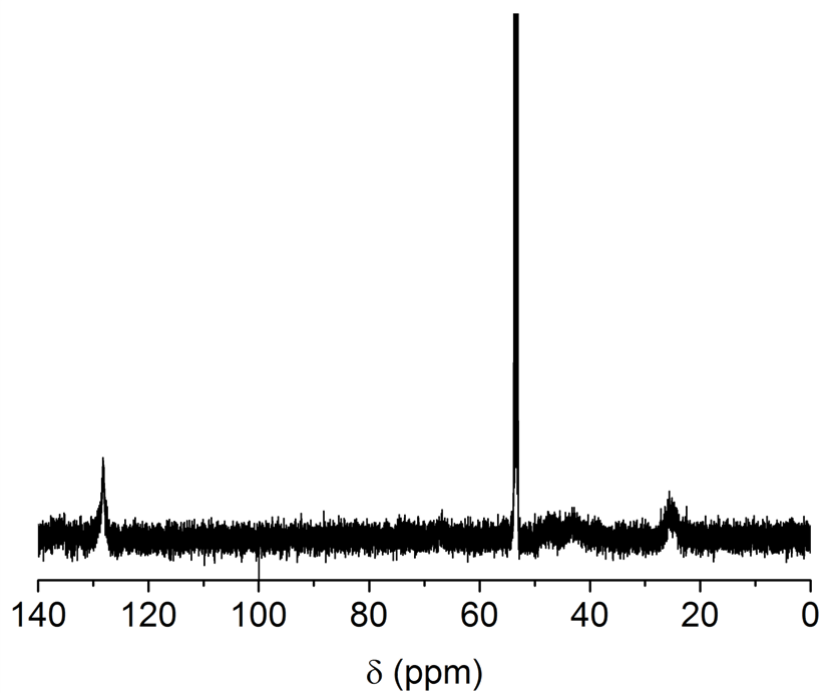
Fig. A.4.: ^{13}C NMR spectrum of poly(benzyl 2-ylidene-acetate) **PBnA_C1** functionalized with piperidine. Spectrum was measured in CD_2Cl_2 (150 MHz spectrum).

^{1}H NMR Spectrum of Poly(benzyl 2-ylidene-acetate) (PBnA_C1) Functionalized with 2-Ethylhexylamine
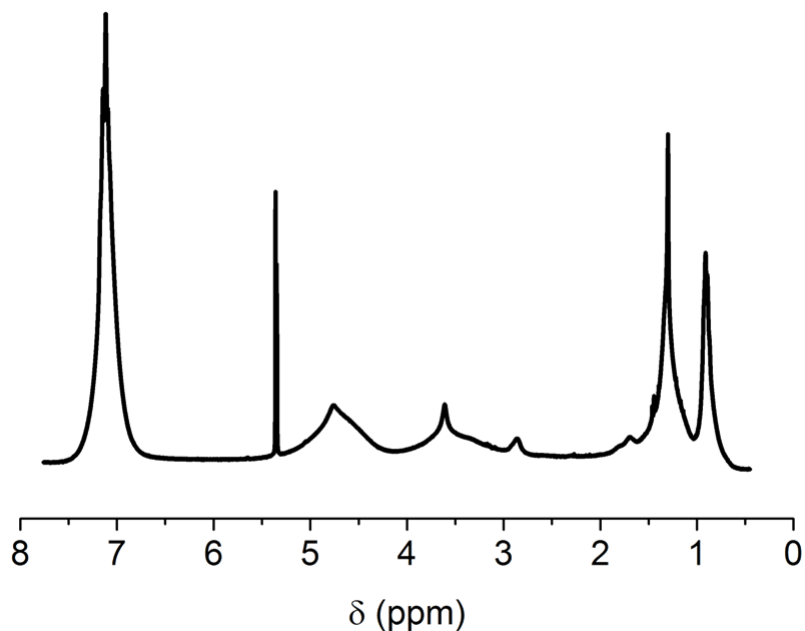
Fig. A.5.: ^{1}H NMR spectrum of poly(benzyl 2-ylidene-acetate) **PBnA_C1** functionalized with 2-ethylhexylamine. The spectrum was measured in CD_2Cl_2 (300 MHz spectrum).

^{1}H NMR Spectrum of Poly(benzyl 2-ylidene-acetate) (PBnA_C1) Functionalized with Benzylamine
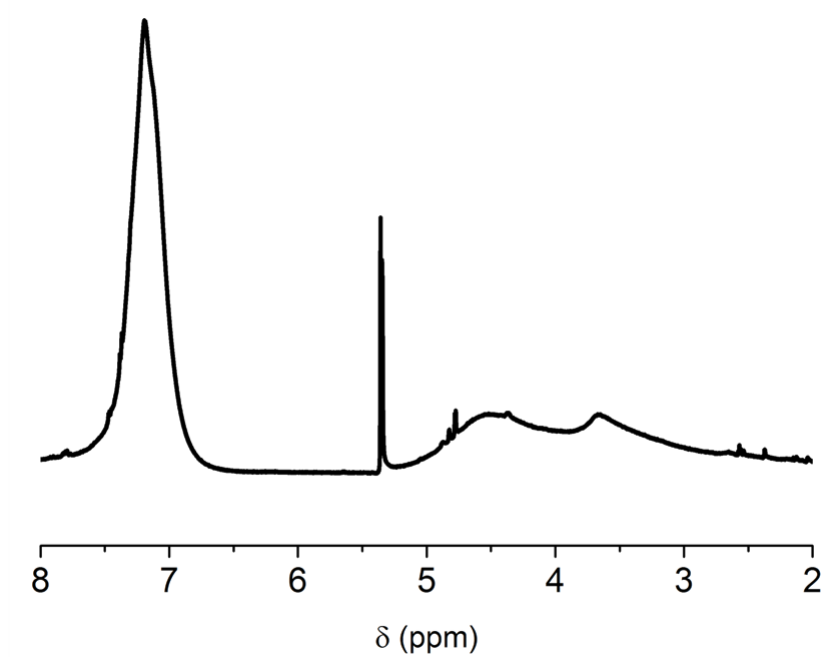
Fig. A.6.: ^{1}H NMR spectrum of poly(benzyl 2-ylidene-acetate) **PBnA_C1** functionalized with benzylamine. The spectrum was measured in CD_2Cl_2 (300 MHz spectrum).

TGA Data of Poly(benzyl 2-ylidene-acetate) (PBnA_C1), PBnA_C1 Functionalized with n-Hexylamine and PBnA_C1 Functionalized with Piperidine
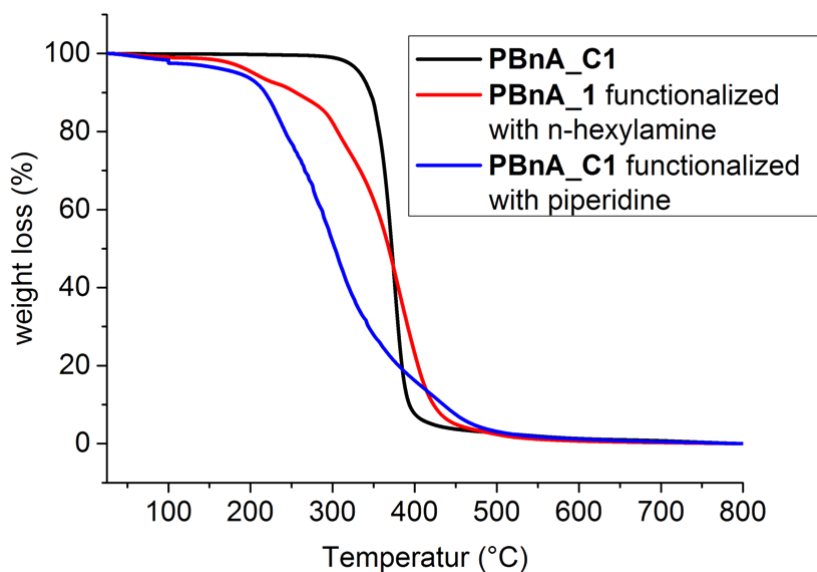
Fig. A.7.: TGA data of of poly(benzyl 2-ylidene-acetate) **PBnA_C1**, **PBnA_C1** functionalized with n-hexylamine and **PBnA_C1** functionalized with piperidine. The investigated temperature range is 25 °C to 800 °C at 10 °C min⁻¹ under air. The pristine polymeric starting material has a distinct weight loss between 300 to 400 °C. Both functionalized polymers show a broader weight loss region with an earlier onset temperature compared to the C1 polymeric material. This can be attributed to non-quantitative conversion and the formation of pseudo-copolymers.

DSC Data of Poly(benzyl 2-ylidene-acetate) (PBnA_C1) and PBnA_C1 Functionalized with *n*-Hexylamine
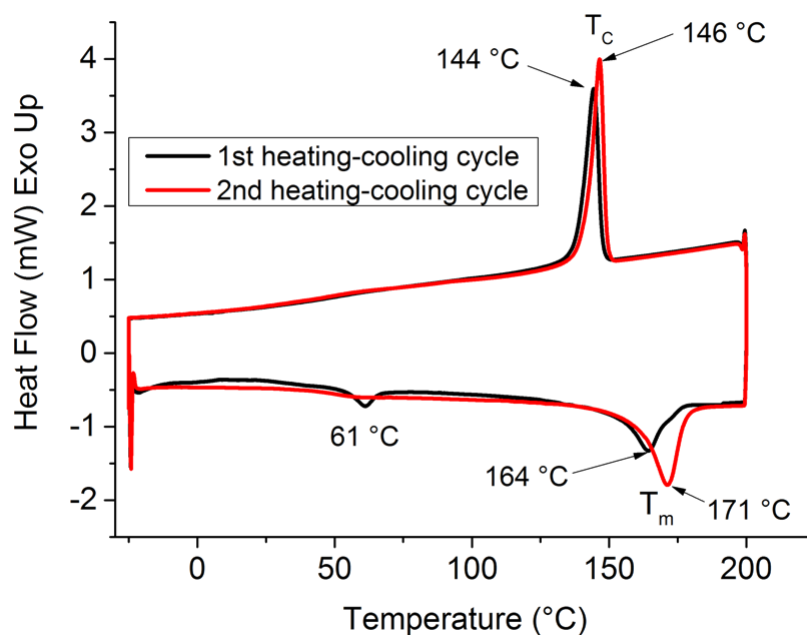
Fig. A.8.: DSC scan of of poly(benzyl 2-ylidene-acetate) **PBnA_C1**. The investigated temperature range is -25 °C to 200 °C at 10 °C min^{-1}. Data of the first and second run were collected. Transition temperatures are determined at the peak maximum.
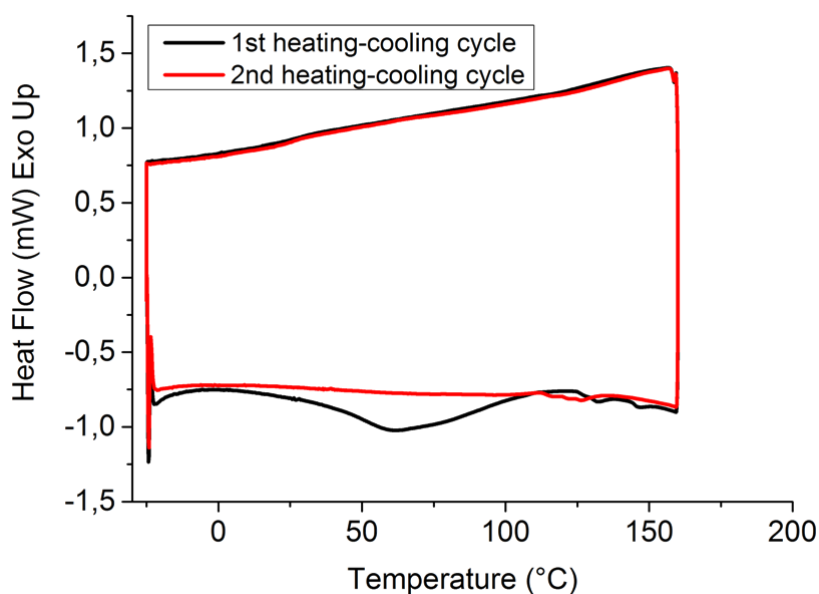
Fig. A.9.: DSC scan of of poly(benzyl 2-ylidene-acetate) **PBnA_C1** functionalized with *n*-hexylamine. The investigated temperature range is -25 °C to 160 °C at 10 °C min^{-1}. Data of the first and second run were collected. Solely a broad signal in the first heating run can be observed with a signal maximum at 61 °C.

SLS Data of Poly(benzyl 2-ylidene-acetate) (PBnA_C1) and PBnA_C1 Functionalized with *n*-Hexylamine

The data depicted below were obtained from a different batch of C1 polymer poly(benzyl 2-ylidene-acetate) than the one used in Chapter 3.1. Analysis by SLS resulted in a molecular weight of $M_w(c) = 686{,}000\,\text{g}\,\text{mol}^{-1}$ for the starting C1 polymer with a refractive index increment of $0.10805\,\text{mL}\,\text{g}^{-1}$ calculated as average value out of two measurement series. The modified polymer results in a decreased molecular weight $(M_w(c) = 254{,}000\,\text{g}\,\text{mol}^{-1})$ compared to the starting C1 polymer. Again the refractive index increment $(0.08683\,\text{mL/g})$ has been determined twice and averaged over both runs. A decrease was expected as two repeating units will form one new repeating unit. SLS data were determined from the following solutions in chloroform:

Table A.1.: Concentrations used for SLS analysis.

PBnA_C1 $(\text{dn/dc} = 0.10805\,\text{mL}\,\text{g}^{-1})$	**PBnA_C1** functionalized with *n*-hexylamine $(\text{dn/dc} = 0.08683\,\text{mL}\,\text{g}^{-1})$
$0.998\,\text{mg}\,\text{mL}^{-1}$	$1.720\,\text{mg}\,\text{mL}^{-1}$
$1.310\,\text{mg}\,\text{mL}^{-1}$	$2.566\,\text{mg}\,\text{mL}^{-1}$
$2.372\,\text{mg}\,\text{mL}^{-1}$	$3.105\,\text{mg}\,\text{mL}^{-1}$
$3.043\,\text{mg}\,\text{mL}^{-1}$	$4.067\,\text{mg}\,\text{mL}^{-1}$
$3.665\,\text{mg}\,\text{mL}^{-1}$	
$4.770\,\text{mg}\,\text{mL}^{-1}$	

Mw(c): 6.864e+05 g/mol   Mw(q²): 6.864e+05 g/mol
A2: 2.747e-07 mol dm³/g²   Rg: 5.463e+01 nm
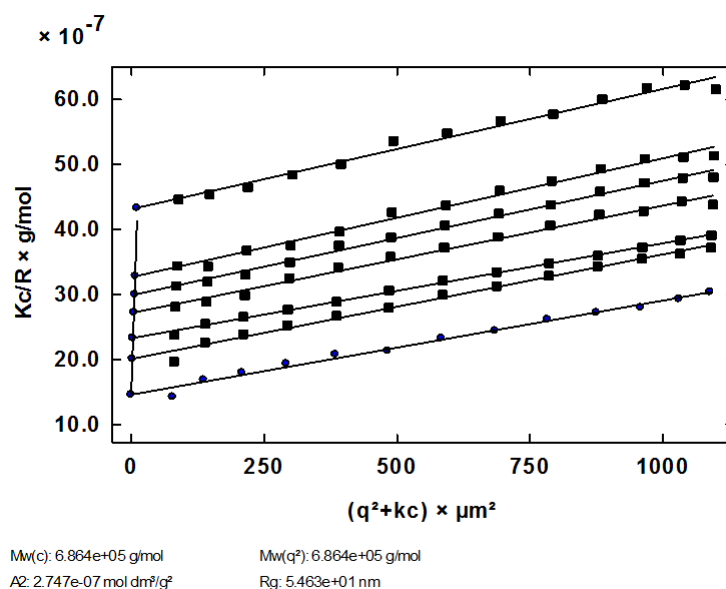
Fig. A.10.: Zimm-plot of poly(benzyl 2-ylidene-acetate) **PBnA_C1**.
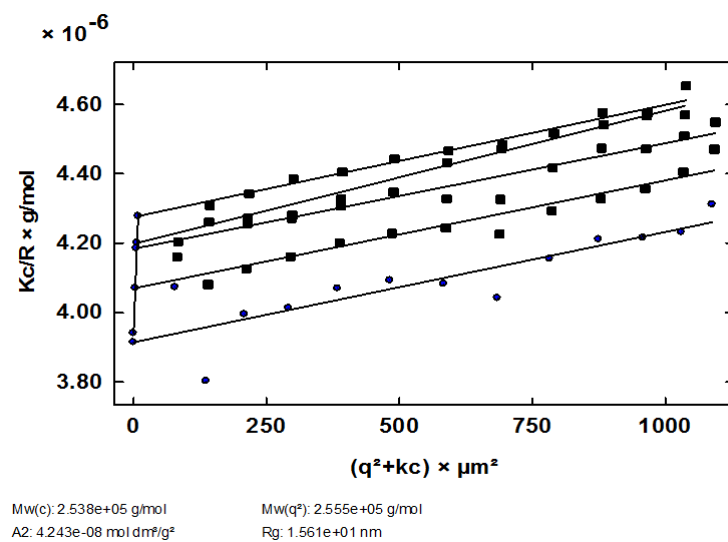
Fig. A.11.: Zimm-plot of poly(benzyl 2-ylidene-acetate) **PBnA_C1** functionalized with n-hexylamine.

A.2. Supporting Information for Chapter 3.2

The supporting information for chapter 3.2 is partially adapted from Ref.[80]- *Polym. Chem.*, **2016**, 7, 4525–4530 - with permission from The Royal Society of Chemistry. The online content can be accessed by using the following URL:

`http://xlink.rsc.org/?DOI=C6PY00818F`

Real-Time In-Situ FT-IR (Masked Points Included)
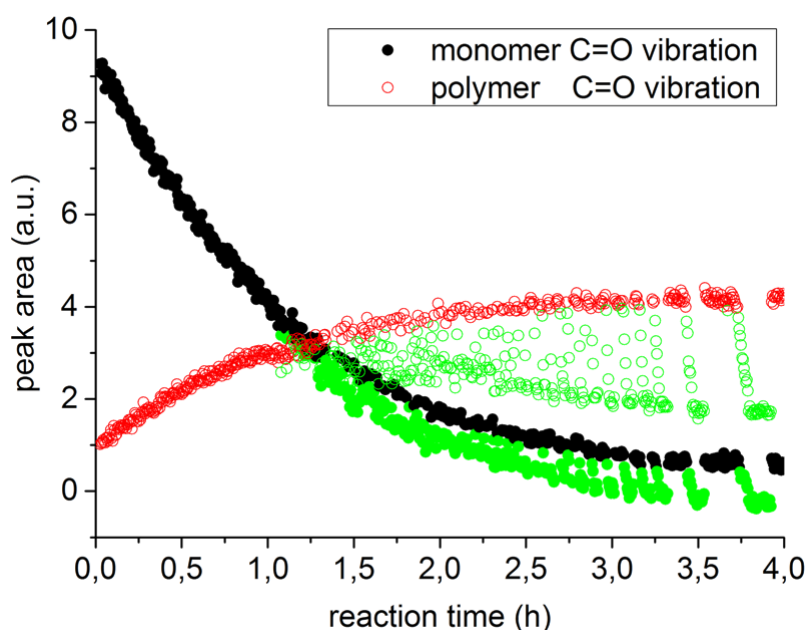
Fig. A.12.: Peak areas of the C=O vibration modes tracked over time by real-time in-situ FT-IR spectroscopy. Black circles resemble the peak area trend of the monomer C=O vibration mode. Red open circles resemble the peak area trend of the polymer C=O vibration mode. Green open and closed circles are masked points. Points were masked as the recorded IR signal tended to drop in intensity at later reaction times. This intensity drop was recorded for both C=O vibration modes, monomer and polymer.

Spectral Data for PAA_C1 After Bromination
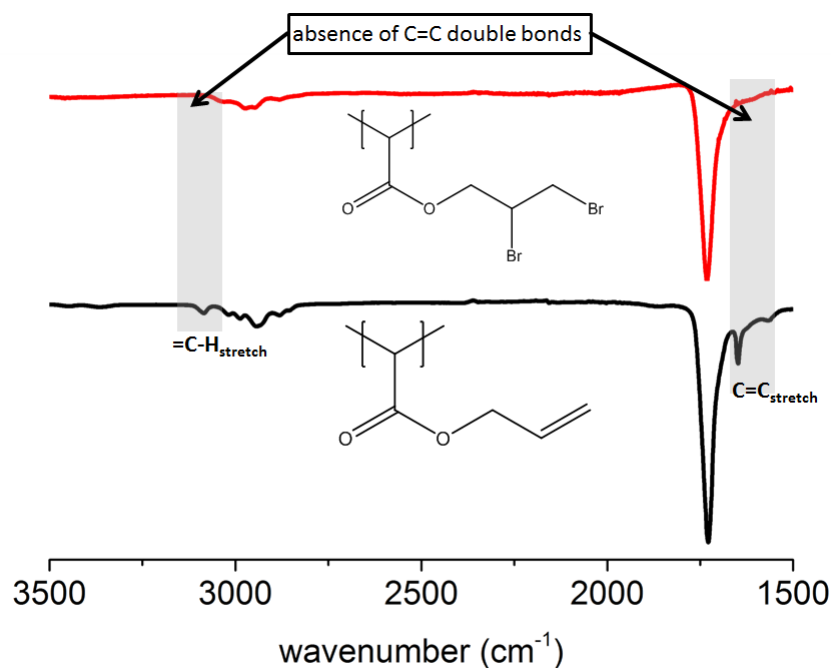
Fig. A.13.: FT-IR spectra of **PAA_C1** prior to and after bromination, showing quantitative conversion of double bonds. Bromination of $54.6\,\mathrm{mg}$ **PAA_C1** in $20\,\mathrm{mL}$ chloroform was done by adding a large excess of bromine $(1\,\mathrm{mL})$ and subsequent storage in the fridge for three days. Afterwards the polymer was precipitated in methanol. The obtained polymer was insoluble in all tested solvents.

A.3. Supporting Information for Chapter 3.3

The supporting information for chapter 3.3 is partially adapted from Ref.[87] - *Macromolecules*, **201**7, 50, 1415-1421 - with permission from The American Chemical Society. The online content can be accessed by using the following URL:

`http://pubs.acs.org/doi/abs/10.1021/acs.macromol.6b02465`

FT-IR Spectra of PGA_C1 Before and After Bromination
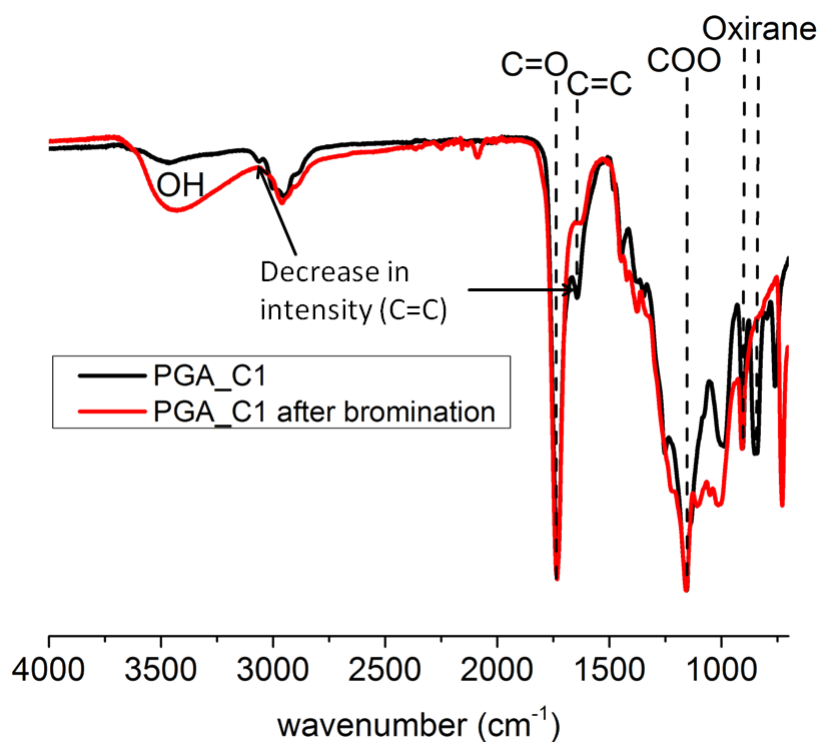
Fig. A.14.: Obtained FT-IR spectra before and after bromination. Black: **PGA_C1**; Red: **PGA_C1** after bromination. Ring-opening is clearly observed, by absence of the oxirane signals at 905 and 852 cm^{-1} as well as the OH vibration at 3427 cm^{-1}. Furthermore, a decrease in the vibration intensity of the carbon-carbon double bond at 1644 cm^{-1} can be noticed.

Spectral Changes in the ¹H NMR Spectra After Functionalization of PGA_C1 with Amines
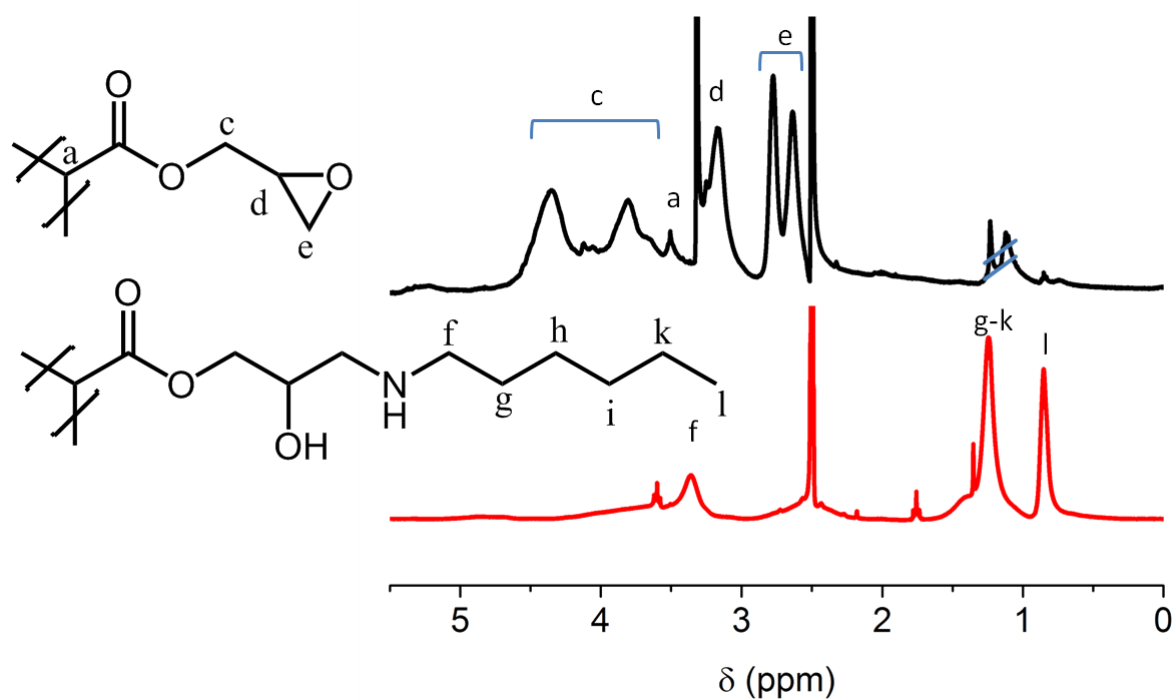
Fig. A.15.: Post-polymerization modification of **PGA_C1** with n-hexylamine – ^{1}H NMR spectrum recorded in DMSO-d^6.
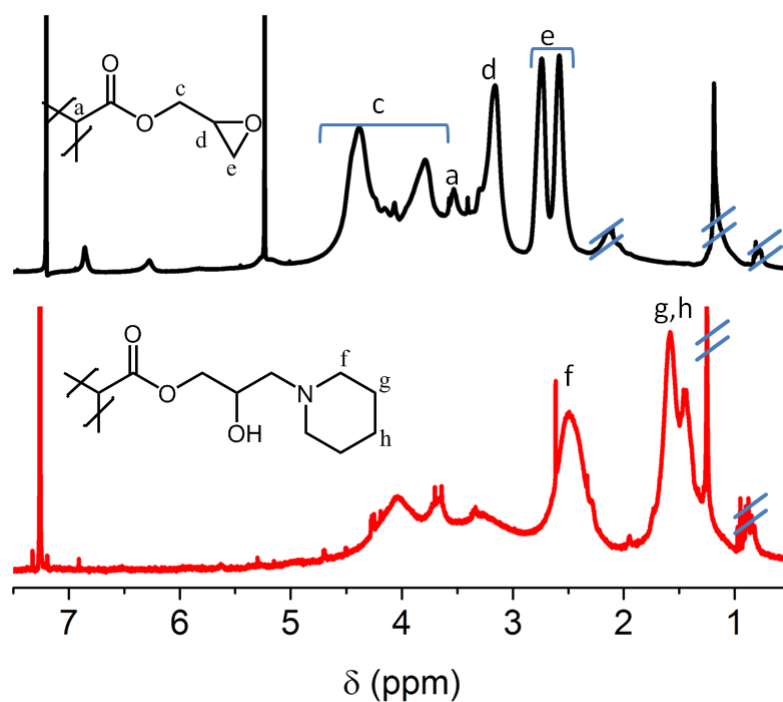
Fig. A.16.: Post-polymerization modification of **PGA_C1** with piperidine – ^{1}H NMR spectrum recorded in CDCl$_3$.
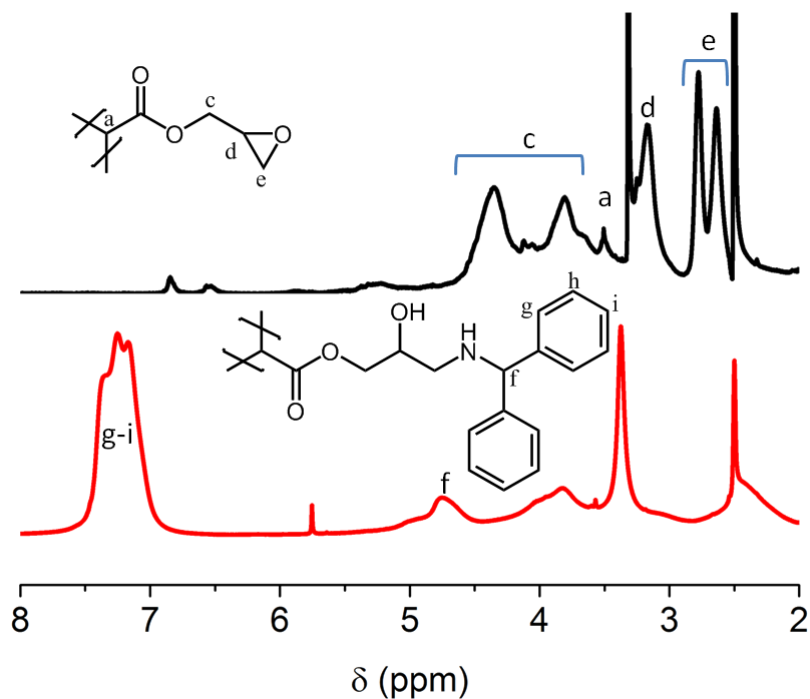
Fig. A.17.: Post-polymerization modification of **PGA_C1** with α-aminodiphenyl-methane -^{1}H NMR spectrum recorded in DMSO-d[6].

Spectral Changes in the FT-IR Spectra After Functionalization of PGA_C1 with Amines
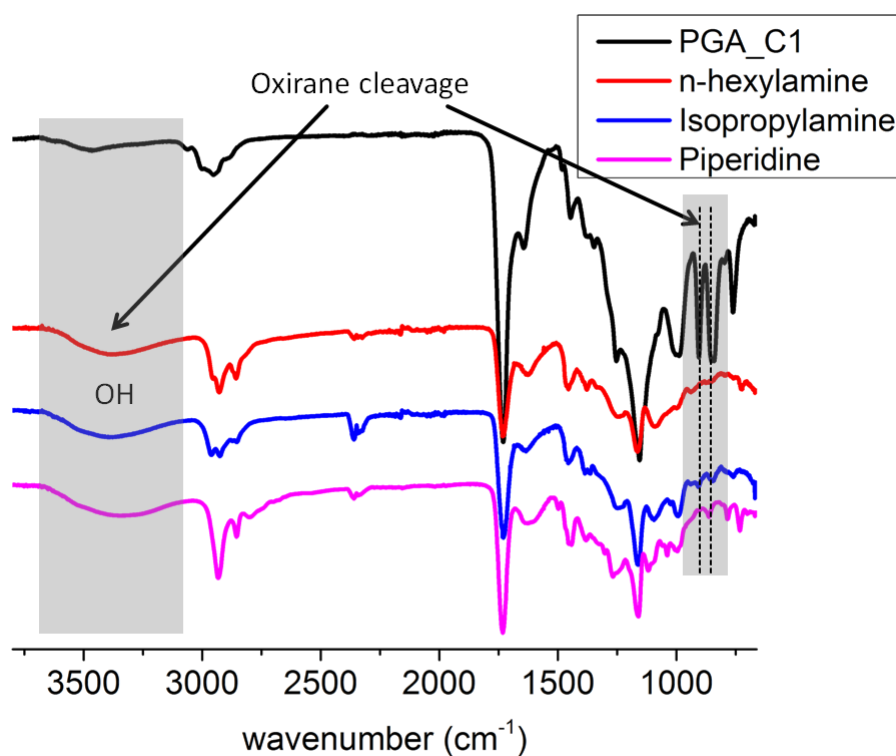
Fig. A.18.: Oxirane cleavage of **PGA_C1** with various amines as observed via FT-IR spectroscopy.

Spectral Changes in the ¹H NMR Spectra After Functionalization of PGA_C1 with Thiols
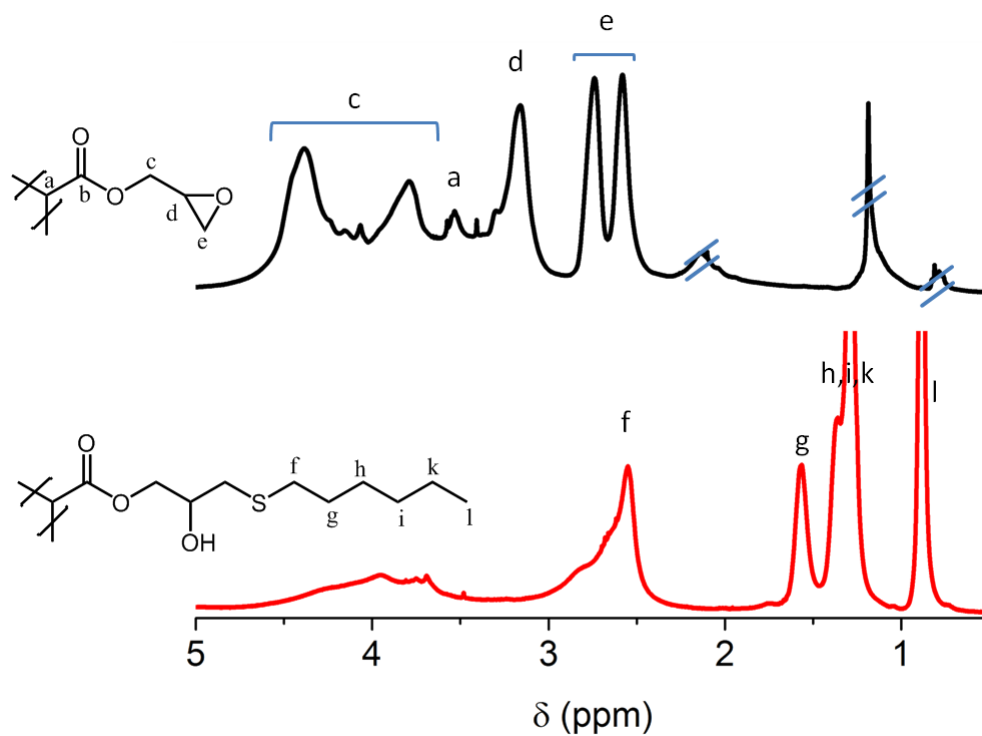
Fig. A.19.: Post-polymerization modification of **PGA_C1** with 1-mercaptohexane -¹H NMR spectrum recorded in CDCl₃.
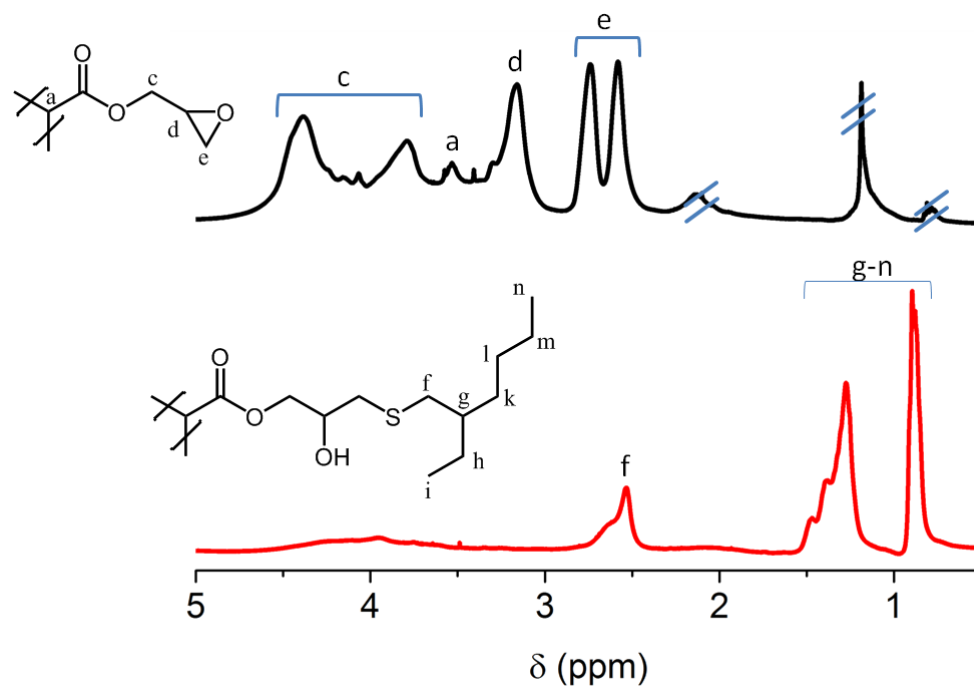
Fig. A.20.: Post-polymerization modification of **PGA_C1** with 2-ethylhexylthiol – ¹H NMR spectrum recorded in CDCl₃.
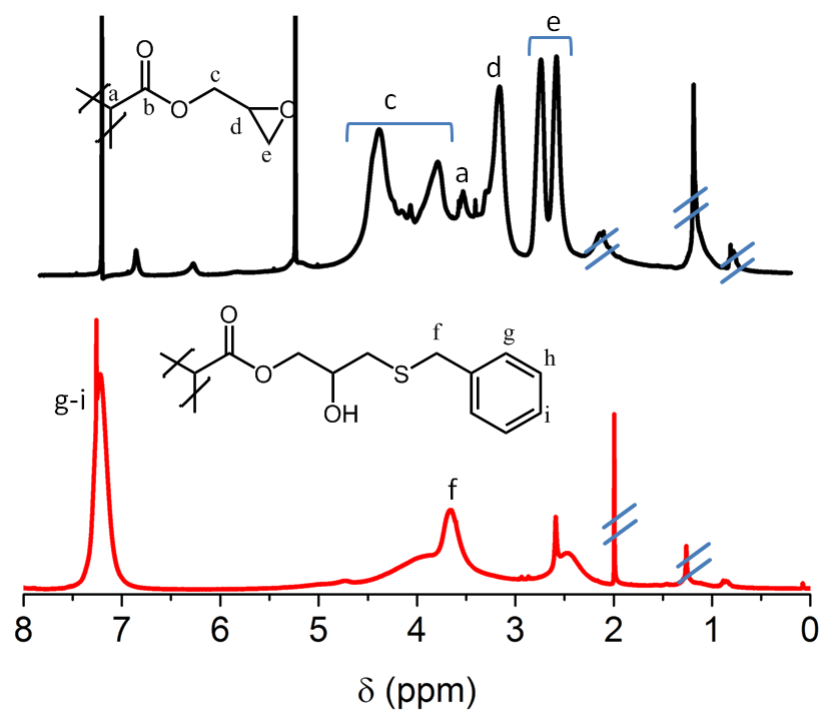
Fig. A.21.: Post-polymerization modification of **PGA_C1** with benzylmercaptan – ^{1}H NMR spectrum recorded in CDCl$_3$.
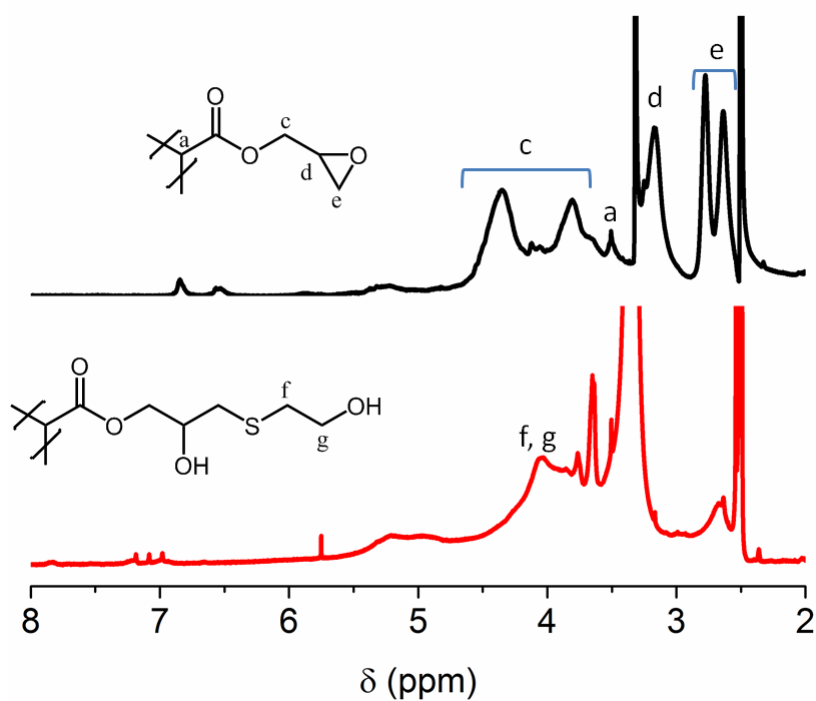
Fig. A.22.: Post-polymerization modification of **PGA_C1** with mercaptoethanol – ^{1}H NMR spectrum recorded in DMSO-d[6]. The product was acidified prior to analysis.
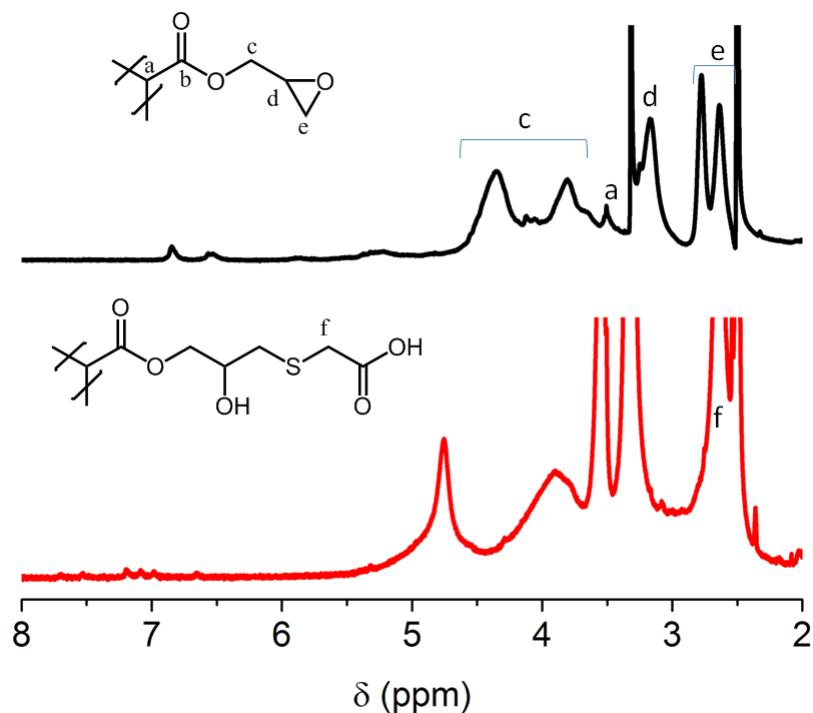
Fig. A.23.: Post-polymerization modification of **PGA_C1** with thioglycolic acid – ^{1}H NMR spectrum recorded in DMSO-d^6. The product was acidified prior to analysis.

Spectral Changes in the FT-IR spectra After Functionalization of PGA_C1 with Thiols
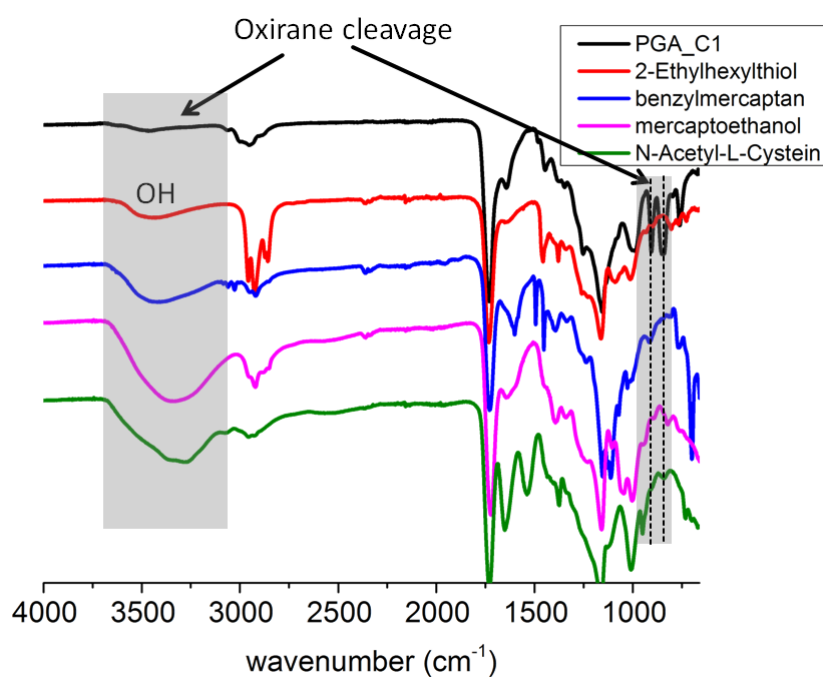
Fig. A.24.: Oxirane cleavages with various thiols as observed via FT-IR spectroscopy.

Comparison of ¹H NMR Data Derived from PGA_C1 and PGMA_C2 After Post-Polymerization Modification with Thiols
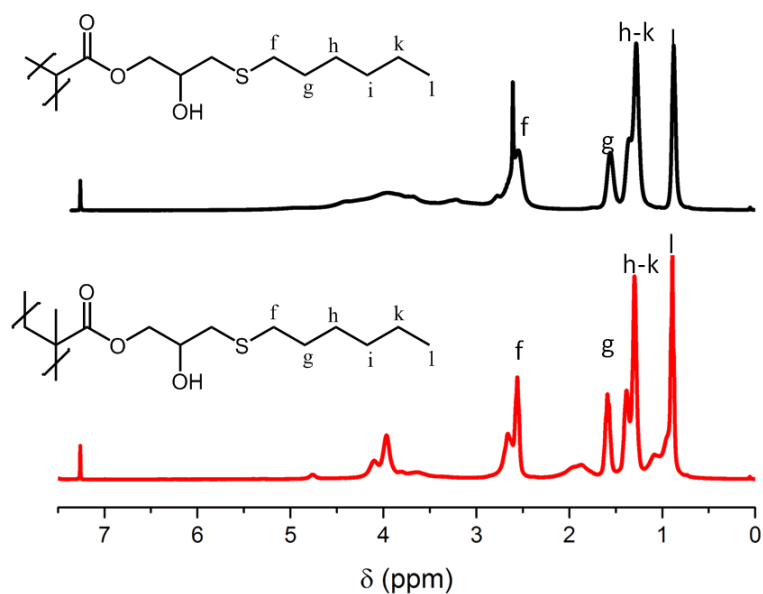
Fig. A.25.: ¹H NMR spectra in CDCl$_3$. Poly(glycidyl methacrylate) **PGMA_C2** functionalized with 1-mercaptohexane (upper spectrum). Poly(glycidyl 2-ylidene-acetate) **PGA_C1** functionalized with 1-mercaptohexane (bottom spectrum).
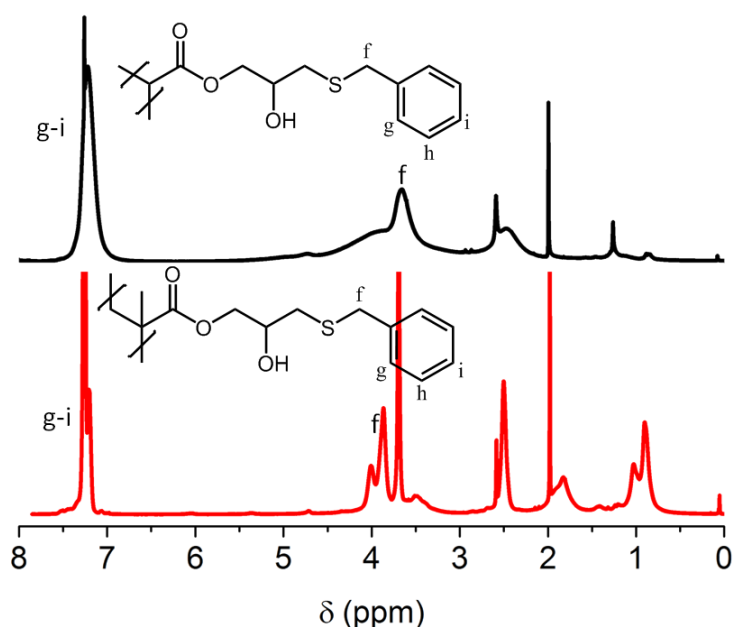
Fig. A.26.: ¹H NMR spectra in CDCl$_3$. Poly(glycidyl methacrylate) **PGMA_C2** functionalized with benzylmercaptan (upper spectrum). Poly(glycidyl 2-ylidene-acetate) **PGA_C1** functionalized with benzylmercaptan (bottom spectrum).

B. List of Hazardous Substances

Informations were extracted from `http://www.sigmaaldrich.com`.

Chemicals (CAS number)	Hazard class	H-Phrases	P-Phrases
Acetone (67-64-1)	GHS02 GHS07	H225-H319-H336	P210-P305 + P351 + P338-P370 + P378-P403 + P235
Acetonitrile (75-05-8)	GHS02 GHS07	H225-H302 + H312 + H332-H319	P210-P261-P280-P305 + P351 + P338-P370 + P378-P403 + P235
N-Acetyl-L-cysteine (616-91-1)	/	/	/
Allyl alcohol (107-18-6)	GHS02 GHS06 GHS09	H225-H301 + H311 + H331-H315-H319-H335-H400	P210-P261-P273-P280-P301 + P310 + P330-P403 + P233
α-Aminodiphenyl-methane (91-00-9)	GHS07	H302-H315-H319-H335	P261-P305 + P351 + P338
Azobisisobutyronitrile (78-67-1)	GHS02 GHS07	H242-H302 + H332-H412	P210-P220-P234-P261-P280-P370 + P378
Benzyl acrylate (2495-35-4)	GHS07	H315 + H319	P264 + P280 + P302-P352-P332-P313-P362-P364 + P305-P351-P338-P337-P313
Benzyl alcohol (100-51-6)	GHS07	H302 + H332-H319	P261-P301 + P312 + P330-P304 + P340 + P312-P305 + P351 + P338

B. List of Hazardous Substances

Chemicals (CAS number)	Hazard class	H-Phrases	P-Phrases
Benzyl mercaptan (100-53-8)	GHS06	H302-H330	P260-P284-P310
Benzylamine (100-46-9)	GHS05 GHS07	H302 + H312-H314	P301 + P312 + P330-P303 + P361 + P353-P304 + P340 + P310-P305 + P351 + P338
Benzyl bromide (100-39-0)	GHS07	H315-H319-H335	P261-P305 + P351 + P338
Bromoacetyl bromide (598-21-0)	GHS05	H314	P280-P305 + P351 + P338-P310
α-Bromoisobutyryl bromide (20769-85-1)	GHS05 GHS07	H302-H314	P280-P305 + P351 + P338-P310
tert-Butyl mercaptan (75-66-1)	GHS02 GHS07 GHS09	H225-H317-H411	P210-P273-P280
Chloroform (67-66-3)	GHS06 GHS08	H302-H315-H319-H331-H336-H351-H361d-H372	P201-P261-P304 + P340 + P312-P305 + P351 + P338-P308 + P313-P403 + P233
1,5-Cyclooctadiene (111-78-4)	GHS02 GHS07	H226-H302 + H332-H315-H317-H319	P280-P305 + P351 + P338
1,8-diazabicyclo-[5.4.0]undec-7-ene (6674-22-2)	GHS05 GHS06	H290-H301-H314-H412	P273-P280-P301 + P310-P305 + P351 + P338-P310
Dichloromethane (75-09-2)	GHS07 GHS08	H315-H319-H335-H336-H351-H373	P260-P280-P305 + P351 + P338
Diethylether (60-29-7)	GHS02 GHS07	H224-H302-H336	P210-P261

B. List of Hazardous Substances

Chemicals (CAS number)	Hazard class	H-Phrases	P-Phrases
Dihexylamine (143-16-8)	GHS05 GHS06 GHS09	H302-H311-H314-H400	P273-P280-P305 + P351 + P338-P310
2,2-Dimethoxy-2-phenylacetophenone (24650-42-8)	GHS07 GHS09	H317-H410	P273-P280-P501
1,5-Dimethyl-1,5-cyclooctadiene (3760-14-3)	GHS02	H226	P210 + P233 + P240 + P241 + P242 + P243 + P261 + P264 + P271 + P280 + P303-P361-P353 + P370-P378 + P403-P235 + P501
Dimethylsulfoxide (67-68-5)	/	/	/
1,4-Dioxane (123-91-1)	GHS02 GHS07 GHS08	H225-H319-H335-H351	P210-P280-P305 + P351 + P338-P370 + P378-P403 + P235
Ethyl acetate (141-78-6)	GHS02 GHS07	H225-H319-H336	P210-P305 + P351 + P338-P370 + P378-P403 + P235
Ethyleneglycol (107-21-1)	GHS07 GHS08	H302-H373	P260-P301 + P312 + P330
2-Ethyl-1-hexylamine (104-75-6)	GHS02 GHS05 GHS06	H226-H302-H311 + H331-H314	P261-P280-P305 + P351 + P338-P310
2-Ethylhexylmercaptan (7341-17-5)	GHS02 GHS08	H226-H319-H334-H412	P261-P273-P305 + P351 + P338-P342 + P311
Glycidol (556-52-5)	GHS02 GHS06 GHS08	H242-H302 + H312-H315-H319-H331-H335-H341-H350-H360F	P201-P261-P280-P304 + P340 + P312-P308 + P313-P403 + P233

B. List of Hazardous Substances

Chemicals (CAS number)	Hazard class	H-Phrases	P-Phrases
Glycidyl methacrylate (106-91-2)	GHS05 GHS06 GHS08	H302 + H332-H311-H314-H317-H341-H350-H360F-H370	P201-P260-P280-P305 + P351 + P338-P310
n-Hexane (110-54-3)	GHS02 GHS07 GHS08 GHS09	H225-H304-H315-H336-H361f-H373-H411	P201-P210-P273-P301 + P310-P308 + P313-P331
Hexylamine (111-26-2)	GHS02 GHS05 GHS06 GHS09	H226-H301 + H311-H314-H411	P273-P280-P301 + P310-P305 + P351 + P338-P310
Lithium hydroxide (1310-65-2)	GHS05 GHS07	H302-H314	P280-P305 + P351 + P338-P310
Magnesium sulfate (7487-88-9)	/	/	/
Mercaptoacetic acid (68-11-1)	GHS05 GHS06	H301 + H311 + H331-H314	P280-P301 + P310 + P330-P303 + P361 + P353-P304 + P340 + P310-P305 + P351 + P338-P403 + P233
2-Mercaptoethanol (60-24-2)	GHS05 GHS06 GHS08 GHS09	H301 + H331-H310-H315-H317-H318-H373-H410	P261-P280-P301 + P310 + P330-P302 + P352 + P310-P305 + P351 + P338 + P310-P403 + P233
1-Mercaptohexane (111-31-9)	GHS02 GHS06	H226-H302-H331	P261-P311
Methanol (67-56-1)	GHS02 GHS06 GHS08	H225-H301 + H311 + H331-H370	P210-P280-P302 + P352 + P312-P304 + P340 + P312-P370 + P378-P403 + P235

B. List of Hazardous Substances

Chemicals (CAS number)	Hazard class	H-Phrases	P-Phrases
Petrol ether (101316-46-5)	GHS02 GHS07 GHS08 GHS09	H225-H304-H315-H336-H361f-H373-H411	P210-P260-P280-P301 + P310-P370 + P378-P403 + P235
Piperidine (110-89-4)	GHS02 GHS05 GHS06	H225-H302-H311 + H331-H314-H412	P210-P280-P304 + P340 + P310-P305 + P351 + P338-P370 + P378-P403 + P235
L-Prolin (147-85-3)	/	/	/
Propargyl alcohol (107-19-7)	GHS02 GHS05 GHS06 GHS09	H226-H301-H311-H314-H331-H411	P261-P273-P280-P301 + P310-P305 + P351 + P338-P310
Sodium bicarbonate (144-55-8)	/	/	/
Sodium azide (26628-22-8)	GHS06 GHS08 GHS09	H300 + H310-H373-H410	P273-P280-P301 + P310 + P330-P302 + P352 + P310-P391-P501
Tetrahydrofurane (109-99-9)	GHS02 GHS07 GHS08	H225-H302-H319-H335-H351	P210-P280-P301 + P312 + P330-P305 + P351 + P338-P370 + P378-P403 + P235
Toluene (108-88-3)	GHS02 GHS07 GHS08	H225-H304-H315-H336-H361d-H373	P210-P260-P280-P301 + P310-P370 + P378-P403 + P235
p-Toluenesulfonyl chloride (98-59-9)	GHS05	H315-H318	P280-P305 + P351 + P338

B. List of Hazardous Substances

Chemicals (CAS number)	Hazard class	H-Phrases	P-Phrases
p-Toluenesulfonyl hydrazide (1576-35-8)	GHS02 GHS06	H242-H301	P301 + P310
Triethylamine (121-44-8)	GHS02 GHS05 GHS06	H225-H302-H311 + H331-H314-H335	P210-P261-P280-P303 + P361 + P353-P305 + P351 + P338-P370 + P378
2,2,6-Tri- methyl-4H-1,3-dioxin-4-one (5394-63-8)	GHS02 GHS07	H225-H319	P210-P305 + P351 + P338

Acknowledgements

Declaration on Oath

I hereby declare on oath, that I have written the present dissertation by my own and have not used other than the acknowledged resources and aids. The submitted written version corresponds to the version on the electronic storage medium. I hereby declare that I have not previously applied or pursued for a doctorate (Ph.D. studies).

Hamburg, February 2, 2017

Hiermit versichere ich an Eides statt, die vorliegende Dissertation selbst verfasst und keine anderen als die angegebenen Hilfsmittel benutzt zu haben. Die eingereichte schriftliche Fassung entspricht der auf dem elektronischen Speichermedium. Ich versichere, dass diese Dissertation nicht in einem früheren Promotionsverfahren eingereicht wurde.

Hamburg, February 2, 2017